Optimisation Of Methods For The Differentiation Of Human Embryonic Stem Cells Into Retinal Progenitor Cells

By

Subashini Sabapathy

Department of Biochemical Engineering

University College London

Torrington Place

London WC1E 7JE

Declaration

I Subashini Sabapathy, confirm that the work presented in this thesis is my own. Where information has been derived from other sources, I confirm that this has been indicated.

Subashini Sabapathy.

Acknowledgements

I dedicate this to my mum and my (late) grandfather- the best teacher I have ever known!

These last four years have been a rollercoaster of a journey with many, many lessons learnt- academically and in life. I have had many amazing people that have helped me to get through this and without these people I would not be where I am today. I am very, very grateful to all of those people.

Firstly my sincere thanks go to Prof. Nigel Tichener-Hooker for giving me this opportunity in the first instance. Heartfelt thanks also go to Prof. Gary Lye for all his advice and help before and during the process of this MPhil. Thank you also to Dr Farlan Veraitch , my supervisor, for his guidance and support.

I would also like to thank Mrs Ludmila Ruban sincerely, for being my mum in the lab and also for her great efforts in helping me to complete my thesis and also for her genuine care.

A big thank you goes to Dr Dae Bae for his tireless efforts, guidance and support throughout this journey. My thanks also go to Kate Fynes for all her support and also for putting up with my rants!

I could not have completed this without my loving mum, whose endless support and physical help has been completely selfless. I could never thank you enough! My thanks also go to my aunt, Dhushy (chithy), for all her efforts in helping me complete my thesis- finally you can get away from me and be peaceful at work! A very big thank you to my son, Ishan, whom I've watched grow so quickly since the start of this journey.

His smile, presence and existence has lifted my spirits on so many occasions and given me the determination to persevere.

My sincere thanks to each and every one of you who really have helped me to get to this point.

Contents

Optimisation Of Methods For The Differentiation Of Human Embryonic Stem Cells Into Retinal Progenitor Cells 1

Declaration 2

Acknowledgements 3

List of Figures 9

Abstract 14

1 Introduction 15

1.1 Eye Development 16

1.2 Anatomy of the adult eye 18

1.2.1 Fibrous Tunic 19

1.2.2 Vascular Tunic 21

1.2.3 Neural Tunic (Retina) 22

1.3 The Retina 24

1.3.1 Photoreceptors 24

1.3.2 Bipolar cells 27

1.3.3 Ganglion cells 28

1.4 Photoreceptor Dystrophies 28

1.5 Retinitis Pigmentosa 29

1.5.1 Non syndromic RP 30

1.5.2 Syndromic Retinitis Pigmentosa 34

1.6 Potential Treatment for retinal dystrophies 36

1.6.1 Gene Therapy 36

1.6.2 Cell Therapy 37

1.7 Stem cells 38

1.7.1 The Discovery 38

1.7.2 Human Embryonic Stem Cells (hESCs) and Mouse Stem cells 41

1.7.3 Adult Stem Cells 44

1.7.4 Induced Pluripotent Stem Cells 48

1.8 Differentiation of Human Stem Cells 51

1.8.1 Differentiation of Human Stem cells through EBs 51

1.8.2 Monolayer Differentiation of hESCs 54

1.9 Retinal Differentiation of pluripotent hESCs 55

1.9.1 Wnt signalling 55

1.9.2 Current Methods of Photoreceptor Differentiation of Stem Cells 57

1.10 Retinal Co-culture with hESCs and Photoreceptor Differentiation 68

1.11 Retinal Transplantation 71

1.12 Summary 79

2 Aims and Objectives 81

3 Materials and Methods 82

3.1 Human Pluripotent Cell Culture 82

3.2 Isolation of Mouse Embryonic Fibroblasts 82

3.3 Feeder Preparation 83
3.4 Retinal Differentiation of Human Pluripotent Stem Cells 83
3.4.1 Embryoid Body Differentiation of Human Pluripotent Stem Cells . 83
3.4.2 Optimisation of Dissociation Buffer For EB Retinal Differentiation 84
3.4.3 Monolayer Retinal Differentiation 84
3.5 Immunocytochemistry 85
3.6 RNA Extraction and cDNA Synthesis 86
3.7 Real-time Quantitative Polymerase Chain Reaction (qPCR) 86
4 Characterisation of Shef3 hESCs 88
4.1 Introduction 88
4.1.1 Aim 88
4.2 Morphology of undifferentiated Shef3-hESCs 88
4.3 Differentiation of Shef3 hESCs 92
4.4 Formation EBs from pluripotent Shef3 hESCs 94
4.5 Karyotype analysis of Shef3 hESCs 95
5 Differentiation of Pluripotent Human Embryonic Stem Cells using the Lamba protocol 97
5.1 Introduction 97
5.1.1 Aim 98
5.2 Differentiation of Shef 3 hESCs following the protocol devised by Lamba 98
5.3 Generation of Early RPCs 108

5.4 Optimisation of the Lamba Differentiation Process 111

5.4.1 Aim 111

5.4.2 Differentiation of Shef3 hESCs using dissociation enzyme Accutase and dissociation reagent TrypLE Express 112

5.4.3 Generation of early RPCs 121

5.5 Discussion 125

5.6 Conclusion 129

6 Monolayer Differentiation of Human Pluripotent Stem Cells 130

6.1 Introduction 130

6.2 Aim 130

6.3 Monolayer Differentiation of Shef-3 hES cells 130

6.4 Differentiation of Retinal cells on various ECMs 141

6.5 Generation of Early RPCs Using a Monolayer Differentiation 144

6.6 Discussion and Conclusion 151

7 Concluding Remarks and Future work 158

7.1 Summary of results 158

7.2 Future Work 160

Bibliography 167

List of Figures

Figure 1.1: Development of the eye……17

Figure 1.2: A simplified horizontal section of the eye……18

Figure 1.3: A detailed horizontal section of the right eye……..….20

Figure 1.4: Diagram of pupillary muscles during decrease and increase of light intensity……...22

Figure 1.5: Detailed diagram of the retina……...23

Figure 1.6: Structure of a rod and a cone……25

Figure 1.7: Detailed structure of rods and cones…….26

Figure 1.8: Images of the fundus…….31

Figure 1.9: Visionary field……...31

Figure 1.10: Derived H9 cell……...39

Figure 1.11: Teratomas formed by human ES cell lines after injection onto 4 week old SCID mice……...40

Figure 1.12: LIF-dependent activation of STAT3 block ES cell differentiation and promotes self-renewal…….43

Figure 1.13: A diagram of adult stem cell (ASC) healing response to damage……..47

Figure 1.14: The process of reprogramming between embryonic stem cells (ES) and somatic cells……50

Figure 1.15: Image of AggrWell plates from Stem Cell Technologies……...53

Figure 1.16: qPCR of cells treat with and without (control) endogenous Wnt3A and BMP4 during the first 10 days of differentiation process of eye field cells……61

Figure 1.17: qPCR analysis of eye field transcription factors after 1 week culture with combination of IGF1, Dkk1 and noggin……..62

Figure 1.18: Response of mouse embryonic stem cells cultured in varying concentrations of retinoic acid…….63

Figure 1.19: Expression of retinal markers from retinal induced hESCs……66

Figure 1.20: RT-PCR of gene expression during first 16 days of eye field differentiation of hESCs……..66

Figure 1.21: QPCR analysis of various genes between cells from a 91 day human foetal retina and hESCs after a 3 week culture condition……..67

Figure 1.22: Generation of photoreceptors from mES cell co-culture with mature retinal cells……..69

Figure 1.23: hESCs derived retinal progenitor cell co-culture with Aip1-/- GFP mice retina labelled with human nuclear marker (blue) and recoverin (red)……...70

Figure 1.24: Transplantation of P1 transgenic retinal cells into immature wild type littermate (3 weeks post transplantation)…….71

Figure 1.25: Transplantation of P1 cells from transgenic mice into wild-type mature retina……72

Figure 1.26: A chart of the number of integrated cells from each population of transplanted cells…….73

Figure 1.27: Transplantation of rod-precursor cells in Gnat1-/- mice……75

Figure 4.1: Immunocytochemistry results of pluripotency markers Oct4, TRA-160 and SSEA-3 for Shef3 hESCs……90

Figure 4.2: Morphology of healthy undifferentiated state……...91

Figure 4.3: Morphology of Shef3 hESCs undergoing differentiation…….92

Figure 4.4: Immunocytochemistry results for SSEA1 on a population of hESCs……..93

Figure 4.5: Image of EBs formed from Shef3 hESCs after 5 days of suspended culture……95

Figure 4.6: Cytogenetic analysis of Shef 3 hESCs. Image shows results of karyotyping of these cells……..96

Figure 5.1: Morphology of EBs…….99

Figure 5.2: Morphology of cell aggregates formed from cells mechanically dissected with Collagenase VI at various time points in the differentiation……100

Figure 5.3: Morphology of cells on day 5 of the differentiation of Shef 3 hESCs……102

Figure 5.4: Morphology of cells on days 6 and 7 of the differentiation process……...104

Figure 5.5: Morphology of cells on day 10 of the EB incorporated differentiatio process (A)…….....105

Figure 5.6: Morphology of cells during days 11, 12, 13 and 19 of the differentiation process……...107

Figure 5.7: Cell monolayer detachment from the matrigel coating on day 20 of the differentiation process…….....108

Figure 5.8: Generation of Pax6 and Chx10 positive cells from Shef3 cells differentiated using the EB incorporated differentiation protocol……...109

Figure 5.9: qPCR analysis of retinal gene expression of cells mechanically dissected with Collagenase IV……..110

Figure 5.10: Morphology of day 1 aggregates formed from cells dissociated with Accutase and TrypLE Express……..114

Figure 5.11: Morphology of day 4 aggregates……..114

Figure 5.12: Morphology of cells on day 6 of the differentiation process……116

Figure 5.13: Morphology of cells during different time point of the differentiation process……...118

Figure 5.14: Morphology of cells dissociated with TrypLE Express and Accutase on days 11 & 12 of the differentiation process……...119

Figure 5.15: Morphology of cells dissociated with TrypLE Express on day 20 of the investigations…….120

Figure 5.16: Pax 6 expression of cells dissociated with Accutase and TrypLE Express……...122

Figure 5.17: Immunocytochemistry results of Chx10 Express from cells dissociated buffers Accutase and TrypLE Express. Arrows indicate examples of multi-layered structures……123

Figure 5.18: qPCR analysis of retinal gene expression in cells dissociated with Accutase, TrypLE Express and mechanical dissection with Collagenase…….125

Figure 6.1: Morphology of Shef-3 hESCs on day 1(A & B) and day3 (C & D) of the monolayer differentiation……..132

Figure 6.2: Morphology of differentiated Shef 3 hESCs on day 4. A: Image of compacted cells on a lower magnification……133

Figure 6.3: Shef-3 hESCs on various points of the monolayer differentiation…….133

Figure 6.4: Images of Shef 3 hESCs on day 10 of the monolayer differentiation process……...135

Figure 6.5: Images of Shef3 hESCs on day 11 of the differentiation process……..136

Figure 6.6: Images of Shef3 hESCs at various time points of the differentiation…….138

Figure 6.7: Image of Shef3 hESCs on day 17 of the differentiation process……139

Figure 6.8 Images of Shef3 hESCs at various time points of the differentiation process……...140

Figure 6.9: Image of cells on day 25 of the differentiation process on various ECM coatings.....143

Figure 6.10: Immunocytochemistry for β-III-Tubulin, DAPI Staining and phase images for cells cultured on various ECMs……...145

Figure 6.11: Immunocytochemistry for Pax6, DAPI staining and phase images for cells cultured on various ECMs……147

Figure 6.12: Immunocytochemistry results for Chx10 for monolayer differentiated Shef3 cells cultured on various ECM coatings……..149

Figure 6.13: qPCR results for monolayer differentiation of pluripotent Shef 3 hESCs samples taken at various time points during the differentiation process……...151

Figure 7.1: Quantification using flow cytometry for the differentiation of hESCs under normal and hypoxic conditions……..165

List of Tables

Table 1.1: A summary of the main photoreceptor differentiation protocols with results……...64

Table 1.2: Classification of early-, mid- and late- stage retinal degeneration mouse models used…….77

Table 3.1: A list of qPCR primers used for analysis……...87

Abstract

Many ocular diseases result in visual impairment often leading to blindness with disease progression, one such example is Retinitis pigmentosa (RP). The underlying cause for blindness is often due to the degeneration of photoreceptors and supporting cells in the retina. Photoreceptors are responsible for the conversion of light signals into electrical impulses which are processed by the brain to form a visual image. Unlike other cells, photoreceptors cannot be regenerated by the body. For this reason current treatment for many ocular diseases aims to preserve what little vision patients hold. The only way such diseases could be cured is by regenerating photoreceptors and transplanting them into patients to replace lost cells and function.

The differentiation of retinal cells from human embryonic stem cells (hESCs) is a difficult process. Current strategies produce low efficiencies of retinal cells which could not supply cells in a clinical environment. It is evident that the key lies within the tight control of the microenvironment of these cells at various stages of the differentiation process.

In this study various optimisation avenues were investigated in order to increase the yield of retinal cells. By investigating the impact of various dissociation reagents and enzymes it was found that, the dissociation of cells using TrypLE Express significantly increased retinal gene expression. Using this reagent resulted in over a 100 fold increase in expression of photoreceptor precursor marker Nrl in comparison to the mechanical dissection with Collagenase IV (the control). In this investigation it was also found that the dissociation of cells during the process, in order to reduce cell densities is highly detrimental.

The investigations were successful in finding some changes to the published protocols that optimised the differentiation process of pluripotent Shef3 hESCs into retinal cells.

1 Introduction

The eye although a comparatively small structure of the human anatomy, in history, has been the centre of many conflicting theories for centuries. Famous scholars including Plato and Aristotle have all contributed to the discussion of its process.

In summary, it is a complex system capable of rapidly processing light into electrical impulses to produce the important sense of vision; and the underlying cause of ocular diseases is often degeneration, damage or loss of one or more of the components involved in this system.

Loss of vision has become widely accepted as “the norm” in the aging population with a whole subset of ocular diseases shown to be more prevalent with ageing. Examples of diseases from this subset are macular degeneration and retinitis pigmentosa, resulting in partial or total blindness respectively, due to damage in components associated with light processing. These components are known as photoreceptors and reside in the back of the eye in the retina. Degeneration of photoreceptors can be both inherited or acquired.

The discovery of stem cells has taken science and therapy to new horizons with the potential to be used in therapy for many age-related ocular diseases. Before these cells become clinically available however, there are several hurdles to overcome concerning the efficiency, reproducibility and safety in the production of these cells. Once key hurdles have been conquered, the transplantation of photoreceptors to replace degenerate photoreceptor cells could be the answer to the restoration vision in suffering patients.

1.1 Eye Development

The development of the human eye begins around day 22 of embryogenesis lasting several months until completion (Sernagor, 2006). It is structured using three tissue types: the neural ectoderm, mesoderm and the ectoderm. The retina and retinal pigmented epithelium (RPE) is formed from the neural ectoderm, whilst the sclera and cornea are formed from the mesoderm. Lastly the lens is formed from the ectoderm. During the developmental process, optic vesicles which form from the neural tube, form the two eyes (Sernagor, 2006).

The development of the eye results from the contact of the optic vesicle with the ectoderm. This induces the thickening of the ectoderm, producing a lens placode which in turn pushes into the optic vesicle leading to its invagination and formation of the optic cup, lens and vesicle (Sernagor 2006). This is connected to the central nervous system by a stalk which later becomes the optic nerve. The outer surface of the optic cup later becomes the retinal pigment epithelium (RPE), whilst the inner surface becomes the retina (Figure 1.1) (Wawersik and Maas 2000; Sernagor 2006).

Several important eye field transcription factors have been found to hold important roles in the formation of the eye. These include the following: ET, Rx1, Pax6, Six3, Lhx2, tll and Six6 which are all expressed at the neural plate (Zuber *et al.*, 2003).

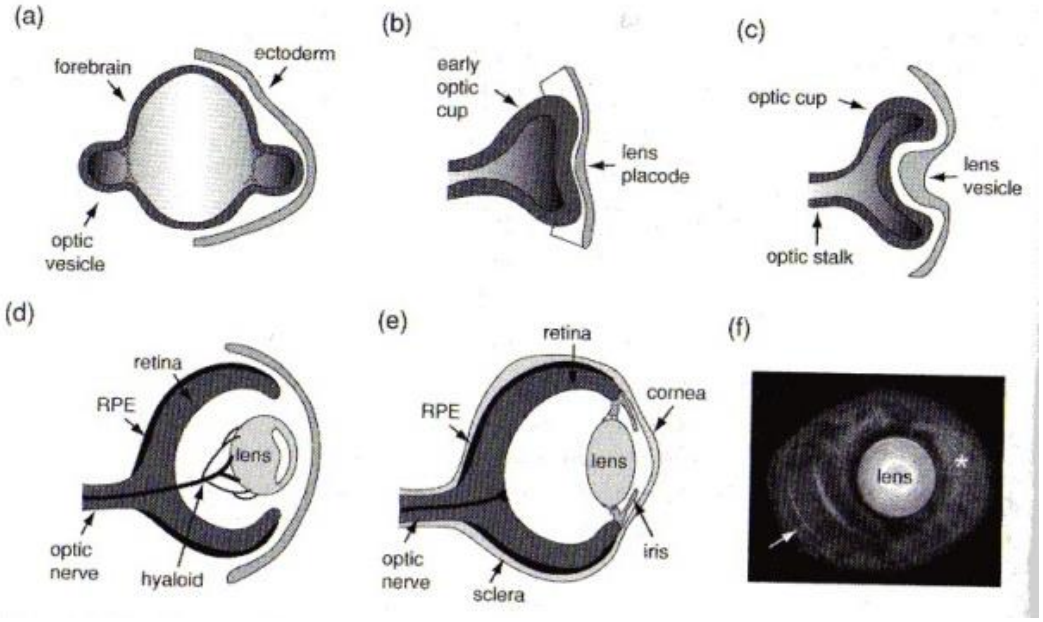

Figure 1.1: Development of the eye. (a): Optic vesicles from the neural tube form the two eyes. (b): The lens placode is produce as a result of the contact between the surface ectoderm and optic vesicles. (c): The invagination of the lens placode results in the formation of the optic cup. (d): The outer surface of the optic cup later becomes the retinal pigment epitheilum and the inner surface the retina. (e): The mature eye and location of the retina. Image retrieved from Sernagor 2006.

Pax6 especially, has been found to play a prominent role in the early development of the eye. The expression of Pax6 has been found to be present in the head ectoderm and optic vesicle. This has then found to later become restricted in the lens placode prior to ectoderm thickening, suggesting a regulatory role of Pax6 expression by the optic vesicle.

The importance of Pax6 in eye development is clear from studies that have found mutations resulting in a range of severe ocular diseases including: aniridia, a disease resulting in the absence (complete or partial) of the iris and anophthalmia, a disease resulting in the absence of the eye structure affecting either one or both eyes.

Other studies have also found that homozygous mutants for Pax6 fail to form the lens placode, whilst chimera studies have highlighted a cell autonomous role for Pax6 in retina development (Wawersik and Maas 2000).

There are several transcription factors that have been identified to play an important role in and also mark the various stages of photoreceptor differentiation.

1.2 Anatomy of the adult eye

The complex system of the eye is compacted into a slightly irregular spheroid with a diameter of approximately 24mm and weighs an estimated 8g. Structurally it is divided into three layers (i) fibrous tunic- the outer layer, (ii) vascular tunic- the intermediate layer, and (iii) the neural tunic (retina)- the inner layer (Figure 1.2) (Martini et al. 2009).

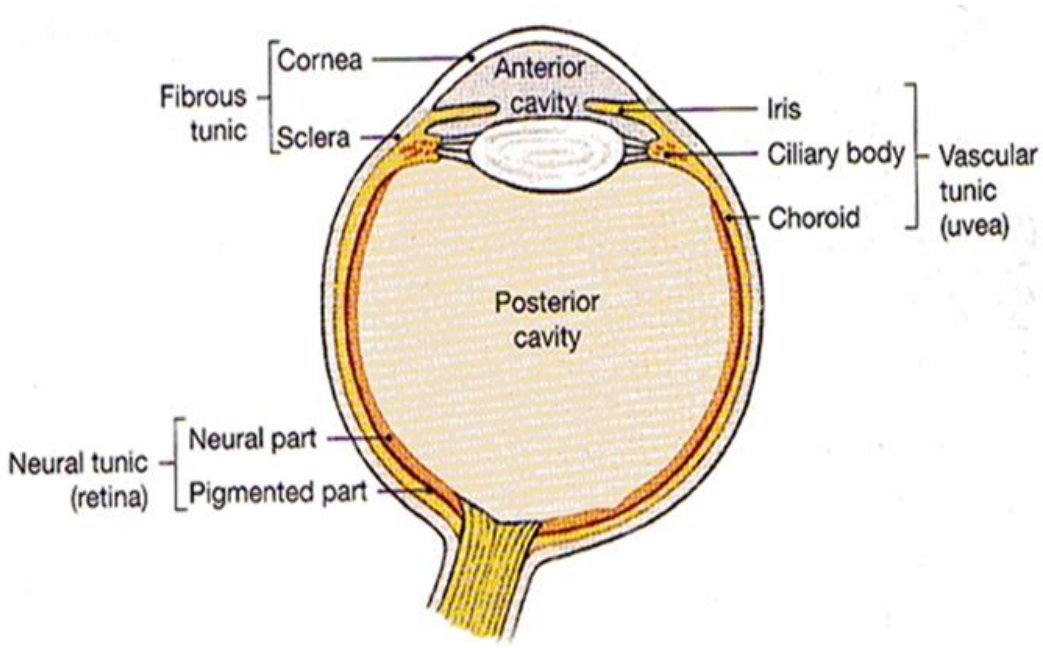

Figure 1.2: A simplified horizontal section of the eye. Image taken from Martini et al., 2009.

1.2.1 Fibrous Tunic

The fibrous tunic is the outermost layer containing the sclera and cornea. The majority consists of the sclera. This structure is a strong layer of connective tissue made up of collagen and elastic fibres that functions as (i) a protective shield for internal structures that are more delicate, (ii) an attachment point for extrinsic muscles and (iii) contains structures involved in focussing.

Towards the anterior section of the eye, the surface closest to the entrance of light, the sclera becomes more curved in structure and transparent to form the cornea. The cornea consists of dense collagen layers organised not to impede on the path of light entering the eye (Figure 1.3) (Martini et al. 2009; Tortora and Nielsen 2009). In contrast to the sclera, the cornea does not contain any blood vessels. Epithelial cells absorb oxygen and nutrients from the free flowing tears across the eye instead. It also has a limited ability for self-repair, maybe owing to the lack of blood supply. Damage could therefore easily result in blindness, although intrinsic structures are fully functional.

The advantage of lacking a capillary network is that it remains one of the few transplantation procedures readily carried out without danger of immunorejection, as no white blood cells are present to initiate an immune response (Martini et al. 2009). Corneal transplantation is a common procedure with approximately 3615 successful procedures resulting in the restoration of sight carried out in the UK last year (2012/2013)(NHSBT,2013).

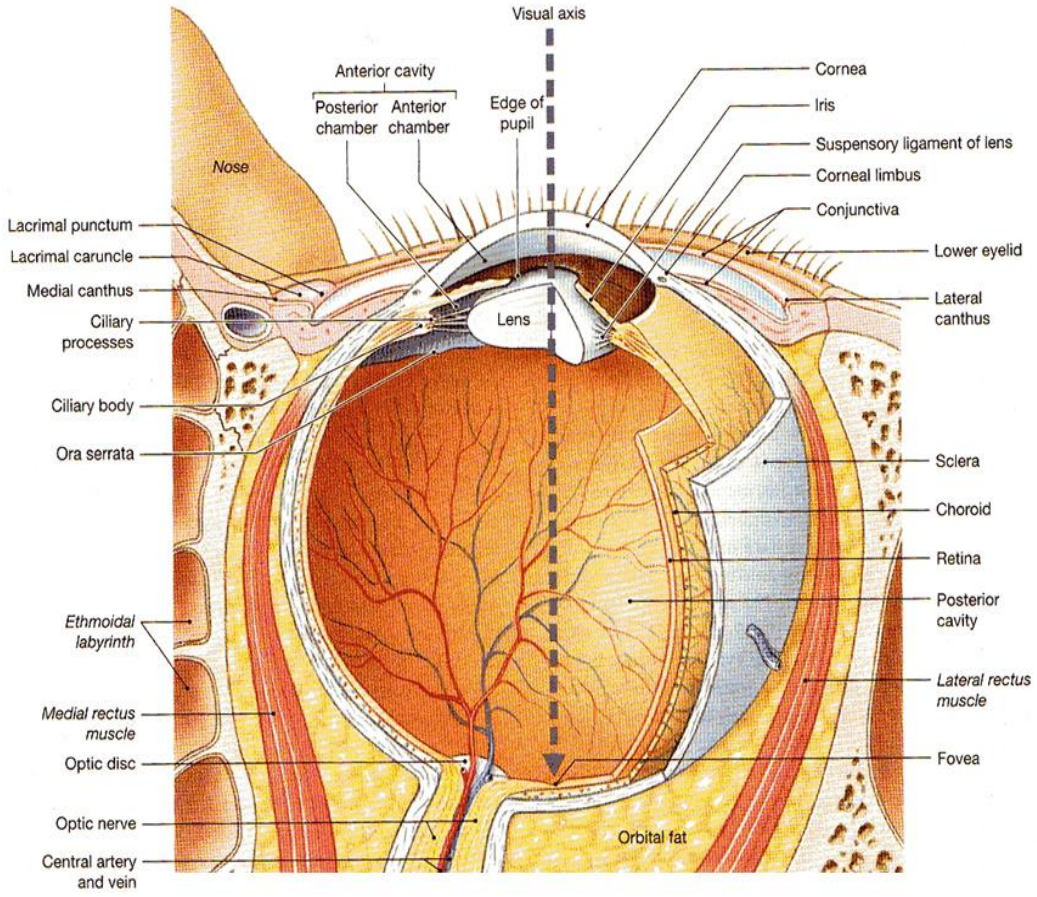

Figure 1.3: A detailed horizontal section of the right eye. (Martini et al. 2009).

1.2.2 Vascular Tunic

The vascular tunic is the middle layer of the eye and regulates the lens shape, aqueous humor volume, quantity of light entering the eye and supplies blood and nutrients to the eye (Martini *et al.,* 2009). This layer is primarily made up of three main components: iris, ciliary body and the choroid.

The iris is positioned between the cornea and the lens, morphologically shaped like a donut, with the opening referred to as the pupil and the ring made up of two groups of smooth muscle (Martini*et al.,* 2009). The pupillary constrictor located towards the inner ring (i.e. closest to the pupil) and the pupillary dilator located towards the outer ring (Figure 1.4) (Martini et al. 2009). As the names suggest, these are involved in regulating the diameter of the pupil depending on the intensity of entering light in the eye. Melanin producing cells (melanocytes) also reside in the iris, the density of which governs eye colour. A dense organisation of melanocytes restricts the quantity of light reflecting back from the pigmented epithelium. This results in a brown eye colour, whereas a less dense organisation allows more light to be reflected from the pigmented epithelium giving the appearance of blue eye colour.

The iris is firmly attached to the ciliary body, a thickened region of the sclera at the corneal junction. The ciliary body is made up of smooth muscle (ciliary muscle) which regulates lens shape. The epithelium of ciliary muscle are organised into folds referred to as ciliary process and fibres (suspensory ligaments), the lens attach to the ciliary body from these folds. Contraction and relaxation of the ciliary muscles affects the tension on the suspensory ligaments which in turn alters the lens shape (Martini et al. 2009; Tortora and Nielsen 2009).

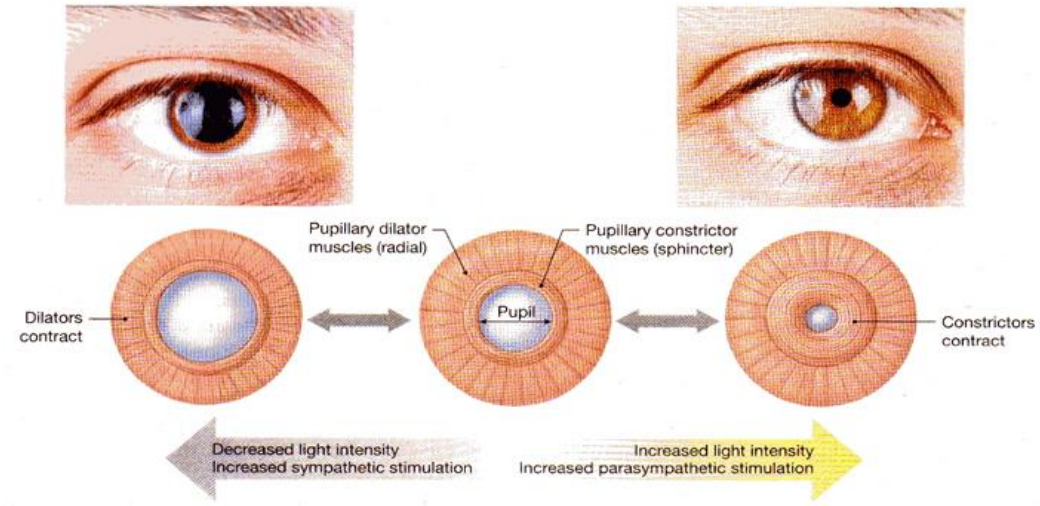

Figure 1.4: Diagram of pupillary muscles during decrease and increase of light intensity. (Martini et al. 2009).

Separation of the vascular tunic and the fibrous tunic is provided primarily by the choroid. The choroid is equipped with a capillary network which is used to supply nutrients and oxygen to the retina. It also contains melanocytes giving this structure a dark brown appearance. The melanin absorbs lights rays entering the eye and restricts reflection of the rays within the eye so that a sharp image is cast on the retina.

1.2.3 Neural Tunic (Retina)

The retina is the innermost layer of the eye made up of a pigmented layer and a neural layer. A single sheet of epithelial cells containing melanin constructs the pigmented layer and runs over the ciliary body and iris. The role of the melanin remains the same as that in the choroid. In contrast to the pigmented layer, the neural layer is a multi-layered structure constructed of three distinct layers of neurons: (i) photoreceptor layer, (ii) bipolar cell layer and (iii) ganglion cell layer, which only continues as far as the ciliary body (Martini et al. 2009; Tortora and Nielsen 2009) (Figure 1.5).

In addition to these neurons the retina also contains a number of other supporting neurons, including horizontal cells and amacrine cells which are involved in modulation of the activity of the three primary neurons (Snell and Lemp 1998).

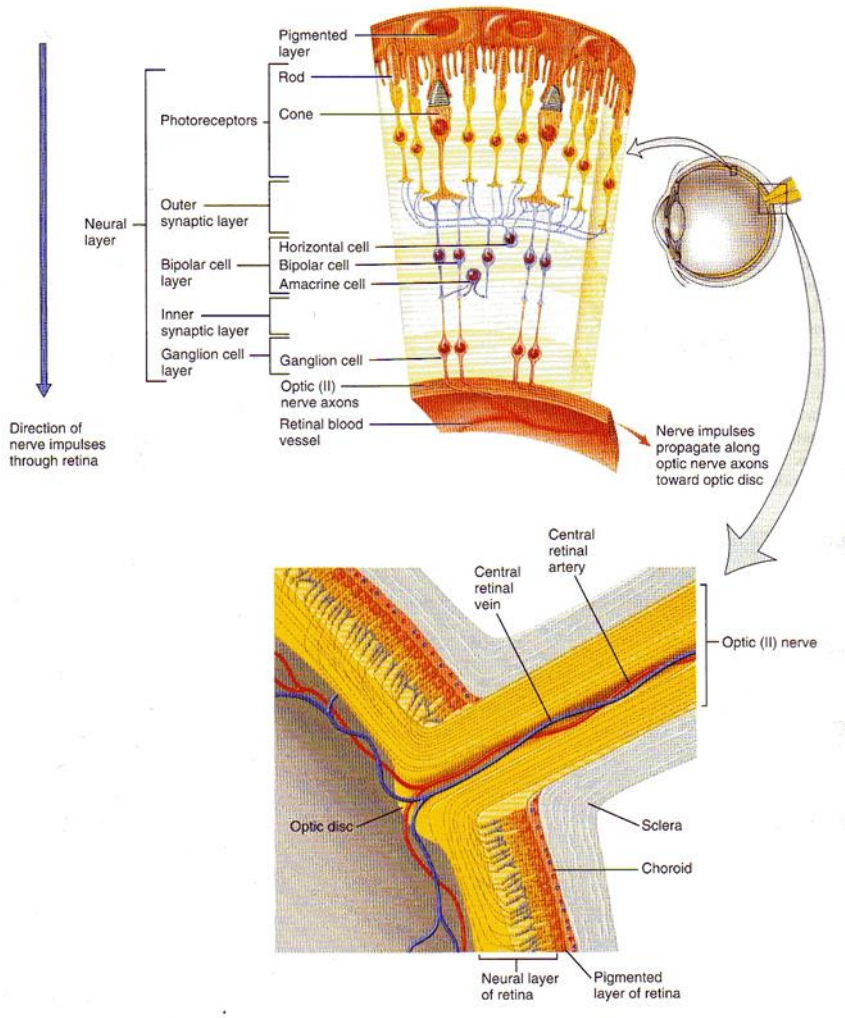

Figure 1.5: Detailed diagram of the retina. (Tortora and Nielsen 2009).

1.3 The Retina

1.3.1 Photoreceptors

This layer is located closest to the pigmented layer of the retina and is packed with numerous photoreceptors- as the name suggests! Photoreceptors, in short, are sensory receptors capable of detecting light. There are two types of photoreceptors: **rods** involved in dim vision and **cones** involved in colour vision. The latter is responsible for producing sharper and clearer images. Rods, approximately 120μm in length, are more sensitive to light and produce vision when light is sparse, but cannot distinguish colours in contrast to cones. There are three types of cones, each approximately 75μm in length, and colour perception is dependent on the combination of which of the different types are stimulated.

The distribution of rods and cones are by no means equal within the retina. The population of cones are by far outweighed by that of rods. An estimated 125 million rods are distributed in the periphery of the retina gradually decreasing in density towards the centre of the retina. In contrast, there is an estimated 6 million cones with the highest concentration lying at the fovea, the central point of the macula lutea, the region where most distinct vision occurs. Both rods and cones appear as narrow cells and are constructed of three parts: (i) an outer segment responsible for the detection of light, (ii) an inner segment and (iii) a synaptic terminal (Figure 1.6) (Snell and Lemp 1998; Martini et al. 2009).

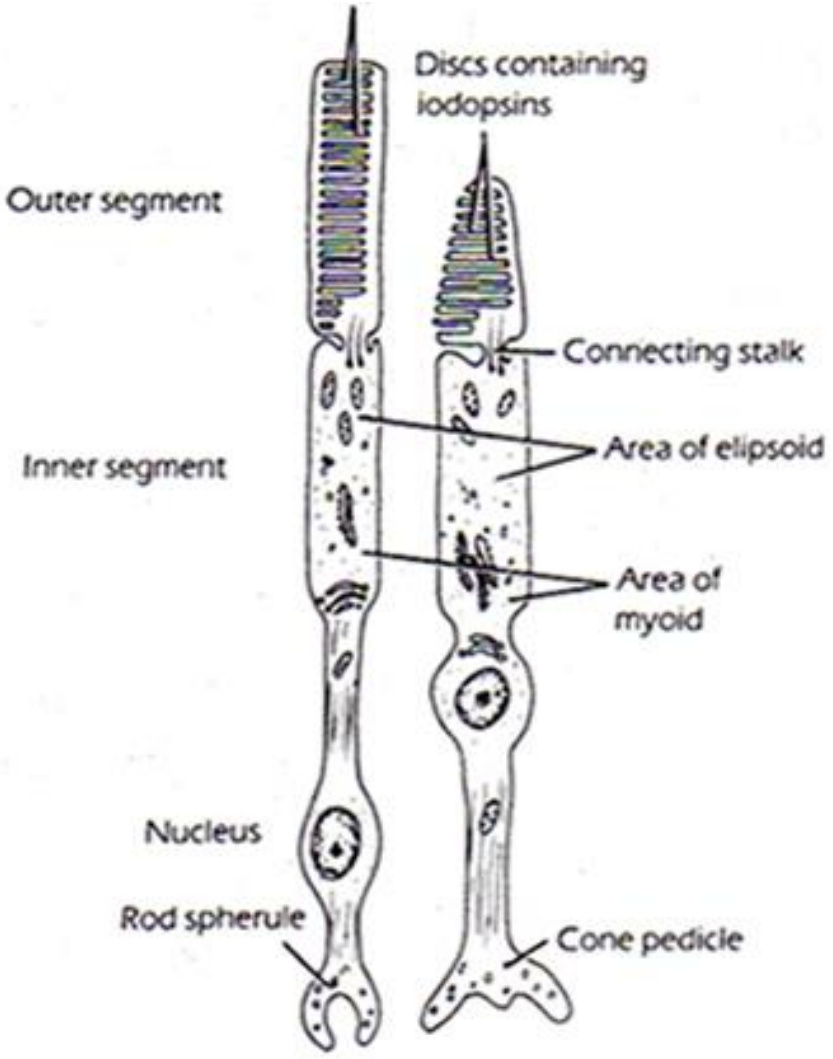

Figure 1.6: Structure of a rod and a cone. Image retrieved from Snell and Lemp 1998.

The shape of both photoreceptors in the outer segment, the region responsible for light detection, is what lends its name to the receptors. Rods take the shape of a rod-like structure whilst cones take the shape of a cone. The outer segment of both rods and cones have an elongated region of the photoreceptor containing thousands of individual discs; in cones however, as this region lies within the folding of the plasma membrane, the outer segment tapers to a point producing the characteristic cone shape which distinguishes cones (Figure 1.6) (Martini et al. 2009; Tortora and Nielsen 2009).

In both photoreceptor types the discs contain visual pigment which absorbs light photons, the first step light detection. This is known as photoreception. In rods this visual pigment is called rhodopsin, synthesised from vitamin A, whilst in cones the

pigment is called iodopsin (Figure 1.7 A and B). Both are made up of the pigment retinal, bound to the protein opsin. In cones however, the retinal is bound to different forms of opsin which defines the light wavelength that can be absorbed (Martini et al. 2009; Tortora and Nielsen 2009). This is the underlying basis of colour vision.

There is ample evidence showing the continual renewal of the outer segment with discs assembled at the base of the outer segment slowly moving to the tip of the outer segment (Young 1967; Snell and Lemp 1998; Martini et al. 2009). After approximately ten days discs become phagocytosed by pigmented epithelial cells reconverting retinal into vitamin A which the pigmented cells store (Young 1967; Snell and Lemp 1998; Martini et al. 2009). The outer segments of photoreceptors are connected to the inner segment via connecting stalks which in fact have been shown to be modified cilia (Snell and Lemp 1998).

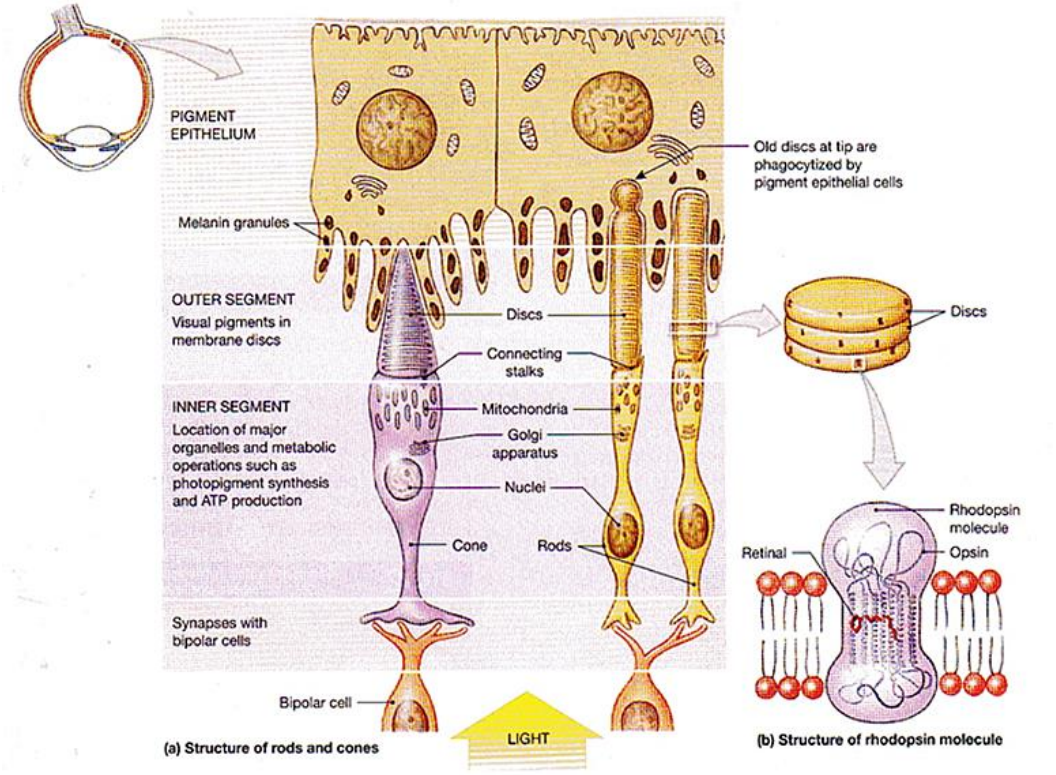

Figure 1.7: Detailed structure of rods and cones. (Martini et al., 2009).

The inner segment is made up of two main areas: (i) the ellipsoid and (ii) the myoid. The ellipsoid was first described by Sjöstrand in 1953 and covers the area closest to the outer segment. It also contains numerous mitochondria. The myoid is located towards the synaptic layer of the photoreceptor. It contains many important organelles such as Golgi apparatus, free ribosomes and endoplasmic reticulum to perform the vital role of providing ATP for the renewal of visual pigment and synthesis of parts of the outer segment (Ishikawa and Yamada 1969; Iwasaki and Inomata 1988; Snell and Lemp 1998).

The remaining compartments of photoreceptors consist of a 1µm wide outer fiber that connects the inner segment to the cell body. An inner fiber in turn connects the cell body to the spherule in the case of a rod; and the pedicle in the case of a cone (Snell and Lemp 1998). The spherule and pedicle contain many pre-synaptic vesicles and microtubules, which form synapses with dendrites of bipolar cells (Snell and Lemp 1998; Martini et al. 2009). This region is known as the synaptic terminal. Approximately six million neurons form synapses with both types of photoreceptors and these neurons are known as bipolar cells (Snell and Lemp 1998; Martini et al. 2009).

1.3.2 Bipolar cells

Bipolar cells form synapses with photoreceptors at one end and ganglion cells at the other. The input received from photoreceptors are delivered to ganglion cells through horizontal cells located at the base of photoreceptors, and are involved in the inhibition of bipolar cells producing sharpened contrast and spatial resolution (Snell and Lemp 1998). There are specific bipolar cells for both rods and cones so that a single bipolar cell will never receive input from both rods and cones (Masland, 2001). The number of cone-driven bipolar cells outnumber that of rod-driven cells. Approximately 9-11 varieties of cone-driven bipolar cells have been identified in mammals, most likely due to the fact that more rods converge to a single bipolar cell whereas many single cones converge to a single bipolar cell although there are also bipolar cells that connect many cones to ganglion cells (Snell and Lemp 1998; Masland, 2001).

1.3.3 Ganglion cells

Ganglion cells are neuronal cells that form synapses with bipolar and amacrine cells within the retina. Amacrine cells are excited by bipolar cells which in turn excite ganglion cells. Ganglion cells have long axons which extend to form the optic nerve leading to the brain. They are involved in transporting information from photoreceptors to the brain. Largely, a single layer of ganglion cells occupy the retina but the layers increase from the periphery of the retina to the macula (Snell and Lemp 1998). Up to 10 layers can be found to be present in areas containing multi-layered ganglion cells, decreasing towards the fovea (Snell and Lemp 1998).

From what has been discussed, it is easy to see why diseases causing damage or degeneration to components such as photoreceptors in the retina can have detrimental effects on vision. The importance of the role of photoreceptors in producing visual images can also be appreciated.

1.4 Photoreceptor Dystrophies

Photoreceptors are light sensing cells located in the outer nuclear layer (ONL) of the retina. These cells absorb light and transform these into electrical signals, the process known as phototransduction. This process makes up the initial stage of the visual cycle. These signals are then transported and interpreted by the brain to produce a visual image.

There are two types of photoreceptors: rods, involved in phototransduction in dim light and cone which are involved in phototransduction of colour vision. The healthy function of both types of photoreceptors is key for normal vision.

There are many devastating ocular disease which can grossly effect visual clarity and often result in blindness. Some of these include age-related macular degeneration (AMD), retinitis pigmentosa (RP) and cone-rod dystrophy (CRD) (Nag and Wadhwa, 2012).

AMD is a disease affecting the choroid and RPE, the photoreceptor support system. Lesions form on the choroid and ingrowth of vessels in the choroid can lead to visual impairment (Nag and Wadhwa 2012). The choroid is the layer located between the

retina and the sclera and provides oxygen and other nutrients to the retina for its maintenance. RP and CRD affect the function of photoreceptors directly.

Of the photoreceptor dystrophies mentioned above, RP is the more prevalent of ocular diseases and is discussed in further detail in the following chapter.

1.5 Retinitis Pigmentosa

Pigmentary retinopathies are a classification of ocular diseases as a result of the loss of photoreceptors and retinal pigmented deposits. This is also the classification under which retinitis pigmentosa (RP) appears. In contrast to some other ocular diseases, RP is both genetically and clinically heterogenetic. It has also become the most common subtype of retinal degeneration related diseases in the world, with 1 in 4000 individuals being affected (Petra-Silva and Linden, 2013). A defect in any one of over 60 genes can result in RP which can be inherited (Petra-Silva and Linden, 2013). Characteristic to RP, alterations occur in the retinal pigmented epithelium resulting in the deposits of pigments (Anasagasti *et al.,* 2012). These pigments are predominantly deposited in the peripheral retina often with initial degeneration of rod photoreceptors followed by the secondary degeneration of cones (Hamel, 2006). In light of this, it is no surprise that sufferers often experience the loss of night vision initially, eventually leading to visual impairment and often blindness with progression of the disease. The disease progression evolves over several decades (Hamel, 2006). In some cases the cone function is lost first, leading to the loss of central vision (Petra-Silva and Linden, 2013).

All RP are progressive but the rate of deterioration varies greatly. Even in the case of the same gene mutation resulting in RP can still result in varied symptoms which can also be affected by the environment (Petra-Silva and Linden, 2013). There are two forms of RP that exist: syndromic and non-syndromic.

1.5.1 Non syndromic RP

Non-syndromic RP is inherited in most cases and is the term given to RP where only the eye is affected with no other non-ocular diseases are associated (Anasagasti *et al.*, 2012). In rare cases, RP can also be caused due to mutations in mitochondrial DNA (Mansergh *et al.*, 1999). The course of RP can easily be divided into 3 stages: early, mid and late. Diagnosis of RP during early stages of the disease is difficult. This is because night blindness is often the main symptom of the disease with minimal or no defects during day light. For this reason it is often ignored by sufferers (Figure 1.8 B). Additionally, fundus examination may appear as normal as deposits are rarely present (Hamel 2006). A key test is that of the electroretinogram (ERG) which can expose the presence of the disease by the characteristic decrease in the b-wave amplitude. It must be noted however, that the ERG may seem normal although the retina is partially affected (Hamel 2006).

By the mid stage of the disease symptoms are clearly obvious with night blindness and loss of peripheral vision during day light. Sufferers may become photophobic and also suffer a decrease in visual accuracy; pigmented deposits also become clearly evident in fundus examinations by this stage of the disease (Figure 1.8 C). Additionally, the optic disc may appear pale with a narrowing of retinal vessels (Hamel, 2006).

At this stage of the disease the ERG is often not recordable with flickering responses and various yearly assessments are mandatory in order to keep records of the progression of the disease (Hamel, 2006).

By the end stage of the disease, patients lose all autonomous movement due to loss of peripheral vision often termed tunnel vision (Figure 1.9B). Reading remains extremely difficult without the aid of magnification glasses and photophobia becomes more intense. Fundus examinations exhibit widespread pigmented deposits spreading as far as the macular (Figure 1.8 D) and retinal vessels become more narrow with the optic disc becoming even more pale (Hamel, 2006). Disease progression at this stage is still slow, with patients able to read short passages for several years although unable to move. This is only lost once central visual fields also become affected and lost (Hamel, 2006).

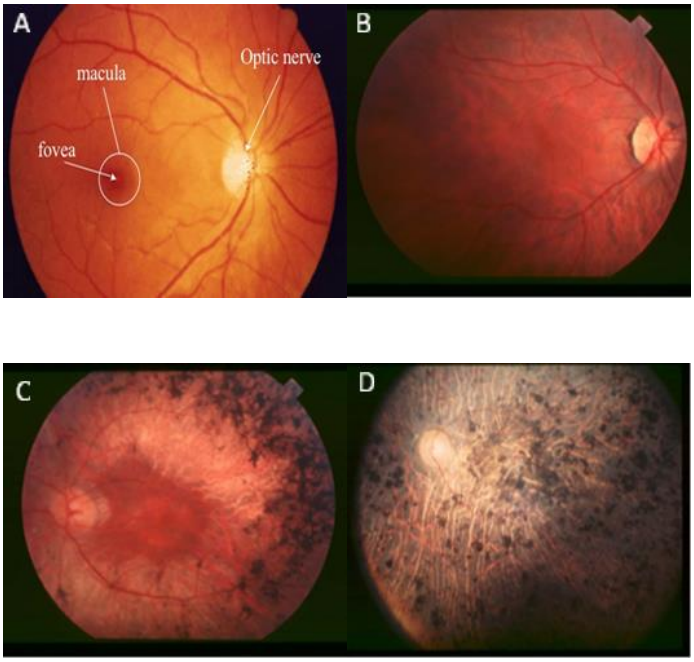

Figure 1.8: Images of the fundus. (A) Image of fundus from an individual with normal vision. (B)Fundus image of early stage retinitis pigmentosa (RP) patient. (C) Image of fundus from mid stage RP patient. (D) Fundus image from end stage RP sufferer. Retrieved from (Hamel 2006).

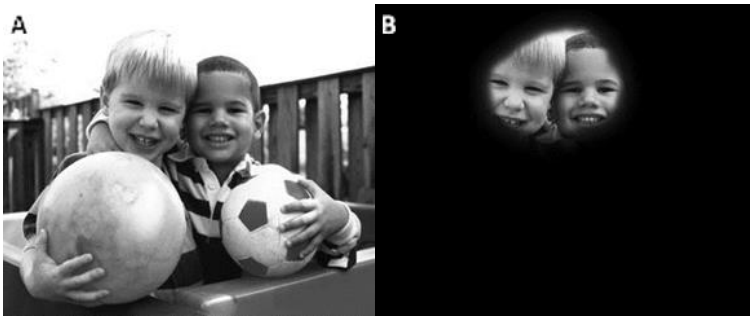

Figure 1.9: Visionary field. (A) Normal visionary field. (B) RP visionary field. Retrieved from (http://www.retinitis-pigmentosa.com.au/ 2009).

The inheritance of RP can be divided into three groups: autosomal dominant, autosomal recessive and X-linked.

1.5.1.1 Autosomal Dominant RP

Autosomal dominant RP is generally the least severe of RPs with the onset of the disease generally seen later and it also maintains fairly good vision (Chang *et al.*,2011). Approximately 30-40% of RP is autosomal dominant RP (http://www.patient.co.uk/doctor/retinitis-pigmentosa). There are three main genes where mutations can result in autosomal dominant RP, and these are: rhodopsin (Rho), oxygen-related proteins (RP1) and peripherin (RDS) (Chang *et al.*,2011).

Rhodopsin is a photo-pigment found in rod photoreceptors and is involved in the absorption of light and is responsible for phototransduction (Chang *et al.*,2011). This transmembrane makes up 85% of the total protein content in rods and with rods being made up with three domains, mutations have been identified in all three domain (Chang *et al.*,2011).

As the name suggests, RP1 is regulated by oxygen levels in the retina and has been found to play an important role in the correct stacking of photoreceptor outer segments (Chang *et al.*,2011). Over 50 mutations that cause the disease have been identified in this gene and most commonly in those suffering from dominant RP these mutations are usually a frameshift or nonsense mutations in a region located on the exon 4 of this gene (Siemiatkowska *et al.*,2012).

Peripherin is found abundantly in the outer segments of photoreceptors and is extremely important in maintaining the structure and stability of photoreceptors (Chang *et al.*,2011).

1.5.1.2 Autosomal Recessive RP

Autosomal recessive RP is one of the most common inherited forms of the disease although associated genes are very rare. This disease often has an early onset of the disease with more severe symptoms (Chang *et al.*,2011). Approximately 50%-60% of suffers of RP are affected by this type (Patient.co.uk). The most common gene mutations that result in the disease include: ABCA4, RPE65, PDE6A and PDE6B, and USH2A amongst others that are common to other ocular disease (Chang *et al.*,2011).

ABCA4 is a photoreceptor specific ATP-binding cassette transporter gene. This protein is found in the outer segments of photoreceptors and is responsible for the breakdown of N-retinylidene-PE into vitamin A which is involved in the visual process (Chang *et al.*,2011). This mutation has also been found to be present in other ocular disease including age related macular dystrophy and cone rod dystrophies to name a few (Chang *et al.*,2011).

RPE65 is also involved in the breaking down of retinoids, mutation in which results in the disease. Both PDE6a and PDE 6b play important roles in the rod photoreceptor visual transduction cascade and hold vital roles in the correct function and maintenance of photoreceptors (Sakamoto *et al.,* 2009).

USH2A is found in two isoforms in the body; a short and long form, the latter of which is predominantly found in the retina (Mèndez-Vidal *et al., 2013).* This gene produces multidomained proteins called usherins which are involved in the delivery of substituents from the inner segments of photoreceptors to the outer segment. Thus they play important roles in the maintenance of photoreceptors (Mèndez-Vidal *et al., 2013).*

1.5.1.3 X-linked RP

X-linked RP causes the most severe forms of the disease with an early onset and also fast disease progression (Chang *et al.,* 2011). This has also been found to account for 6%-20% of RP (Petrs-Silva & Linden, 2013). This disease affects males more severely than females, caused by a random X-inactivation (Chang *et al.,* 2011). Mutations in two genes: RPGR/RP3 and RP2 have been found to be responsible for the majority of X-linked RP (Chang *et al.,* 2011).

The protein produced by the gene RP3 is imminent for cell viability and is localised in the base of photoreceptors and cilia bodies. This protein also possibly plays important roles in protein transportation and organisation of microtubules (Petrs-Silva & Linden, 2013). Almost 70% of X-linked RP is caused by a mutation in this gene (Petrs-Silva & Linden, 2013).

It is very clear that in the majority of cases, RP is caused by the failure of vital components to function as normal. This occurs either in photoreceptors or supporting components which in some way affect the normal functioning of photoreceptors.

Currently there is no cure for RP and existing treatment only aid in preserving what little vision is left using visionary aids. Some treatments aim at treating various symptoms of RP such as photophobia, by reducing the effect of photophobia. Other treatments include the supply of antioxidants such as vitamin A and E to protect and prolong the life of existing photoreceptors, although studies have shown that the supply of vitamin A may not be suitable for sufferers of RP due to specific mutations (Mansergh et al. 1999).

1.5.2 Syndromic Retinitis Pigmentosa

Syndromic RP refers to a number of other syndromes that have been associated with retinopathies. This chapter only discusses the two most common syndromes associated with RP: Usher syndrome (USH) and Bardet Biedl syndrome (BBS).

1.5.2.1 Usher syndrome

This syndrome is characterised by retinitis pigmentosa, loss of hearing and in some cases vestibular dysfunction and is often a disease that is inherited in an autosomal recessive manner (Ferrari *et al.,* 2011). This syndrome is the most common syndrome affecting deaf-blind individuals and accounts for approximately 50% of these individuals (Ferrari *et al.,* 2011). Approximately 10%-30% of all cases of autosomal recessive RP are sufferes of Usher syndrome (Ferrari *et al.,* 2011).

This syndrome can be divided into three categories with the severity of deafness defined by the syndrome type. Type 1 (USH1) is profound and thus the most severe of the three types. In USH1 the onset of RP is pre-pubertal (Ferrari *et al.,* 2011). Type 2 (USH2) is mild or moderate in comparison with USH1 with a later onset of RP progression (Ferrari *et al.,* 2011). In type 3 (USH3), deafness can occur within the first decade worsening with disease progression (Boughman *et al.,* 1983; Hamel 2006). The onset of RP is also variable in this type of the sydrome (Ferrari *et al.,* 2011).

Unfortunately, there is no treatment available to cure this syndrome. Detection for the syndrome has been greatly aided by the discovery of mutations of specific genes associated with the disease. Currently five genes have been identified to be associated with USH1 and three associated with USH2 (Ferrari *et al.,* 2011). In the case of USH3, this is a very rare form of the disease, with the prevalence seen only in certain populations (namely Finns and Ashkenazi Jews) (Ferrari *et al.,* 2011).

1.5.2.2 Bardet Biedl syndrome (BBS)

Bardet Biedl syndrome (BBS) is less frequent than usher syndrome, affecting 1 in 150,000 people (Hamel 2006). Similar to Usher syndrome, this is another syndrome that is inherited in an autosomal recessive manner (Ferrari *et al.,* 2011). Characteristics of this syndrome include child obesity, mental retardation or mild psychomotor delay and renal abnormalities leading to renal failure amongst sufferers (Hamel 2006). A major cause of morbidity and mortality in this syndrome has been a result of renal failure (Ferrari *et al.,* 2011).

Although sufferers of this syndrome are usually born with a normal birth weight, a continuous substantial weight gain is often observed within the first year; this then later becomes a fighting battle throughout adult life (Ferrari *et al.,* 2011). Night blindness in many sufferers is usually observed by the age of seven, with blindness often diagnosed by the age of 15 (Ferrari *et al.,* 2011).

Some population have a higher incidence of this syndrome than others, such as some population of Newfoundland where 1 in 13000 is affected. A total of 14 genes have been associated with BBS which again is useful for diagnosis purposes although

approximately 20% of sufferers have gene mutation that have not yet been identified (Ferrari *et al.*, 2011). Again, as of yet, there is no current cure for sufferers of BBS.

1.6 Potential Treatment for retinal dystrophies

1.6.1 Gene Therapy

Gene therapy is currently the most promising treatments for many ocular diseases. In a short summary, this form of therapy involves the transportation of normal genes into an area of mutated genes causing disease to correct the disease. This type of therapy often requires the use of retroviral vectors for the transplantation stage. These then infect cells of the patient to correct the mutation and thus aid in treatment of the disease.

One of the most popular types of vectors to transport genes into ocular cells is the recombinant adenoassociated virus (rAAV) (Petrs-Silva and Linden, 2013). The AAV vector is relatively smaller in size in comparison to other available vectors and thus holds a great advantage in that it is capable of tranducing to a range of retinal cells, both dividing and single cells (Petrs-Silva and Linden, 2013).

One ocular disease which has had success in clinical trials via gene therapy is the treatment of Leber's congenital amaurosis (LCA). LCA is one of the most severe forms of inherited ocular diseases with severe loss of vision detected at early infancy and childhood. Although the disease can be caused as a result of mutations in any one of 13 genes, a mutation in the retinal pigment epithelium (RPE65) causes approximately 6% of all cases of LCA (Maguire *et al.*, 2009).

Maguire and his group carried out phase 1 clinical trials for the treatment of LCA. In this investigation 12 sufferers of various ages were injected with the recombinant vector (AAV2-hRPE65v2) containing the sequence of a normal RPE65 gene in the subretinal space. Three doses of low, medium and high were administered to patient. The AAV2-hRPE65v2 vector was well tolerated by all patients with increased visual acuity observed in children and benefits of the trial was sustained at the 2 year follow-up

investigation. The study also found that the high dosage of the vector ($1.5x10^{11}$) may be edging towards the limit of toxicity and thus will be omitted in following investigations.

This provides great hope for young suffers as the greatest level of benefits were observed in children.

1.6.2 Cell Therapy

As the name suggests, cell replacement therapy is the transport of healthy cells into an organ in order to restore functionality of deteriorated or damaged cells. This type of treatment is especially convenient for treating photoreceptors dystrophies as the intraocular space is in fact immunoprivilaged. As the subretinal space has also been found to hold this property, it is immediately protected by the harmful effects of immunological inflammatory responses which can lead to blindness (Masli & Vega, 2011).

For this type of treatment to become successful, this requires initially the transplanted cells to survive in the retina and then become integrated as part of the ONL of the host retina where it can then form synaptic connections for transmission.

Carr *et al.,* 2009 readily differentiated iPS cells from human foetal lung fibroblast cells and differentiated these cells into RPE cells. The iPS-RPE was then injected into the subretinal space of 22-23 day old dystrophic rats. The disease progression in untreated rats is such that the ONL is usually diminished along with the reduction in the photoreceptor outer segment layer.

Transplantation however, found that 13 weeks post-transplantation the structure of the retinal was well preserved with a significant increase in visual acuity. This provided great potential for the treatment of AMD.

A partnership between UCL and Pfizer has now been formed. This partnership has been approved to begin phase 1 clinical trials for the treatment of wet AMD in March 2014. In this trial patients over 60 years of age, suffering with wet AMD, whereby the blood vessels are affected in the retina resulting in a rapid progression of AMD are to be investigated. The trial will involve the transplantation of hESCs derived RPE cells, which will be immobilised on a polyester membrane, into the eye

(http://clinicaltrials.gov). If successful, this will provide a cure for sufferers as the procedure is intended to be life-long.

Current times are extremely exciting times in terms of the development of therapies for some retinal dystrophies, although there are far more ocular diseases where no treatment is currently available, like for example RP. It is clear that for some ocular diseases such as RP, the way forward would be to develop a means by which target cells such as photoreceptors could be delivered in a safe, secure and permanent manner. The possibility of using hESCs to reach this target definitely holds great potential.

1.7 Stem cells

During early stages of mammalian embryo development cells are capable of existing in an undifferentiated state for an indefinite period of time. They also have the capability of differentiating into various cell types of the 3 germ layers: (i) endoderm, (ii) mesoderm or (iii) ectoderm, a term commonly defined as **pluripotency**. These early developmental cell types are what became known as **stem cells**.

1.7.1 The Discovery

Using mouse-derived cells Thomson and his group defined that for a cell to be defined as a stem cell, it must exhibit the following characteristics: (i) it must be derived from a peri-implantated or pre-implanted embryo, (ii) it must be able to proliferate in an undifferentiated state for a prolonged period and (iii) that it must demonstrate potential to form derivatives of all three germ layers, and only then can a cell be defined as a stem cell (Thomson *et al.*, 1998).

Using donated fresh/frozen cleavage stage embryos intended for use in, *in vitro* fertilization,embryos were cultured into a blastocyst stage. Thomson and his group (1998) then isolated 14 inner cell masses from the blastocyst and they obtained 5 embryos from which 5 stem cell lines (H1, H13, H14, H7 and H9) were derived. These cell lines produced characteristic morphology to stem cells such as, a high nucleus to cytoplasm ratio, prominent nucleoli and colony morphology to stem cells (Figure 1.10).

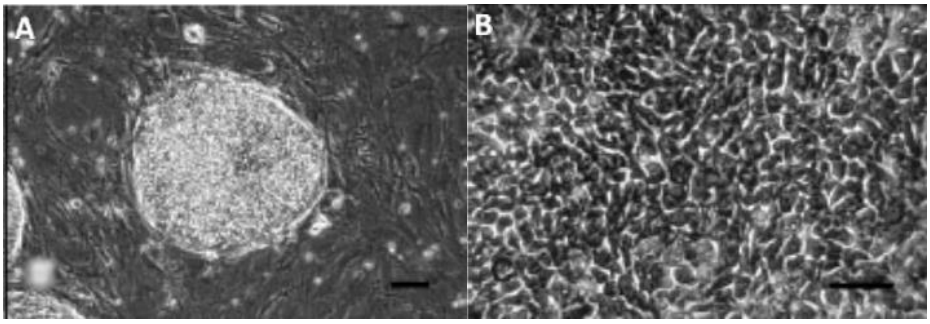

Figure 1.10: Derived H9 cell. (A) H9 colony, scale bar 100µm. (B) H9 colony , scale bar 50 µm. Modified from Thomson et al. (1998)

Of the five cell lines derived by Thomson and his group (1998), 4 cell lines were stably cultured in an undifferentiated state for 5-6 months before being cryopreserved. The last cell line, H9 was stably cultured for 8 months (32 passages) in an undifferentiated state, fulfilling the second characteristic of a stem cell discussed earlier.

When telomerase activity was investigated by this group, it was found that all cell lines exhibited high telomerase activity. Telomerase is an enzyme that functions to add G-rich repetitive sequences to the ends to chromosomes (Yang *et al.,* 2008). This action protects the chromosomes from degradation and end-to-end fusion (Yang *et al.,* 2008). The activity of telomerase to maintain telomere length has readily been associated with cell immortality in cancer cells, germ line cells and embryonic stem cells (Hiyama and Hiyama 2007).

Given the infinite, undifferentiated, proliferative nature of stem cells, it would be rational to assume that stem cells must have some way of maintaining telomere length. They therefore must express telomerase highly in order to be capable of proliferating (undifferentiated) infinitely. The fact that high telomerase activity was recorded in all 5 cell lines isolated by Thomson *et al.,* 1998 is further evidence that these cell lines were in fact stem cells.

It is however also important to note that other studies have found low expression of telomerase activity in human stem cells (Hiyama and Hiyama 2007). An up regulation of telomerase acitivity has also been observed in cells which rapidly expand, such as committed haematopoietic progenitor cells (Hiyama and Hiyama 2007). In the case of cells isolated by Thomson however, these cells are embryonic stem cells and not adult

stem cells and therefore these finding are in line with other research into telomerase activity in stem cells.

After being injected to severe combined immunodeficient (SCID) mice, all cell lines produced teratomas of all three germ layers (Figure 1.11), exhibiting the third property of a stem cell, although only images for three of the cell lines are shown.

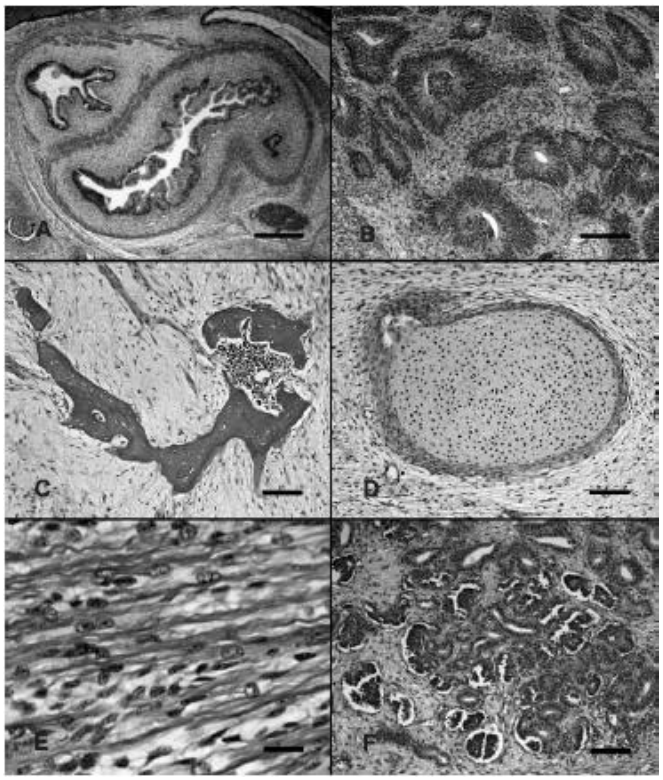

Figure 1.11: Teratomas formed by human ES cell lines after injection onto 4 week old SCID mice. (A) Gut-like structures from H9 cell line. Scale bar, 400mm. (B) Rosettes of neural epithelium from H14 cell line. Scale bar, 200mm. (C) Bone from H1 cell line. Scale bar, 100mm. (D) Cartilage from H9 cell line. Scale bar, 100mm. (E) Striated muscle from H13 cell line. Scale bar, 25mm. (F) Tubules interspersed with structures resembling foetal glomeruli from H9 cell line. Scale bar, 100mm. Image retrieved from Thomson et al., 1998.

Stage-specific embryonic antigen 3 (SSEA3), stage-specific embryonic antigen 4 (SSEA4), TRA160 and TRA181 are all markers of pluripotency originally developed from human embryonic carcinoma cells. These markers are also recognised in human embryonic stem (hESCs) cells, which were shown to be present in all cells isolated by Thompson and his group (1998). This provided even further evidence for the nature of these derived cells.

It is important to note that conflicting research emerged, suggesting SSEA3 and 4 were invalid markers for pluripotency as it was not essential (Brimble *et al.*, 2007). The international stem cell initiative, which compared characteristics of 59 hESCs cell derived from 17 laboratories worldwide found that in fact the expression of these antigens were valuable markers of pluripotency in hESCs (Adewumi *et al.*, 2007).

The cells isolated by Thomson and his group in 1998 clearly fulfilled all the defined characteristics of stem cells with ample evidence. This protocol has since been widely used to isolate many more stem cell lines through the years of stem cell history. A list of current stem cells approved by the National Institutes for Health (NIH) can be found on their website (http://grants.nih.gov/stem_cells/registry/current.htm).

1.7.2 Human Embryonic Stem Cells (hESCs) and Mouse Stem cells

Although mouse models provide a reliable source for medical research in the field of stem cell research it has been found that mouse development is considerably different to human development. One such difference is the timing of gene expression in developing embryos.

An investigation was carried out by Braude *et al.*, 1988, where human pre-embryos were inseminated and gene expression analysed at various time points. This investigation found that unlike mouse gene expression which was known to be detected in the mid two-cell-stage of development, in human development gene expression was not detected until between the four-cell and eight-cell stage (Braude *et al.*, 1988). In the case of hESCs, as discussed earlier, there are also major differences in surface makers. Stage-specific antigens 3 (SSEA3) and 4 (SSEA4), glycoproteins TRA-1-60 and TRA-1-81 and GCTM2 are not detected in mouse stem cells while they are readily detected in human stem cells (hESCs) (Thomson *et al.*, 1998; Reubinoff and Pera *et al.*, 2000).

In the case of mouse stem cells, surface marker Stage-specific antigen 1(SSEA1) is readily detected as a marker for pluripotency but remains undetected in human stem cells (Solter and Knowles, 1978).

Major differences in the culture methods between mouse and hESCs also exist. The primary difference being that in order to maintain hESCs in a state of pluripotency, a feeder layer of mouse embryonic fibroblasts (MEF) is required. MEFs are known as "feeder cells" and provide hESCs with important growth factors, which still remain unknown, and play important roles in the maintenance of pluripotency in culture.

The introduction of animal cells however raises many safety concerns especially in terms of cross-contamination for intended clinical use. The use of MEFs in culture systems introduces potential non-human pathogens which could then be transfer into human if the same hESCs are used in a clinical environment. The introduction of non-human pathogens in humans could have devastating effects on the health of patients. Additionally, non-human pathogens can evoke immune responses in recipients and thus alter hESCs therapeutic capacities (Kibschull *et al.,* 2011). For these reasons, all animal constituents are used with caution in research, especially when intended for use in therapy.

For this reason MEFs are best avoided when investigating hESCs for the purpose of regenerative medicine increasingly so at the point of clinical trials. In order to avoid issues of contamination, technology has since evolved from the original procedure of hESCs culture. Currently many commercial products are available which mimic the role of MEFs using a range of extracellular matrices (ECMs) without the introduction of animal counterparts.

One such product is Matrigel (BD Biosciences) for example, containing components such as collagen IV, laminin, heparin sulphate proteoglycans and entactin, amongst others, are now available to overcome this issue of cross contamination (Thomson *et al.,* 1998; Loring *et al.,* 2007).

Using such products to culture hESCs is termed a "feeder-free" culture system. In the past the transition from a feeder culture system to a feeder-free culture system was a gradual process but with time this has also become a fairly easy process (Loring *et al.,* 2007). Cells are now almost instantaneously changed between the two culture systems

Unlike hESCs, mouse stem cells do not require co-culturing with a feeder layer and can be easily be maintained in the same manner as normal mammalian cell culture (Loring *et al.,* 2007).

In mouse stem cell (ES) culture, Leukaemia inhibitory factor (LIF), a cytokine from the interleukin family (IL-6) is required for the proliferation of mouse ES (Burdon *et al.*, 2002; Conley *et al.*, 2004). LIF has been found to block differentiation in mouse ES by stabilising the LIF receptor (LIFR) and gp130 cytokine receptor heterodimer complex. This results in the activation of the Janus-associated tyrosine kinases (JAK) / signal transducer and activator of transcription (STAT3) cascade resulting in the translocation of STAT3 into the nucleus (Burdon *et al.*, 2002; Conley *et al.*, 2004). In the nucleus STAT3 binds onto essential ES self-renewal locations on the DNA (Figure 1.12) (Burdon *et al.*, 2002; Conley *et al.*, 2004).

In the case of hESCs however, the presence of LIF seems to have no effect in sustaining the cells in an undifferentiated state. Research has shown that differentiation takes place both in the presence and absence of LIF in hESCs (Thomson *et al.*, 1998).

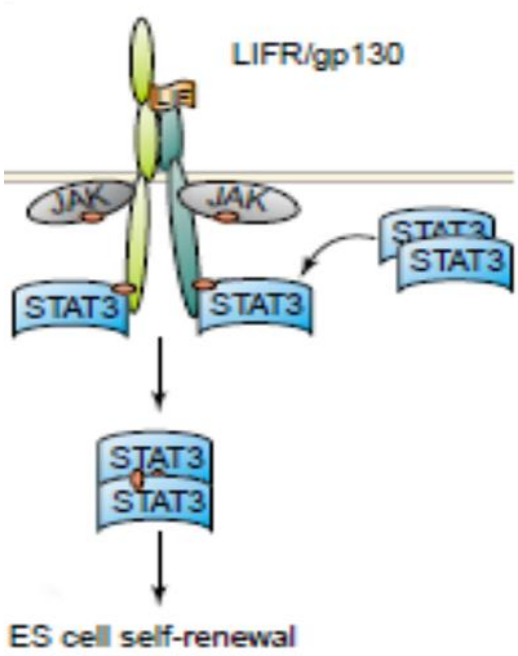

Figure 1.12: LIF-dependent activation of STAT3 blocks ES cell differentiation and promotes self-renewal. Leukaemia inhibitory factor (LIF) stabilizes the association of LIFR and gp130 cytokine receptors activating JAK kinases, causes the recruitment, tyrosine phosphorylation and dimerization of STAT3 resulting in the translocation of STAT3 into regions of the DNA in the nucleus to important controls of self-renewal transcriptional genes. Image modified from (Burdon, Smith et al. 2002).

1.7.3 Adult Stem Cells

Pluripotent stem cells exist in adults in various tissues and organs. These cells are known as adult stem cells (ASCs) or somatic stem cells. The purpose of these cells is to repair and maintain damaged cells or tissue in organs through the lifetime of the organism. These cells lie in a state of activity or quiescence within their location until they are required to repair or maintain damaged cells (Li & Clevers, 2010; Maguire & Friedman, 2014). ASCs have been found in various locations in the body, with the list of locations increasing with research; some of these locations include (but is not by any means exclusive): hair, bone marrow, gut, skeletal muscle and the brain (Li &Clevers., 2010).

When damage has occurred in the body, there are many stem cell types which migrate to initiate a healing response (Maguire & Friedman, 2014). ASCs migrate from various locations in the body and release a pool of stem cell released molecules (SRM) at the site of damage (Maguire & Friedman, 2014). These SRMs are specific to some degree to each stem cell type with some level of overlap between pools released (Figure 1.13) (Maguire & Friedman, 2014).

These pools of SRM are made up of a range of molecules including (but not exclusive): cytokines, growth factors, chaperone molecules, microRNA and antioxidants (Maguire & Friedman, 2014). All these molecules are collectively referred to as SRMs. When two pools of SRMs are released from two different ASCs they are referred to as S^2RM (Maguire & Friedman, 2014). As is obvious, all these molecules play important roles in the healing and maintenance process of cells.

Studies have found that although ASCs are extensively capable of repair and maintenance of damaged tissue, the mere transplantation of ASCs from a young adult into an older adult may not reach optimal results regarding tissue regeneration and age-related conditions (Maguire & Friedman, 2014). This is because stem cells must come from similar stem cell niches in order to keep their optimal regenerative properties (Maguire & Friedman, 2014).

Other studies have found that the life style of an individual can have an important impact on the health of ASCs in the body as this can have an impact on the telomerase activity (Maguire & Friedman, 2014). Some research has shown that exercise, low

calorie intake and low stress could all contribute to extending the life span of ASCs or increase the lifespan of stem cell renewal activity (Maguire & Friedman, 2014).

Initially it was thought that ASCs were multipotent cells. The term 'multipotent' refers to the capability of cells to specialise into a limited number of cells that are closely related. This idea however, has since changed with various researches exhibiting the differentiation of ASCs into various specialised cells generated from both the same embryonic germ layer as well as different germ layers (Mundra et al, 2013). Differentiation is still however, restricted in terms of lineage in comparison to embryonic stem cells (Mundra et al, 2013).

This capability of ASCs to differentiate into other specialised cells of other embryonic germ layers is referred to as "transdifferentiation". These findings have opened new doors for the potential exploitation of ASCs in the clinical environment. The added advantage of ASCs for use in therapy is that, unlike embryonic stem cells (ESCs), ASCs do not form teratomas in the body and thus holds great potential in regenerative medicine.

One example of ASCs that has received tremendous amounts of attention is a type of ASCs derived from bone marrow. There are two types of ASCs found in the bone marrow: Mesenchymal stem cells (MSCs) and Hematopoietic stem cells (HSCs) (Mundra et al, 2013).

MSCs were discovered by Friedenstein and his colleagues over 40 years ago. This group found that a small population of cells resident in the bone marrow were adherent to tissue culture surfaces and were capable of differentiating into osteoblasts, chondrocytes, and adipocytes- cells of the mesoderm germ layer (Prockop *et al.,* 2003). Following the discovery of MSCs, a number of other investigations have shown the differentiation of MSCs into muscle cells, neural cells as well and cardiomyocytes (Prockop *et al.,* 2003). Such investigations showed that MSCs were in fact, capable of differentiating into specialised cells from other germ layers other than that of their own. This factor had therefore caused interest in MSCs for use in therapy for many diseases.

One disease of particular interest is type 1 diabetes (T1D). T1D is an autoimmune disease whereby insulin-producing pancreatic β cells are identified and destroyed by an

autoreactive immune system. This complicates the treatment and therapy for sufferers of this disease.

Current methods of treatment for T1D only provides short term treatment as it focuses on raising antibodies against T cells (Wu & Mahato., 2014). The complication of this treatment is that antibodies are unable to differentiate between autoreactive T cells and those that are required for the healthy maintenance of the immune system (Wu & Mahato., 2014). This, for obvious reasons causes many complications, as the treatment results in the depletion of healthy T cells that are required for the maintenance of a healthy immune system.

The advantage of MSCs is that they are hypoimmunogenic, due to the lack of specific surface markers and additionally are attracted to injured mesenchymal tissue for repair (Wu & Mahato., 2014). At the target location, they can then transport soluble proteins to autoreactive T cells more specifically rather than affecting the whole immune system as a whole (Wu & Mahato., 2014).

One group has been successful in injecting bone marrow stem cells (BMSCs) into the liver into order to reduce levels of anti- islet cell antibodies (ICA) and anti- glutamic acid decarboxylase antibodies (GAD); two important antibodies the presence of which has been detected in approximately 90% of cases of T1D (Wu & Mahato., 2014; Mesples *et al.,* 2013). In this clinical study, 2 patients were treated with autologous BMSC transplantation through the liver with one patient being treated using conventional treatment and thus acted as the control subject. It was found that, 12 months after the treatment, those patients treated with the BMSCs had a significant reduction in anti-ICA and anti-GAD levels. Results from this study provided great potential for the use of MSCs for an easy and effective treatment for T1D.

The ease of which ASCs can be harvested gives good potential for the use of these cells in a clinical environment. Especially in terms of yield and cost as a small sample could easily be harvested and then potentially be expanded for use for treatment.

Potentially, ASCs from patients needing treatment could be harvested from their own body; differentiated into specialised cells and transplanted back into the patient- a term referred to as “autologous transplantation”. This has the advantage of ruling out almost

all autoimmune reactivity that may be associated with this type of treatment, as the patient's immune system is unlikely to reject cells from its own body.

The disadvantage of these types of stem cells is however that the differentiation potential is somewhat still limited in comparison to other stem cell types. Additionally, the extent to the capability of these cells to differentiate into other functionally mature cells of other embryonic germ layers is yet to be understood. More research is still required before these cells can comfortably be brought from the bench to the bedside as many safety issues still remain unanswered. Furthermore, the potential of the use of APSCs would be greatly increased once issues concerning environmental niches surrounding these cells have been resolved. This could open new doors to the concept of donors which would have a significantly, positive effect in terms of cell therapy and regenerative medicine.

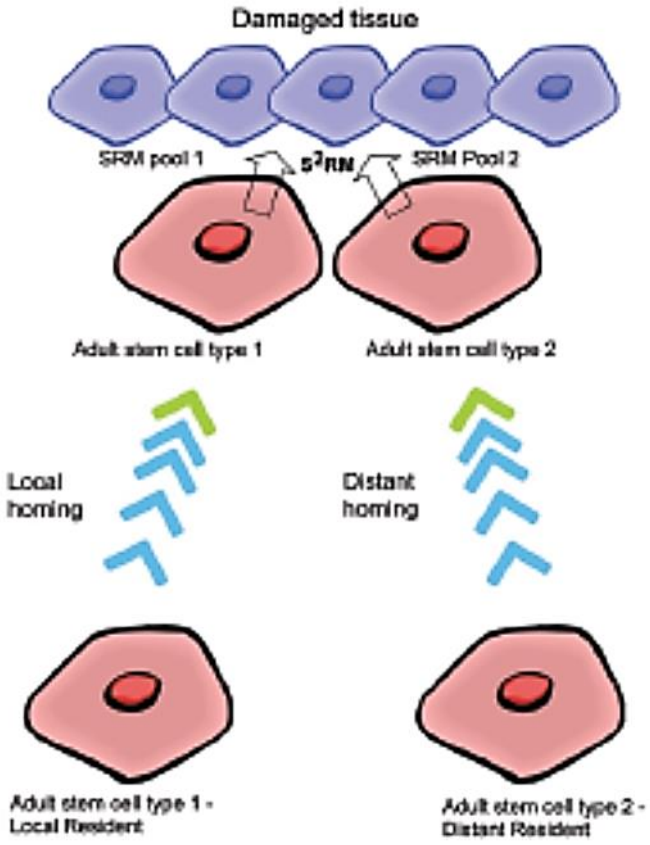

Figure 1.13: A diagram of adult stem cell (ASC) healing response to damage. The image was taken from Maguire & Friedman., 2014.

1.7.4 Induced Pluripotent Stem Cells

In 2006, Takahashi and Yamanaka showed that by exposing somatic cells to transcription factors Oct3/4, Sox2 as well as tumour-related factors c-Myc and Klf4, the differentiation commitment could be reprogrammed to produce cells with a pluripotent nature. These cells were named induced pluripotent stem cells (iPSC). Initially a panel of 24 genes that played important roles in maintaining pluripotency was transfected into MEF cells using a retrovirus. Other investigations have used other delivery systems using adenoviruses to avoid potential introductions of mutations, but with a significant decrease in yield (Stadtfeld *et al.,* 2008). These cells were then exposed to a combination of factors Oct3/4, Sox2, c-Myc and Klf4. By culturing cells in ES conditions, somatic cells were reprogrammed to become cells resembling those in an embryonic state (Figure 1.14). Further research has found that other combinations can be used to substitute c-Myc and Klf4 to produce both mouse and human iPSCs (Nishikawa *et al.,* 2008).

The method of creating iPSCs since its origin has become a robust and practically straight forward process. The major advantage of this process is that it takes away the ethical issues surrounding the use of original stem cells, as these involve invasive methods of cell collection from the inner cell mass of a blastocyst of a pre-implanted embryo. It also opens up great potential for regenerative therapy and customised therapy. This is because this technology has potential to de-differentiate cells from a patient and to re-direct differentiation of these cells to replace degenerate cells from the same patient, overriding many difficulties facing autoimmune rejection.

iPSCs could also provide vast information on disease pathways at a cellular level which could be used to gain a better understanding of some diseases providing great human models for research purposes. For example, cancer is an extremely prevalent disease many types for which, a lack of understanding stands in the way of treatment. It is well known that along with many other factors, epigenetic programming plays an important role in cancer formation (Nishikawa *et al.,* 2008).

By de-differentiating cancerous cells and allowing cancer derived iPSCs to form cells of its original state, a better understanding of the epigenetic changes that take place in the progression of cancer could be gained. This could aid immensely in the treatment of many cancers.

An example of the use of iPSCs is a proof of concept study carried out in 2007, by Hanna and her group, for a mouse model for sickle-cell anaemia (Tahashi & Yamanaka, 2013). This study involved the harvest of mouse fibroblasts from a humanised sickle cell anaemic mouse, which were then de-differentiated to create iPSCs. The genetic mutation causing β sickle cell anaemia was then corrected and the cells were then differentiated into haematopoietic progenitor cells and transplanted back into the mouse (Hanna *et al.,* 2007).

Such investigations provide great scope for potential therapy but in more realistic terms such customised approaches will be extremely costly. In addition to this, if only cells from the patient is used in this technology for treatment of disease, it could be very time consuming, which for some diseases such as spinal cord injury will not be a feasible approach in terms of treatment regimes.

Another advantage of these cells is that because they can be produced from any human cells. Any side effects caused from specific drugs or even the lack of effectiveness could be well investigated using these iPSCs and thus has potential to provide an essential tool in monitoring drug safety in drugs that are already on the market (Nishikawa *et al.,* 2008).

Whilst hurdles are still to be overcome in terms of use in therapy, iPSCs could also be an important tool to gain vital information concerning the progression of diseases. This may in turn aid profusely in the develop treatment for diseases where little is still known.

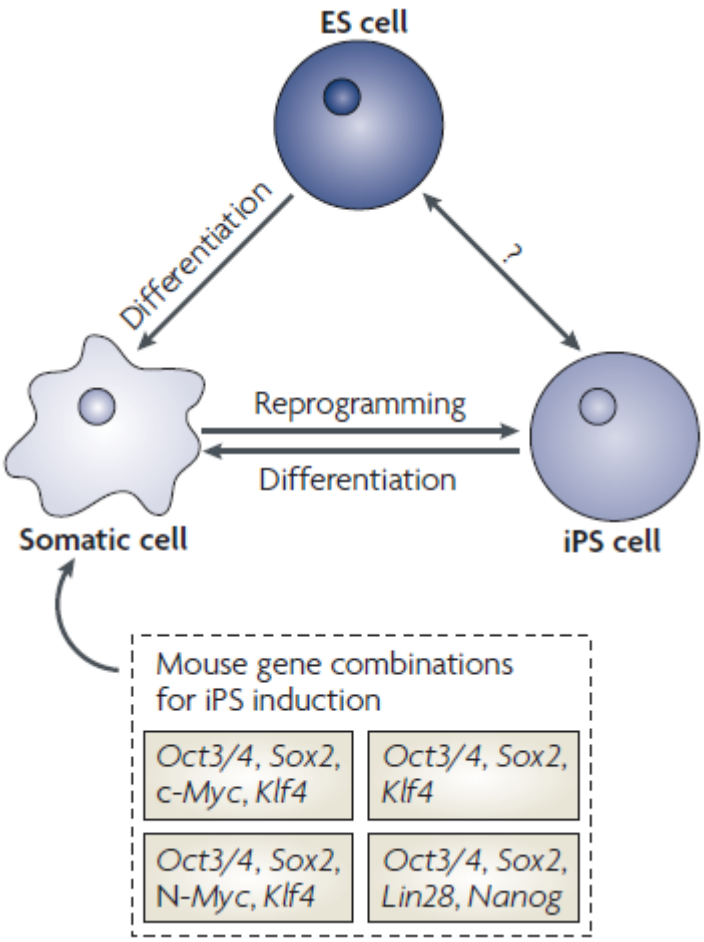

Figure 1.14: The process of reprogramming between embryonic stem cells (ES) and somatic cells. The diagram depicts that all differentiated cells (somatic cells) in the body are derived from pluripotent ES cells. Somatic cells can then be reprogrammed into iPSC cells using a combination of transcription factors, the successful combinations of which are shown in the indicated box. The question mark represents that the lack of understanding between ES cells and iPSCs. Image taken from Nishikawa et al., 2008.

1.8 Differentiation of Human Stem Cells

One of the major challenges of human stem cell culture is to find an efficient protocol to direct hESCs into specific lines of differentiation; and although various methods exist for the differentiation of mouse ES cells, variations in success have been found when these same methods have been applied to hESCs. There are 2 main methods of differentiation in hESCs: embryoid-body (EB) protocol and monolayer protocol.

1.8.1 Differentiation of Human Stem cells through EBs

Mouse ES cells can simply be differentiated by dissociating the culture into single cells, a process that has been found to be fairly detrimental to hESCs.

It has been found that by dissociating hESCs into smaller, free-floating aggregates termed **embryoid bodies**, cells can be directed into different lineages. The route of differentiation hESCs take is dependent on the type of chemically defined media these aggregates are cultured in and the time period (Loring *et al.,* 2007). Aggregates can be directed down various lines of differentiation.

For example, cardiomyocytes have been formed by plating EBs onto gelatin coated dishes after a culture period of 7-10 days in suspension (Kehat *et al.,* 2001). Of the examined EBs approximately 10% exhibited contracting areas which stained positive for cardiac-specific proteins (Kehat *et al.,* 2001).

The formation of EBs has also been used to drive differentiation of hESCs into derivatives of endothelial cells. One such study formed EBs from the H9 hESCs clone and analysed RNA extracted from different time points of the differentiation protocol. This study tested for known endothelial markers PECAM1 (CD31), vascular endothelial-cadherin (VE-cad and CD34) and vascular endothelial growth factor 2 (VEGFR-2/Flk-1/KDR) amongst others (Levenberg *et al.,* 2002). This investigation found that maximum gene expression of PECAM1, VE-cad and CD34 occurred during day 13-15 of EB formation, suggesting that these cells had been directed towards the differentiation of endothelial cells during this period (Levenberg *et al.,* 2002). It is important to note however, that although this protocol produced cells exhibiting the phenotype and specific markers of endothelial cells, the method is not an efficient

process, as only 2% of grown cells were capable of organising into structures indicative to blood vessel formation (Levenberg *et al.*, 2002).

Although only two cell types have been discussed above which use the EB protocol to direct differentiation of hESCs, this protocol has been successfully used to direct differentiation of hESCs into various other cell derivatives including pancreatic cells, neural cells and photoreceptor precursors amongst others (Conley *et al.*, 2004).

Although differentiation can be directed to a certain extent by forming EBs, differentiation of hESCs has also been found to occur spontaneously. Spontaneous differentiation has been found to occur in cells cultured in serum-free conditions as well as serum supplemented media; but the during spontaneous differentiation it is often very difficult to direct the differentiation of hESCs down a specific lineage.

The original differentiation process through EBs remained a fairly unpredictable and in most cases inefficient system. This is largely due to the fact that EB sizes were beyond control and left to the course of nature. Depending on the size of cells mechanically removed from an original culture source, which is by no means a uniform process, would then govern the size of aggregates formed in suspension. A single suspended culture system could therefore hold a number of EBs in varying sizes.

This heterogeneity in cultures then leads to inefficient and uncontrollable differentiation. Additionally, any single cells remaining in suspension that had not conformed to an existing aggregate is then vulnerable to waste. Eventually during culture maintenance processes which may include media change processes, these cells would then eventually be discarded. This can result in the loss of a large cell population, leading to a major reduction in efficiency of the differentiation process.

Whether the size of aggregates can contribute to directing pluripotent hESCs down specific lineages remains unclear. A heavy importance is given to uniformity and creating a homogenous population of cells. Creating uniform EBs would only be beneficial for investigative purposes.

In light of this, recent advances in technology have now addressed this very issue. Currently, Stem Cell Technologies have produced plates called AggrWell in order to address the issue of heterogeneity amongst EB differentiation. These plates have a number of microwells (Figure 1.15A), each specified to a dimension which is dependent

on the plate size. As expected, a larger sized microwell would therefore produce larger aggregates.

A suspension of cells is then added to these plate types and centrifuged in order to distribute cells evenly across the whole plate and are cultured for a minimum period of 24 hours to allow the formation of aggregates in each microwell. This creates a more uniform population of EBs in comparison to the original approach in creating EBs (Figure 1.15 B&C).

EBs formed using this technology are more uniform in terms of size and shape and thus aids in the standardisation of protocols, which was not possible prior to such technologies.

By standardising such methods of differentiation, any results of investigations using such technologies can confidently express results.

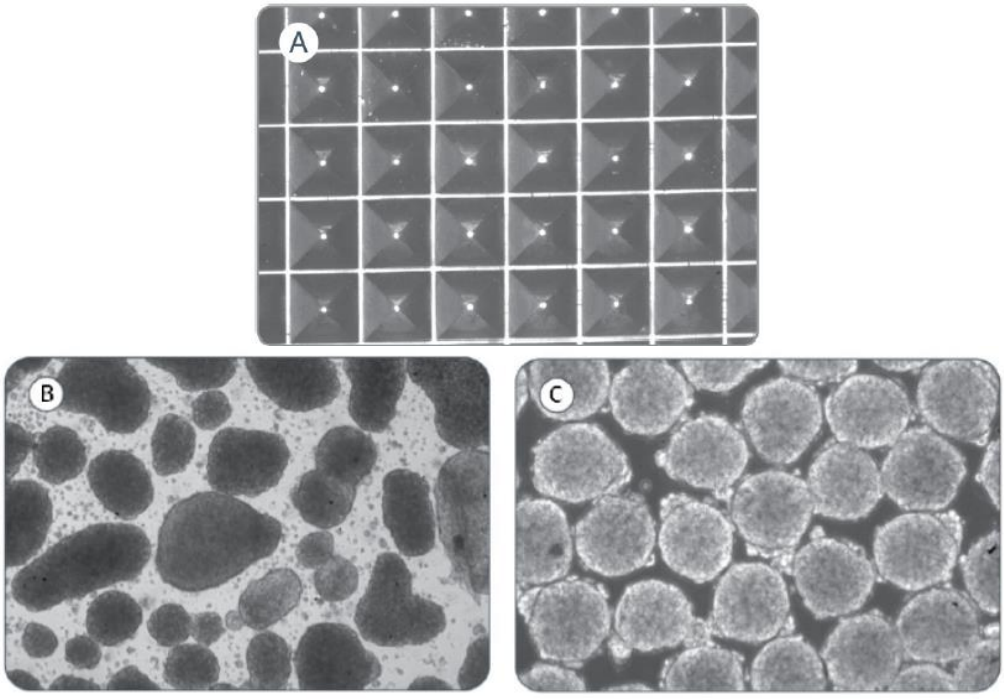

Figure 1.15: Image of AggrWell plates from Stem Cell Technologies. Image of a magnified AggrWell plate. B) Image of heterogeneous population of EBs formed using traditional methods. C) Image of a more uniform population of EBs formed using an AggrWell plate. Images taken from http://www.stemcell.com/~/media/Technical%20Resources/9/29146MAN_3_0_0.pdf

1.8.2 Monolayer Differentiation of hESCs

The term **monolayer differentiation** refers to a process of differentiation whereby EBs are not cultured in a suspended culture system. Instead, in the same way as hESCs are cultured in a monolayer to retain pluripotency, cells are differentiated whilst still attached to a monolayer.

Researchers have found that by culturing undifferentiated hESCs in serum-free media as normal on mouse embryonic fibroblasts and co-culturing with either mouse bone marrow stromal cells or mouse yolk-sac endothelial cells for 17 days, hESCs can be directed to differentiate into hematopoietic cells with differentiated cells being cultured in 20% serum supplemented media (Kaufman *et al.*, 2001). Of the isolated differentiated cells however, only 1-2% exhibited positivity for $CD34^{+}$, a known early hematopoietic cell marker suggesting a small percentage of differentiated cells were successfully directed into hematopoietic-like cells (Kaufman, Hanson et al. 2001).

This method of differentiation can also be referred to as monolayer differentiation as no formations of EBs is required and cells are continually grown on a monolayer.

This type of differentiation has been readily used to direct differentiation of hESCs into cardiomyocytes, trophectoderm and neural cells amongst others with varying degrees of success.

Although both EB and monolayer differentiation process have been successful in differentiating pluripotent hESCs into specific cells types, the differentiation of higher order structure remains to be a challenge (Liu *et al.*, 2013).

The issue with differentiation of pluripotent hESCs is the maintenance of viability of cells as well as creating a homogenous population-which in most cases is almost near impossible using current technologies.

Although protocols have been produced to differentiate hESCs into different cell lines the efficiency and success of these methods require a large amount of optimisation and remains a difficult hurdle in the world of stem cell research, more so for some lineages than others.

1.9 Retinal Differentiation of pluripotent hESCs

As discussed previously, it is extremely difficult to direct hESCs down specific lines of differentiation. The differentiation of photoreceptors has not been found to be an easy process either! There are a number of protocols that have been developed and have shown to direct hESCs into eye field precursors with varying efficiencies. Currently however, no methods to date have been shown to efficiently produce required retinal cells with a pure population. Therefore the struggle to produce a perfect protocol for purposes of treatment for degenerative eye diseases is still present.

Some of the currently available protocols are discussed later in this chapter. One of the hurdles lies within establishing an environment that mimics the retinal environment during embryogenesis. Many pathways have been found to play important roles in the differentiation process of photoreceptors in nature and thus complicating the issue of creating optimal environments for this process *in vitro.* One such pathway which holds great importance in the differentiation of photoreceptors is described in the following.

1.9.1 Wnt signalling

Wingless (Wnt) has been found to be play an important role in many processes of embryonic development and adult tissue. Controlled Wnt signalling has been found to play an extremely important role in forebrain patterning with disruptions resulting in adverse effects on the formation of the eye.

Wnt binds a cell-surface receptor complex made up of Frizzled and low density lipoprotein receptor-related protein (LRP) which activates the dishevelled (Dsh) protein which in turn inhibits a large degradation protein complex, made up of three main proteins: glycogen synthase kinase-3β (GSK3β) which phosphorylates and marks the protein for ubiquitylation, adenomatous polyposis coli (APC) which promotes affinity of the degradation complex to β- and Axin which acts as a scaffold protein holding the complex together.

As a whole this degradation complex functions to phophsphorylate and ubiquitinise β-catenin, therefore the inhibition of this complex result in the accumulation of unphosphorylated β-catenin in the cytoplasm. This accumulation, results in the translocation of the β-catenin into the nucleus where it displaces the Groucho in the

Groucho/Lymphoid enhancing factor 1 (LEF-1)/T cell-specific transcription factor (TCF) complex (Alberts *et al.,* 2002). This induces transcription of Wnt target genes (Alberts *et al.,* 2002).

In the absence of Wnt, β-catenin is readily phosphorylated and degraded. This pathway is referred to as the canonical Wnt pathway.

Wnt signalling can also takes place via the non-canonical pathway in a β-catenin independent manner. Although Wnt is clearly required for the formation of the eye field, overexpression has been found to result in a decrease in eye size while in contrast Wnt antagonists such as dickkopf 1 (dkk1) and Secreted Frizzled related proteins (SFRP) are capable of increasing and expanding eye size and eye field marker expression (Shinya *et al.,* 2000; Esteve *et al.,* 2004).

To add to the confusion, Wnt signalling through non-canonical and canonical pathways can also have opposite effects on eye formation. For example, in zebra fish, whilst the canonical pathway inhibits eye field specification the non-canonical pathway promotes eye field formation (Cavodeassi *et al.,* 2005).This suggests that both canonical and non-canonical signalling of Wnt is a highly controlled process, where different signalling pathways are induced at different stages for the correct development of the eye and is in fact a puzzle within its self, within the world of eye development research.

1.9.2 Current Methods of Photoreceptor Differentiation of Stem Cells

There are currently several protocols available with varying degrees of success to differentiate hESCs into photoreceptors. Each holds its own specific advantages and disadvantages, although no single protocol to date has successfully produced a fool proof method of converting hESCs into photoreceptors with 100% efficiency.

Although not many protocols exist for the differentiation of photoreceptors when comparing differences in methods it is clear that practically not many differences exist. All protocols include the formation of EBs (or EB-like aggregates) as the primary stage followed by a period of free-floating maintenance; a plating stage to adhere cells to a monolayer differentiation system followed by maintenance of cells in chemically defined media for a set period of time. What appear to be minor changes between protocols however may hold the key to success.

The formation of EBs (or EB like aggregates), being the primary stage of photoreceptor differentiation, is one of importance. It is apparent that in the case of EB formation, groups are divided between formation in serum enriched media and the use of a serum replacement, the later method referred to as serum-free culture.

Serum-free culture of EBs involves either culturing cells in suspension for a period of 4 days substituting knockout serum for a commercially available knockout serum replacement (at 20% final volume of media) or culturing in suspension in decreasing concentrations of serum replacement (Meyer *et al.,* 2009; Osakada *et al.,* 2009).

The latter method involves the culture of EBs in an initial concentration of 20% (final volume) for a period of 6 days, proceeding to a concentration of 15% of (final volume) for a further 9 days, down to 10% (final volume) for the rest of the protocol leading to an extended period of EB maintenance of approximately 20 days. EB-like aggregate formation using serum enriched media however, requires no gradual reduction in serum concentration and is only maintained in suspension for a period of 3 days (Lamba *et al.,* 2006; Osakada *et al.,* 2009).

The reason behind the gradual decrease in serum replacement is not clear. This is because, if constituents of the serum replacement resulted in a negative effect on hESCs

differentiation or hESCs cell proliferation then it would be assumed that this would be discussed in studies omitting this stage. On the other hand, the same discussion would be expected if this process had a positive effect towards committing hESCs. The fact that some groups such as Meyer *et al.,* (2009), which have successfully shown to direct differentiation of hESCs into photoreceptors using a serum-free approach without gradual reduction to EB-like aggregate formation, suggests that the incorporation of a gradual reduction in serum replacement, as shown by Osakada *et al.*,(2009), is not an essential part of the process. Especially as this step requires an increased volume of consumables and takes a longer period. On the other hand, the extended time period of EB culture may or may not contribute to the success of the differentiation protocol.

As none of the currently available protocols comment on the number of aggregates produced it is difficult to conclude the success of discrete variations between protocols. From a personal perspective, although long period of suspension culture of EB will essentially allow more time for differentiation to take place within the aggregate conformation, it must be noted that it may not necessarily result in the differentiation of target cells.. This is an important factor that must be taken into consideration when directing hESCs into photoreceptor.

Another difference in protocols is the need to remove feeder cells from the undifferentiated population of hESCs. Whilst some groups direct differentiation of photoreceptors in a mixed population of hESCs and feeder cells, others include steps to create a pure population of hESCs to carry forward with the differentiation.

From a practical perspective, feeders are inactivated cells and therefore should not interfere with any hESCs activity. The removal of these cells from the population however, results in the elimination of any potential interference that may be caused by these cells. Additionally, with any potential therapy, animal contaminants are highly unfavourable therefore removing contaminants early on in the investigation can only be beneficial.

Following the EB formation, common to all current protocols, is the attachment of cells onto a growth surface usually covered in a coat of extracellular matrix (ECM) proteins. Although a common procedure, there is wide variation in the preference of ECM proteins used. It is not surprising that ECM proteins are commonly used during the

attachment stage of the differentiation protocol as the attachment surface has an influence on many cellular pathways such as cell spreading, proliferation ect.

Peptide recognisers known as integrins are responsible for the regulation of intercellular signalling, cell-to-cell signalling as well as surface attachment; the signal regulation is dependent on which peptide the integrin recognises (Hidalgo-Bastida and Cartmell, 2010). As ECM proteins are made up of various different sequences they can be readily used to mimic the cellular micro-environment to encourage processes such as differentiation.

In light of this fact, although initially the variation in ECM proteins used in various protocols of photoreceptor differentiation may have been a fairly small factor to be considered, it is now clearer that these ECM proteins may in fact hold an important role in the direction of photoreceptor differentiation.

While some groups have used a single ECM protein such as laminin, others have opted for a combination of laminin and fibronectin. Some have preferred a commercially available feeder replacement such as Matrigel, discussed earlier in this chapter, as a substitute for feeder cells.

As a matter of opinion, the combination of ECM proteins may greatly impact the process of differentiation. This is due to the fact that they can be used to create a closer match to the natural micro-environment of cells during photoreceptor development. Further investigations are however required to identify whether or not a single ECM protein can significantly increase the efficiency of a specific protocol or whether a combination of ECMs would be more beneficial. If so, which combination would create an optimal environment to efficiently direct differentiation of hESCs into photoreceptors. The use of Matrigel however, is not encouraged, as the constituents of this product remain undefined. This therefore creates many safety concerns for potential use in a clinical environment for therapy.

The culture of cells after attachment in a chemically defined media seems to play an extremely important role in the differentiation process of hESCs into photoreceptors, as all current protocols include this step. Common to all protocols the chemically defined media seem to include an enriched source of neural growth supplements such as N2 supplement and B27 supplement (increases long-term viability of neurons), to steer

hESCs down the retinal lineage with varying concentrations. This is clearly a necessity for the differentiation of photoreceptors. It must be noted however that whilst some positive results has been recorded with only a single addition of a supplement to the chemically defined medium, others have recorded success using a combinations of both neural supplements mentioned above.

Whilst every effort must be made to create an environment as close to the natural environment,, the cost of therapy must also be taken into consideration. In the case of supplement additions, if reduced additions of supplements could still achieve the successful direction of hESCs into photoreceptor precursors, then it is wise to add fewer supplements, purely in terms of cost effectiveness.

Additions of inhibitors of Wnt signalling during the EB formation and maintenance are a common procedure in many protocols attempting to drive differentiation down the photoreceptor lineage. The addition of dickkopf 1 (dkk1), a known Wnt inhibitor is commonly added to the chemically defined media - although at different concentrations depending on the protocol. The importance of the absence of endogenous Wnt3A and bone morphogenetic protein (BMP) 4, especially during early stages of this process holds great importance. The inhibition of both Wnt3A and BMP is known to result in the generation of retinal progeny in blastomeres. The importance of this is more so evident from an investigation carried out by Meyer and his group in 2009. This study showed that the addition of Wnt3A to cultures during the first 10 days of culture, during and briefly after suspension culture of cells, in fact resulted in the abolishment of Pax6 and Rx expression in cells (Figure 1.16) (Meyer *et al.*, 2009).

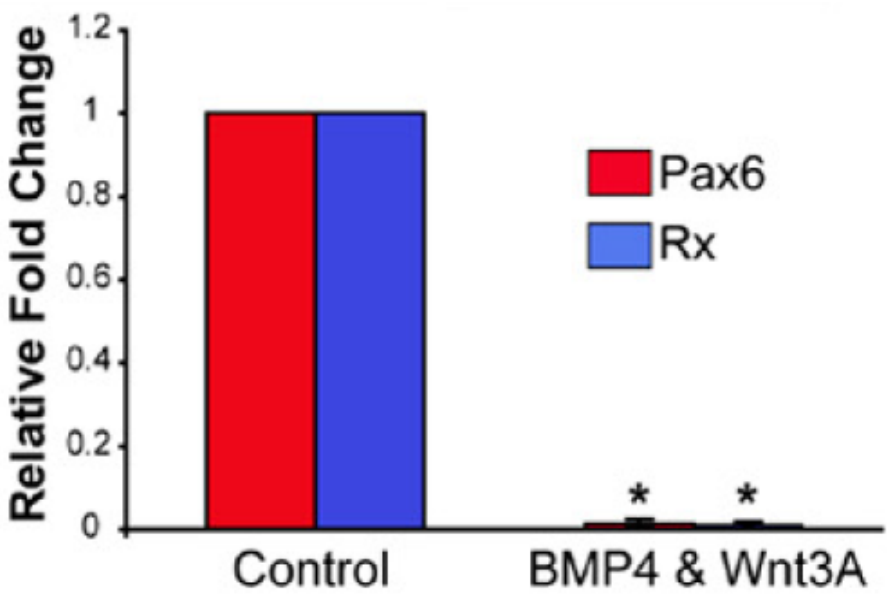

Figure 1.16: qPCR of cells treated with and without (control) endogenous Wnt3A and BMP4 during the first 10 days of differentiation process of eye field cells. Addition of Wnt and BMP4 resulted in loss of Pax6 and Rx expression in comparison to cells treated without endogenous Wnt3A and BMP4. Image retrieved from Meyer et al., 2009.

The absence of endogenous Wnt and BMP is evidently important for the differentiation process of photoreceptors. It is however, questionable whether this requires the addition of inhibitors such as Dkk1, as commonly used. This is because the protocol developed by Meyer *et al.,* in 2009, does not at any point in the protocol add inhibitors such as Dkk1 to the chemically defined media. However, this protocol continued to produce a high percentage of eye field-like cells. Additionally although Meyer *et al.,* 2009, added N2 supplement in the chemically defined media, no other neural inducers such as noggin (used by Lamber *et al.,* 2006) or nodal inhibitors such as LeftyA (as used by other groups) are included. This protocol still remained to successfully produce photoreceptor precursor-like cells. This again questions the necessity of these additions (Osakada *et al.,* 2008;Hirami, Osakada et al. 2009; Osakada *et al.,* 2009).

It must be noted that in the protocol produced by Lamba *et al.,* 2006, the addition of combinations of IGF1, Dkk1 and noggin to attached cultures for a week, resulted in a clear increase in many of the eye field transcription factors (EFTFs) (Figure 1.17).

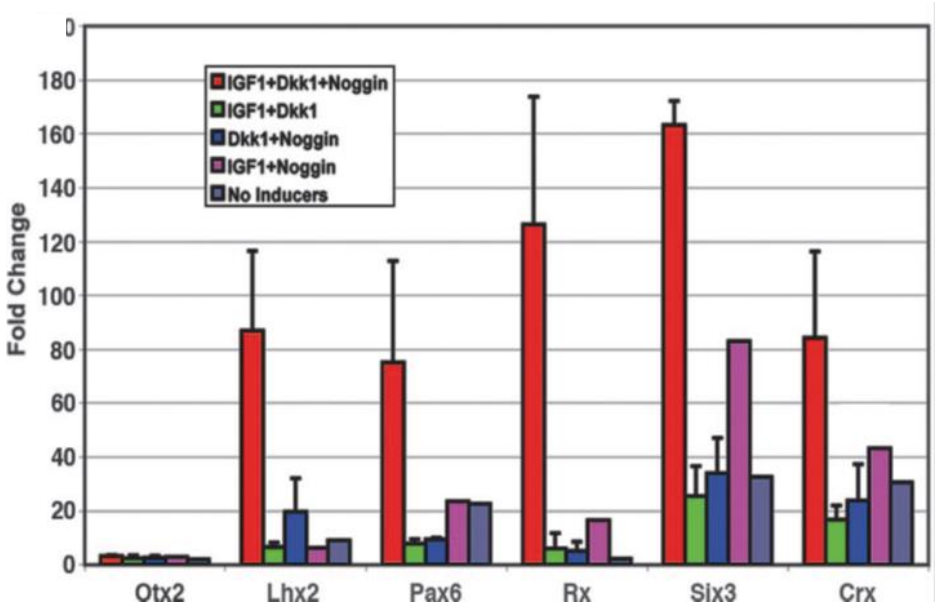

Figure 1.17: QPCR analysis of eye field transcription factors after 1 week culture with combination of IGF1, Dkk1 and noggin. (Lamba et al., 2006).

Retinoic acid has been shown to play an extremely important role in retinal development as has taurine. Retinoic acid has been shown to increase cells that later developed into photoreceptors in a dose-dependent manner when added exogenously in mice (Figure 1.18). This also resulted in having teratogenic effects at high concentrations, clearly reflecting the importance of this acid in eye field development (Kelley *et al.*, 1994; Sernagor and Lemp, 2006).

Investigations have also shown that the deletion of the gene expressing taurine (Taut) results in severe retinal degenerations through photoreceptor apoptosis, again reiterating the importance of the role of taurine (Heller-Stilb *et al.*, 2002). In light of this, the reason behind the addition of retinoic acid and taurine is evident in the differentiation of photoreceptors. Although many groups have included these additions other groups have again, also succeeded in producing photoreceptor precursors without these additions or any replacements.

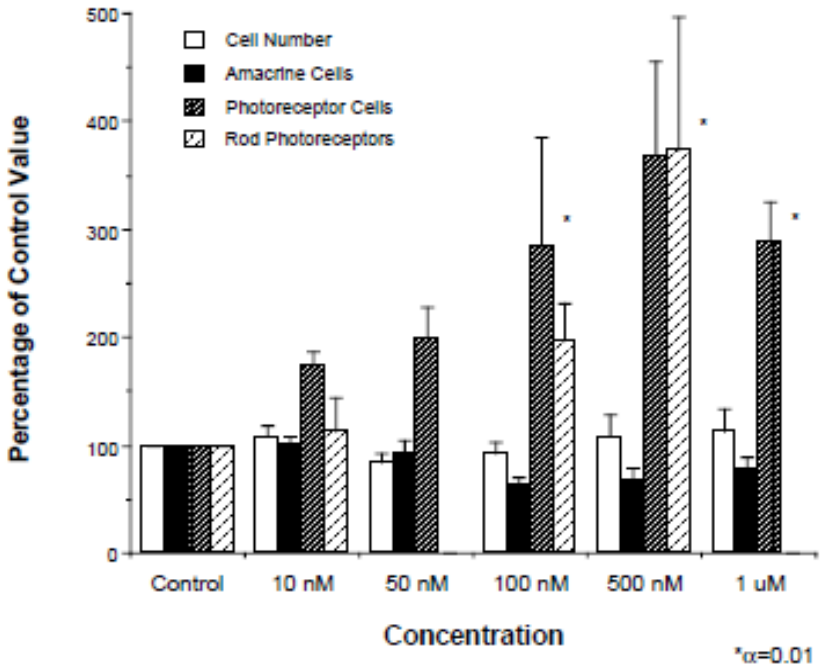

Figure 1.18: Response of mouse embryonic stem cells cultured in varying concentrations of retinoic acid. Image retrieved from Kelley et al., 1994.

In summary, these protocols can be grouped into three main protocols: (1) serum culture and neural growth supplements and only includes a 3-day EB formation protocol as produced by Lamba *et al.*, (2006), (2) serum free culture of EBs in a gradual decrease of serum replacement followed by many groups and (3) the serum free culture without a gradual reduction in concentration as produced by Meyer *et al.*, (2009).

The results obtained by the main groups that have reported successful differentiation of photoreceptors is summarised in Table 1.1.

Table 1.1: A summary of the main photoreceptor differentiation protocols with results.

	Lamba et al., 2006	Osakada et al., 2008	Hirami et al., 2009	Meyer et al., 2009	Osakada et al., 2009
Cell line	H1	khESCsC 1 + 3	201B7, 201B6, 253G1 + Human iPS	H9 + iPS	khESCsC 1
Serum (S)/ Serum-free(SF)	S	SF	SF	SF	SF
Gradual Reduction of knockout serum replacment	-	Y	Y	N	Y
Addition of inducers	Dkk1 Noggin IGF-1	Dkk1 Lefty-A Taurine Retinoic acid	Dkk1 Lefty-A Taurine Retinoic acid	-	Dkk1 Lefty-A Taurine Retinoic acid Y-27632
ECM Proteins	Matrigel	Laminin-Fibronectin	Laminin-Fibronectin	Laminin	Laminin-Fibronectin
Eye field genes expressed & percentage of aggregates expressing genes	Pax6 – 82% Chx10- 70.5%(i) Crx – 12%(i) Nrl- 5.75%(i) Opsin + Rho- <0.01%(i)	Pax6 –30.6% Crx- 19.6% Rho- 8.5%	Pax6 – 19.4% Crx- 14% Recoverin- 26.5% Rho- 3.5% (i)	Pax6 - 95%(i) Chx10- 90.7% Crx- 19.4%(i) Opsin- 46.4%(iii)	Pax6- 79.2% Rx- 25.4% Crx – No data Nrl – No data Rho – No data
Day of eye field gene expression	All genes - Day 21	Pax 6- Day 50 Crx- Day 170 Rho- Day 200	Pax6- Day 35 Crx- Day 80(ii) Recoverin- Day 20 Rho- Day 120	Pax6- Day 16 Chx10- Day 50 Crx- Day 80 Opsin- Day 80	Pax6- Day 35 Rx- Day 35
Duration of protocol	21 Days	200 Days	120 Days	80 Days	140 Days

(i) **Cells** not aggregates

(ii) Note cell line 201B6 did not express Crx or Rho

(iii) Percentage of expressing cells

When comparing results obtained by various groups together with the main differences between groups it is evident, in my opinion, that the increased number of inducers and extended period of gradual reduction in serum replacement is not reflected highly in the results.

The protocol devised by Osakada and his group (2009) requires many inducers with the addition of Y-27632, a Rho-associated kinase inhibitor which aids to stop cell death associated with dissociation. During the extended EB culture, the production of neural retinal progenitor cells and photoreceptor precursors does not match the higher percentages produced by other protocols.

It must also be noted that whilst groups incorporating the serum replacement reduction stage they report results as a percentage of aggregates formed. This does not include the number of cells that are actually expressing specific genes, which would be a more true representation of results. In this case, in extreme circumstances, whether 2 cells or 100 cells in an aggregate expressed a certain gene, this aggregate would be recorded as a "positively expressing" aggregate. This form of analysis has the potential of results being misconstrued.

When comparing protocols it is evident from Table 1.1 that the highest percentage of neural retina progenitor cells have been reported by Lamba *et al.,*(2006) (Figure 1.19 A and B) and Meyer *et al.,* (2009) (Figure 1.20). Whilst Lamba and his group use knockout serum and the addition of other inhibitors, Meyer and his group use serum replacement without reduction of serum replacement, inducers or inhibitors. Additionally these two protocols also require the shortest time periods in comparison to the five protocols discussed.

Although Lamba *et al.,* (2006) have produced the shortest of all protocols with the whole process only lasting 21 days. A good correlation was found in EFTF expression between 91 days (after conception) human foetal retinal cells and differentiated hESCs (Figure 1.21). This builds confidence in this method as a potential therapeutic process although this time period is still a fairly prolonged process.

In the case of photoreceptors production however, it is also important to note that Lamba and his group (2006) were not successful in producing photoreceptor-like cells. This is because expression of opsin and rhodopsin was only recorded in less than 0.01% of cells, a result that would not be satisfactory or feasible for use in therapy.

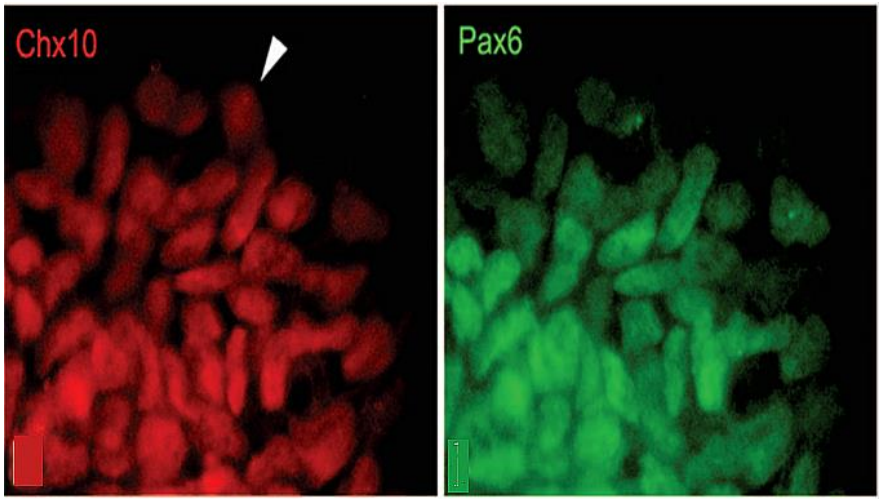

Figure 1.19: Expression of retinal markers from retinal induced hESCs. A) Expression of Chx10 in induced hESCs. Arrows indicate cells that expressed Chx10 (red) but not Pax6. (B) Expression of Pax6 (green) in induced hESCs. Modified from Lamba et al., 2006.

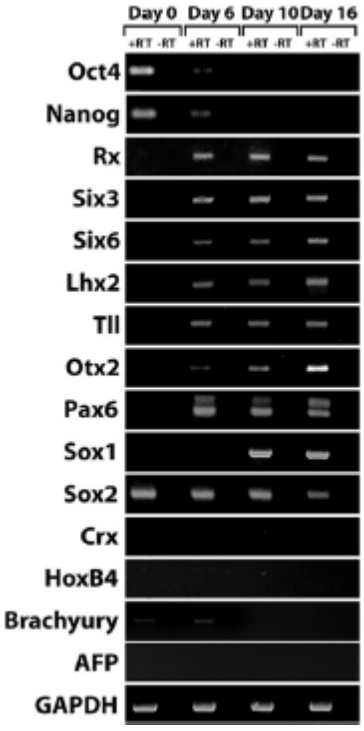

Figure 1.20: RT-PCR of gene expression during first 16 days of eye field differentiation of hESCs. Retrieved from Meyer et al., (2009).

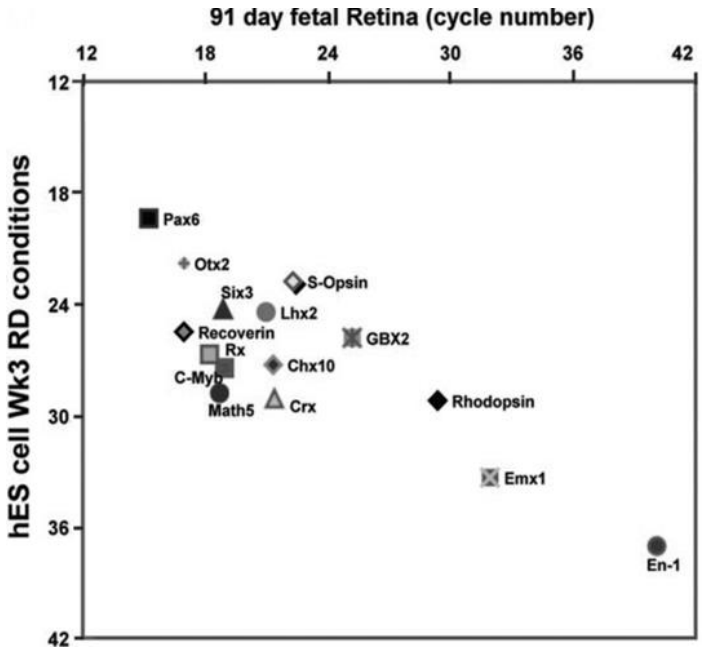

Figure 1.21: QPCR analysis of various genes between cells from a 91 day human foetal retina and hESCs after a 3 week culture condition. (Lamba et al., 2006).

In the case of the protocol produced by Meyer *et al.,* 2009, in comparison to other protocols, the production of photoreceptor-like cells is significantly improved. In terms of use of protocols for the purpose of production of cells for therapy; the protocol produced by Meyer and his group is still extensive. It could however, be argued that from a cost perspective, as this protocol uses minimal reagents in comparison to other protocols, costs may be recuperated from the loss of time endeavoured by the extensive process.

1.10 Retinal Co-culture with hESCs and Photoreceptor Differentiation

Interestingly, it has been found that co-culture of early retinal progenitor cells with mature retinal cells efficiently enhances differentiation of these cells into photoreceptors. Firstly developed in mouse ES cells (mES), rhodamine labelled mES cells (1x104 cells) was cultured in a serum free EB culture system for 5 days. The chemically defined medium had additions of inhibitors such as Dkk1, LeftyA and activin (SFEB/DLFA), a known photoreceptor inducer. These cells were then co-cultured with GFP labelled mouse retinal cells (1:50) for 12 days in chemically defined media (Ikeda *et al.,* 2005; Kanno *et al.,* 2009). This co-cultured medium had the addition of serum (Figure 1.22A) (Ikeda *et al.,* 2005; Kanno *et al.,* 2009). This culture was found to have induced mES cells into expressing photoreceptor genes (Ikeda *et al.,* 2005; Kanno *et al.,* 2009).

This process resulted in 36% of labelled ES cells to be identified in enriched areas of embryo-derived photoreceptors cells (which formed clusters). These clusters of cells were observed to express rhodopsin and recoverin. Interestingly it was also noted that mES cells that were not present near the photoreceptor cluster did not express photoreceptor markers (Figure 1.22 B and C). This suggests that the microenvironment of the immediate vicinity of exogenous photoreceptors may hold an important role in directing differentiation of mES cells towards the photoreceptor lineage (Ikeda *et al.,* 2005).

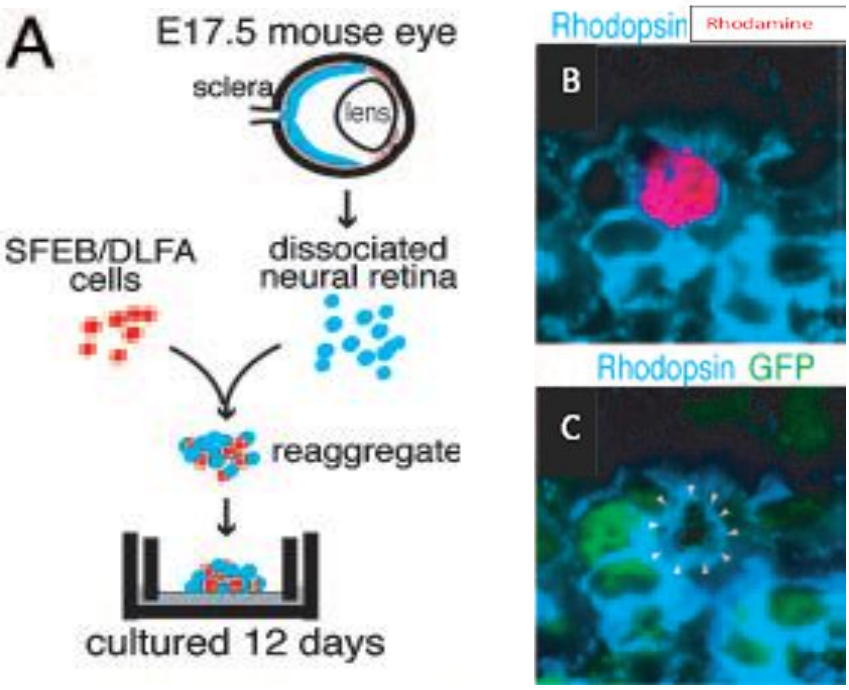

Figure 1.22: Generation of photoreceptors from mES cell co-culture with mature retinal cells. (A)Schematic of mES cells (red) co-culture with mature retinal cells (blue). (B) Rhodamine expressing SFEB/DLFA mES cells (red) were cultured with GFP expressing retinal cells. Rhodopsin (blue) expressing mES cells (red) did not express GFP in C. Modified from (Ikeda et al., 2005).

Following a similar method in hESCs, groups have found that by coculturing hESCs derived progenitor cells with retinal extracts from GFP expressing mice (6 days) these progenitor cells readily integrate into mice retinal extracts with a majority of these cells expressing Pax6 (Lamba *et al.*, 2006). Interestingly, hESCs were co-cultured with both wild-type and mutant mice retina. The later was found to result in photoreceptor degradation, and it was found that hESCs derived retinal progenitor cells expressing recoverin readily integrated into the mouse retina and cells resembling photoreceptors were observed (Figure 1.23) (Lamba *et al.*, 2006).

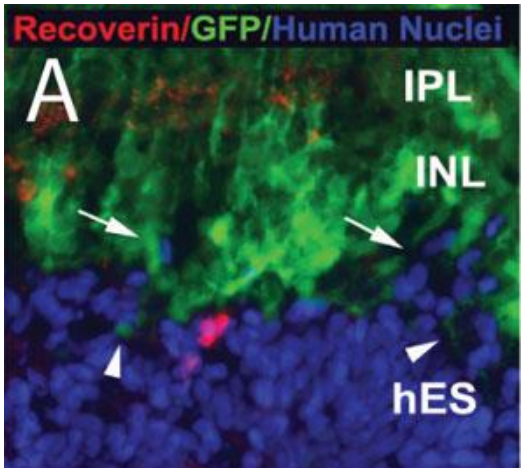

Figure 1.23: hESCs derived retinal progenitor cell co-culture with Aip1-/- GFP mice retina labelled with human nuclear marker (blue) and recoverin (red). Image retrieved from Lamba et al., 2006.

These results are encouraging and give hope that progenitor cells produced by these protocols capable of integrating into the correct part of the retina. It must however, be noted that, to ensure these progenitors are functionally normal, assays are required to stipulate whether this integration does in fact repair visibility in the mice and if so to what extent.

1.11 Retinal Transplantation

Transplantation of brain and retinal derived stem cells have been shown to be unsuccessful in the integration of the outer nuclear layer of the retina failing to differentiate into photoreceptors (MacLaren *et al.*, 2006). An exciting investigation however has found that via transplanting retinal cells taken at the height of rod genesis, into the outer nuclear layer of the retina, these cells are capable of integrating in the correct location with >95% in the correct orientation (MacLaren *et al.*, 2006).

In this particular investigation carried out by MacLaren and his group in 2006, retinal cells from transgenic mice were extracted at postnatal day 1. These cells contained a GFP reporter gene and at this time point cells were at the peak of rod genesis. These cells were then injected to the outer nuclear layer of the retina (~$2x10^5$ cells) of wild-type littermates. Three weeks later approximately 10-200 cells (in each eye) were observed integrate into the correct position with morphological characteristics similar to that of mature photoreceptors (Figure 1.24) (MacLaren *et al.*, 2006).

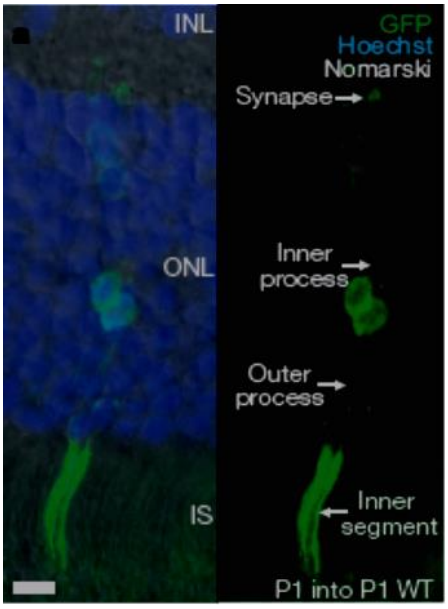

Figure 1.24: Transplantation of P1 transgenic retinal cells into immature wild type littermate (3 weeks post transplantation). Image retrieved from MacLaren et al., 2006.

In order to identify whether this transplantation was only successful in immature retinas, the same population of cells were also transplanted into adult wild-type retina (~$8x10^5$ cells). Contrary to other research it was found that these cells again successfully integrated into the outer nuclear layer (~300-1000 cells) as observed in immature retinas and taken the form of rod photoreceptors (Figure 1.25). The fact that the majority of transplanted cells had taken form into rod-like structures is not surprising, given the transplanted population of cells was taken at a time point which was at the peak of rod genesis.

The majority of the cells within this population must have been in the differentiation process of rod photoreceptors resulting in the further differentiation into rod-like structures after transplantation. This integration was also not due to fusion between host and transplanted cells as DNA labelling confirmed that cells only contained one nucleus from the donor.

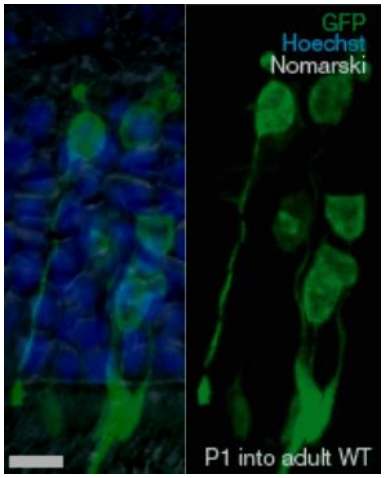

Figure 1.25: Transplantation of P1 cells from transgenic mice into wild-type mature retina. Image retrieved from MacLaren et al., 2006.

As the transplanted population within this investigation contained a mixture of cells at different stages of the differentiation process, in order to identify which specific population was most successful in integrating into the retina cells were extracted at different time points. The first time point of extraction began with embryonic day 11.5 (E11.5), where the majority of cells would consist of progenitor cells; E16.5 and postnatal day 1 (P1)-P15. These populations extracted for transgenic mice were

transplanted into wild-type adult mice and interestingly it was found that cells that cells extracted between P1-P7 had the highest number of integrated cells in comparison to all other ages of cells. The highest cell integration of cells was found between P3-P5, where most cells would have been at the precursor stage (Figure 1.26) (MacLaren *et al.*, 2006).

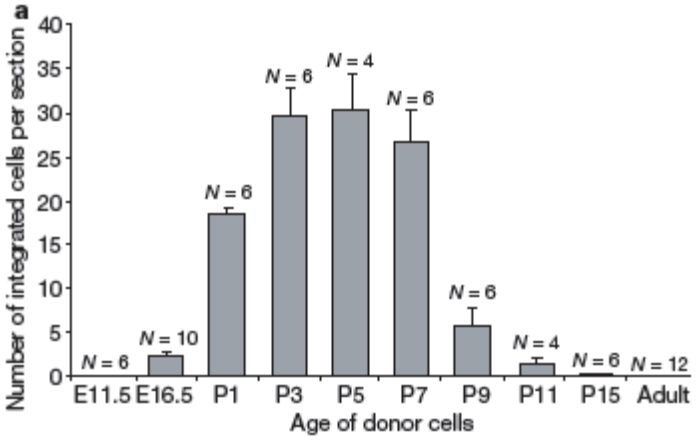

Figure 1.26: A chart of the number of integrated cells from each population of transplanted cells. (MacLaren et al., 2006).

As a large population of viable cells were obtained from each of the transplantations it is apparent that in earlier aged populations, the lack of integration was not due to the lack of cell survival. This was more due to the fact that cells have a higher probability of integration when transplanted at the precursor stage and not at the progenitor or late differentiation stage. This was evident as cells transplanted from an adult retina also did not integrate successfully into the host. Additionally when transplanted cells were tested in rho$^{-/-}$ mice, which do not have functional rod photoreceptors, transplanted mice showed a response to light in comparison to un-injected mice. This suggests that transplanted cells also exhibited functionality, an exciting finding for the therapy of rod regeneration.

The investigation described above clearly shows the successful integration of transplanted rod precursor cells into the retina with cells exhibiting specialised morphologies similar to mature photoreceptors. Although this in itself, this is exciting in the world of regenerative medicine for the treatment of many ocular diseases, it still remains unclear whether transplanted cells are capable of improving vision. Without the

actual improvement of these cells after transplantation, this line of research could potentially be rendered useless in terms of clinical therapy for sufferers of ocular diseases.

Currently no reports of photoreceptor transplantation have actually been found to improve vision. This could possibly be due to the low numbers of transplanted cells, as typically, less than 1000 cells have been transplanted (Pearson *et al.*, 2012). In order to identify whether transplanted rod-precursor cells result in any improvement to vision, Pearson and his group constructed a study in 2012. In this study, rod-precursor cells were tagged with GFP (Green fluorescence protein) under the control of the Nrl promoter.

Nrl is a transcription factor and marker for rod precursors. Transplanted donor cells could then be identified by the GFP. Approximately 200,000 donor cells were transplanted into wild type mice, a vast increase in the number of transplanted cells by most groups. These cells were then injected into the retina of wild type mice and although integrated cells were found to be predominantly located at sights of injection a distribution of donor cells were also found to cover approximately 50% of the retina as a whole.

In order to investigation the functionality of donor cells, rod-precursors were also transplanted into a $Gnat1^{-/-}$ mouse model. This mouse model was chosen as these mice lack α-transducin (Gnat1), which plays an essential role in rod phototransduction. Thus these mice lack any rod function or behavioural response to stimuli. Although these mice lack rod function it is important to note that they do not lack cone function. In fact, these mice have full functional cones, with both histology and behavioural response to visual stimuli.

Transplantation of recombinant rod-precursors, in this study found donor cells to integrate in the outer nuclear layer of the retina (Figure 1.27A). This integration was found to be to similar in numbers as the wild type control exhibiting morphologies also similar to wild type rods. Additionally, integrated donor cells were found to co-express α-transducin. During normal vision, α-transducin is translocated depending on the type of light present; in dim or dark light α-transducin is expressed in the outer segment of the retina whilst in bright light it is found to be expressed in the inner and synaptic

segments (Kerov *et al.*, 2005). Pearson *et al.*, 2012, found that integrated rod-precursor cells also displayed the correct translocations in dim a bright light (Figure 1.27B).

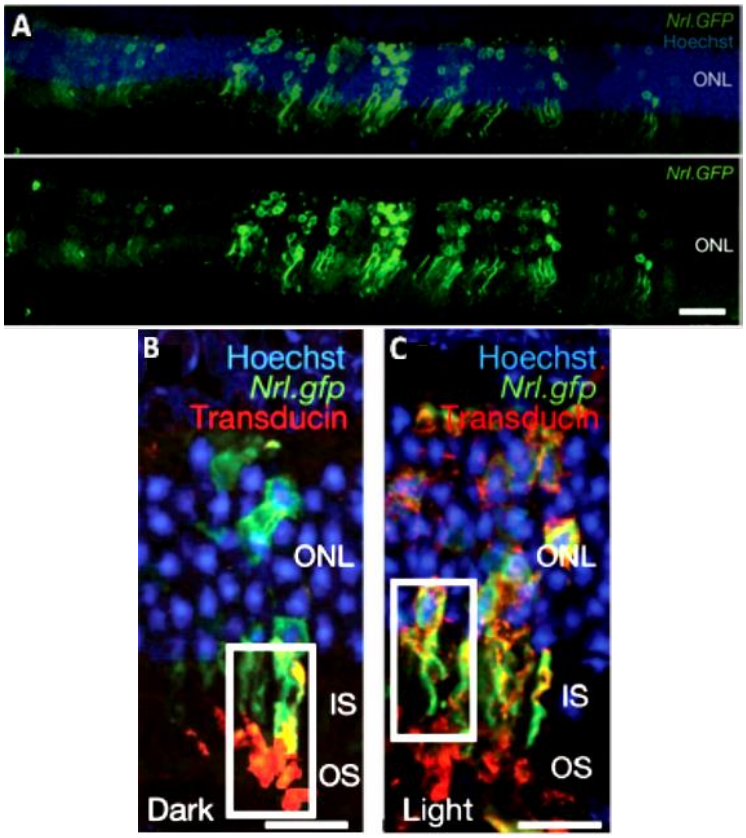

Figure 1.27: Transplantation of rod-precursor cells in Gnat1-/- mice. A: Image of integrated recombinant rod-precursor cells (green) in Gnat1-/- mice. B&C: Image of Translocations of integrated donor cells (in green) in dark light (B) and bright light (C). Image retrieved from Pearsons et al., 2012.

All the results at this point in this investigation give evidence of successful integration of donor cells into the expected regions of the retina. In addition to this, translocation data further showed the correct functioning of these cells in vision. In order to investigate whether the transplantation of these cells had a significant improvement on vision, Pearson and his group then went onto take optomotor head response readings. These readings were taken both before and after transplantation had been carried out in order to give a true reflection of the results of transplantation.

It was found that before transplantation, no responses were made in *Gnat1*$^{-/-}$ mice in scotopic light levels (dim light). This was as expected as these mice lack α trasducin which therefore renders the functionality of rod photoreceptors, which are only function

in dim light. After 4-6 weeks post-transplantations readings were only recorded in mice where the transplantation had been carried out, although visual acuity was found to be poorer in animals in dim conditions than photopic condition.

No change in readings under photopic conditions were found, again an expected results as cone functionality remained unaffected in these models. Mice were also subjected to visually guided water-maze test which would require cognitive processing of visual images. In these tests post-transplantation mice were found to have completed the maze in 70% of trials. Additionally, it was found that mice that mice who had an integration of cell in clusters rather than a wide distribution performed better at completing tasks.

This investigation was successful in the transplantation of rod-precursor cells and also found that transplantations could not only mimic mature cell functionally but could also improve vision. Additionally, results discussed clearly highlight the importance of cell numbers for successful transplantations and also the importance of integrated cells to be in close proximity of one another which may also have a significant effect on improving vision (Pearsons *et al.*, 2012).

Studies described above have shown successful integration of donor photoreceptor precursor cells along with the functionality and improvement of these cells to vision. The next stage of the process of taking such cells from bench side to bedside involves the investigation of transplantations in many more models as well as the study of the success rate of transplantations at varying degrees of retina degeneration. By investing the later of these issues a better idea as to the potential breath of application could be gained to provide a more realistic target for the use of such therapies for blindness in particular.

Transplantation of cells into normal retinal tissue is somewhat different to that of degenerating retina. The reason behind this is that often, degeneration in the retina results in glial scarring as a result of reactive gliosis (Barber *et al.*, 2013). This scarring acts to inhibit many cellular processes within the retina including cell migration and regeneration. Photoreceptor death can also result in reactive gliosis which again result in more scaring and can prevent the migration of transplanted cells within the retina by creating a physical barrier (Barber *et al.*, 2013). Additionally, the death of photoreceptors results in the reduction of the interphotoreceptor matrix (IPM) which impedes on normal barrier functionality (Barber *et al.*, 2013). This in turn affects the

integrity of the outer lining membrane (OLM) located on the outer edge of the outer nuclear layer (ONL) of the retina (Barber *et al.*, 2013).

In light of this knowledge it is clear that there are three main issues which require investigation before transplantation techniques could be employed in a clinical environment. These issues include: the extent of retinal degeneration, the extent of gliosis and integrity of OLM), all of which could potentially have a significant effect on the success of transplantation.

A study carried out by Barber and her group set out to investigate these very issues and published their findings in 2013.

This study investigated six mouse models all of which resulted in the progressive loss of photoreceptors. A range of progressive loss of approximately 10% over a 12 month period ($Gnat^{-/-}$) to almost complete loss of rod photoreceptors (PDE6β) in 3 weeks were covered by the chosen mouse models (Table 1.2). These models therefore represented a good variation in retinal degeneration.

Mouse model	Early (ONL >70% wild-type)	Mid (ONL 30–70% wild-type)	Late (ONL <30% wild-type)
[Wildtype (*C57BL/6*)]	***[6–8 wk]***	[6 mo]	[12 mo]
**Gnat1*$^{-/-}$	***2 mo***	6 mo	12 mo
**Crb1*$^{rd8/rd8}$	3 wk	***6 wk***	12 wk
Prph2$^{+/\Delta 307}$	***2 mo***	4months	6 mo
Rho$^{-/-}$	4 wk	***6 wk***	10 wk
Prph2$^{rds/rds}$	3 wk	***8 wk***	12 wk
**PDE6β*$^{rd1/rd1}$	10 d	—	***3 wk***

A standard time point of 6–8 wk was included to provide information about each model at a time when the retina could be defined as "adult" (boldface, italics). Other stages defined as: early = ONL at >70% thickness of wild-type; mid = 30–70%; and late = <30%. —, not examined.
*Exceptions were Gnat1−/−, which is still 90% of wild-type at 1y and PDE6β $^{rd1/rd1}$, which is ~90% of wild-type at postnatal day 10 but reduced to 20% by postnatal day 21. Crb1 $^{rd8/rd8}$ undergoes focal degeneration, the extent of which broadly follows the criteria above.

Table 1.2: Classification of early-, mid- and late- stage retinal degeneration mouse models used. Table retrieved from supplementary information from Barber *et al.*, 2013.

In these mouse models the retina only reach a stage of maturity during the period of 6-8 weeks. For this reason, murine retinas were only examined 6-8wks, once retinal maturity had been reached. By this timeframe the stage of retinal degeneration was already varied as models used in this study had varied degenerations periods.

(Barber *et al.,* 2013). The most poignant of results recorded from the study carried out by Barber *et al.,* (2013) was that although efficiency of integration of donor cells varies amongst various stages of degeneration, it was prominant to note that integration was still possible in late-stages of retinal degeneration. In most cases integration was found to be comparable to that of wild type controls and thus shows that robust integration of donor cells even at mid-and late-stage retinal degeneration is possible. This is a promising finding that builds confidence for this line of research that endeavours to bring this type of research into use in a clinical environment as it can potentially aid thousands of sufferers irrespective of rate or extent of retinal degeneration.

Investigations concerning the morphology of integrated cells found that all environments tested were capable of forming segment and synaptic formations to some degree (Barber *et al.,* 2013).

The morphology (both segment and synapse) of transplanted cells is however heavily impacted by causes of specific gene defects for each disease, which also has an effect on the number of donor cell integration .Barber and her group also found that the integrity of OLM and glial scarring also has a great impact on transplantation efficiencies. It was interesting to note that in this study, the rate of gliosis and OLM integrity is not have a specific correlation patterns. The increase or decrease of gliosis and OLM integrity with disease progression was dependant on the disease type.

The disease itself can heavily affect the efficiencies of transplantations which if understood could be overcome by manipulating barriers and optimising transplantation cell numbers. By increasing integration of cells transplantation could very well be used to treat and cure many levels of blindness irrespective of the extent of retinal degeneration.

1.12 Summary

Photoreceptor degeneration is the underlying cause of many ocular diseases leading to partial or complete blindness. Current treatments of such diseases aid in preserving as much vision as possible but unfortunately no permanent cure is currently available to completely reverse the effects of these diseases. Many ocular diseases result in progressive loss of vision due to the degeneration of photoreceptors. Unfortunately, photoreceptors cannot repair themselves so that once they are lost there is no way to replace them or their vital function. This results in blindness for many sufferers which in some cases are inevitable depending on the disease type. The only possibility of a permanent cure for such diseases is the permanent replacement of degenerate photoreceptors artificially.

hESCs can potentially be derived into any cell type of the body. The pluripotent nature of these cells holds great potential for cell based therapy for a broad range of degenerate diseases. For example, RP results in progressive blindness as a direct result of photoreceptor degeneration and studies have shown successful differentiation of pluripotent hESCs into retinal cells (Lamba *et al.,* 2010). Additionally, studies have shown that precursor cells have a better ability to integrate into recipients and that transplantations success is possible despite the extent of retinal degeneration (Barber *et al.,* 2013).

Current methods only produce target cells with low efficiencies which are far too small to be exploited in a clinical environment. The key therefore lies in the optimisation of protocols in order to increase target cell production. A large contributing factor may be due to the production of EBs which results in the loss of a large proportion of the cell population which could potentially be differentiated into photoreceptor progenitor cells. By initially creating a protocol which omits the EB stage of photoreceptor differentiation could potentially make a vast increase in efficiency of target cells.

Current protocols have not been successful in creating vast numbers of Chx10 ineural retinal progenitor cells and have the tendency to create higher numbers of other early eye field progenitor cells expressing markers such as Pax 6 Lamba *et al.,* (2006). A protocol that could also be used to create larger populations of late eye field cells such as Nrl positive photoreceptor precursor cells would be extremely beneficial.

An optimised protocol whereby small variants of compounds such as ECM proteins and dissociation buffers and also create a protocol which omits the creating of EBs would be ideal. By achieving this goal a milestone would be reached in the differentiation process of photoreceptors and a platform created with potential of automation to be used for the manufacture of late photoreceptor progenitor cells.

Although at this stage, only part of the goal would have been achieved, once a successful protocol has been identified and used to create a large population of late photoreceptor progenitor cells, the next stage of the system could be investigated in more detail. With co-culture systems with retinal extracts proving to produce functional photoreceptors, investigations can then be made to identify prime factors released by these mature retinal extracts which encourage photoreceptor progenitor cells into mature photoreceptors.

Precursor cells have been proven to be capable of transplanting and maturing into cells that mimic mature photoreceptors and thus once an appropriate protocol has been established cells could possibly then de directly used and tested in transplantations studies. Once key components of the microenvironment are identified, these can then be exploited to artificially mimic the whole differentiation process of photoreceptor progenitor cells and create a breakthrough in therapy for the treatment of blindness caused by the degeneration of photoreceptors.

In general the potential for curative measures for blindness with the use of pluripotent stem cells is theoretically a very viable process. What remains to be difficult is the creation of an efficient protocol that could be used to establish a line of target cells with high efficiency. Once this hurdle has been overcome great potential will be unlocked for the future.

2 Aims and Objectives

Current methods of differentiation of hESCs into retinal cells remain suboptimal. Improvements to the differentiation process could be made by (i) identifying the best dissociation conditions before cells are entered into the differentiation process and (ii) creating a monolayer differentiation system to make the process more efficient.

This study aims to optimise current photoreceptor differentiation protocols to make an improvement to the efficiency of the protocol. In order to investigate various avenues for optimisation this study has been divided into three sections.

Characterisation of hESCs. This chapter investigates the characterisation of Shef3 hESCs using popular pluripotent markers and capabilities of cells to form EBs along with karyotyping analysis.

Differentiation of Shef3 hESCs using current photoreceptor differentiation protocols via EBs. This chapter investigates differentiation capacity of Shef3 hESCs following an already established protocol.

Optimisation of dissociation methods using an EB method of differentiation. This chapter investigate the impact of three different dissociation buffers on the differentiation protocol.

Monolayer differentiation method. This protocol investigates the possibility of a monolayer differentiation method and also explores the impact of various ECMs.

3 Materials and Methods

3.1 Human Pluripotent Cell Culture

Undifferentiated human pluripotent Shef3 cells (obtained from the UK Stem Cell bank) were cultured on mouse embryonic fibroblast (MEF) feeder cells inactivated with Mitomycin-C (1mg/ml, Sigma-Aldrich, Poole, UK) and maintained in hESC media (80% (v/v) Knockout DMEM, 20%(v/v) knockout serum, 1mM Glutamine, 1% (v/v) nonessential amino acids (NEAA), 100mM β-mercaptoethanol, 4.4ng/ml basic human fibroblast growth factor (bFGF) (all Invitrogen, Paisley, UK). Cells were cultured in a Sanyo IncuSafe incubator (Sanyo, MCO-18AIC, Leicestershire, UK) at 37^{O}C and 5%(v/v) CO_2 with an exchange of media every 48 hours.

Non-adapted cells were dissected into smaller colonies using a Fine Tip Mini Pastette (Alpha Laboratories, Hampshire, UK) every 3-4 days after incubation with 0.025mg/ml Collagenase Type IV (Invitrogen, Paisley, UK) at 37^{O}C for 3 minutes and transferred onto newly inactivated MEF feeder cells. Adapted cells were dissociated with TrypLE Express (Invitrogen, Paisley, UK) after incubation at 37^{0}C for 5 minutes.

3.2 Isolation of Mouse Embryonic Fibroblasts

Mouse embryos from day 13 post conception (p.c) were separated from the placenta using sterile tweezers and the brain and dark organs removed using fine surgical scissors. The embryos were then finely minced and incubated with 2mls Trypsin (Invitrogen) at 37^{o}C for 15 minutes. The supernatant was then resuspended in 2ml MEF media (DMEM, 10% (v/v) Foetal bovine serum (all from Invitrogen, Paisley, UK) and 1% (v/v) nonessential amino acids (NEAA) (Gibco)) and centrifuged at 1200 rpm for 3 minutes. The supernatant was discarded and the pellet resuspended in MEF media before being plated out in a T75 (Nunc) flask. This new batch of cells was denoted as "P0".

3.3 Feeder Preparation

Once MEF cells had reached a confluency of approximately 70% cells were inactivated with Mitomycin C (Invitrogen, Paisley, UK) for 2 hours at 37^{o}C, 5% $O_{2.}$ Cell were then washed with Dulbecco's phosphate buffered saline (DPBS) three times and for 10 minutes at 37^{o}C, 5% O_2. Cells were then neutralised with MEF media and centrifuged for 3 minutes at 1200rpm. The pellet was then resuspended in MEF media and counted using a haemocytometer. Cells were then plated onto 0.1% Gelatin (Sigma, Dorset, UK) diluted in sterile H_2O) coated T25flasks at 250,000 cells/cm^2.

3.4 Retinal Differentiation of Human Pluripotent Stem Cells

3.4.1 Embryoid Body Differentiation of Human Pluripotent Stem Cells

The differentiation of human pluripotent stem cells was based on a previously published protocol (Lamba et al., 2006). In accordance with this protocol, undifferentiated human pluripotent stem cells are dissected into smaller clumps with a Fine Tip Mini Pastette (Alph Laboratories) and cultured in suspension as embryoid bodies in a non-adherent 30mm bacterial grade culture dish (Sterilin, Caerphilly, UK). The EBs are maintained for 3 days in EB media (DMEM:F12, Kockout serum replacement (Both Invitrogen, Paisley, UK), GlutaMAX, B27 Supplement (PAA, Somerset, UK), Noggin (1ng/ml), DKK1 (1ng/ml), IGF-1 (5ng/ml)(All R&D Systems, Abingdon, UK). On day 4, EBs were plated onto a 6-well plate pre-coated with Matrigel (BD Bioscience, San Diego, CA) and maintained in differentiation media until day 21 (DMEM:F12, GlutaMAX, B27 Supplement, N2 supplement (All PAA, Somerset, UK), Noggin (10ng/ml), DKK1 (10ng/ml), IGF-1 (10ng/ml) and bFGF (5ng/ml) (All R&D Systems, Abingdon, UK).

3.4.2 Optimisation of Dissociation Buffer For EB Retinal Differentiation

Undifferentiated Shef 3 (P63) cells were induced into early neural retinal differentiation using the protocol described above. To investigate and optimise the dissociation buffer type, one flask of pluripotent hESCs was dissociated with one dissociation buffer or enzyme. One flask of pluripotnet hESC was dissociated by incubation with Collagenase Type IV (Invitrogen, Paisley, UK) for 3 minutes, another flask of pluripotent hESCs was dissociated with TrypLE Express for 5 minutes and another flask with Accutase (Both Invitrogen, Grand Island, NY) for 5 minutes at 37^{o}C. The remainder of the differentiation protocol was carried out as outlined above.

3.4.3 Monolayer Retinal Differentiation

Shef 3 (P52) cell line were maintained in EB media (DMEM:F12, Kockout serum replacement (Both Invitrogen, Paisley, UK), GlutaMAX, B27 Supplement (PAA, Somerset, UK), Noggin (1ng/ml), DKK1 (1ng/ml), IGF-1 (5ng/ml) (All R&D Systems, Abingdon, UK) for 3 days in a T25 culture flask on MEF feeders (250,000 cells per flask). The media was then completely replaced with differentiation media (DMEM:F12, GlutaMAX (Invitrogen, Paisley, UK), B27 Supplement, N2 supplement (Both PAA, Somerset, UK), Noggin (10ng/ml), DKK1 (10ng/ml), IGF-1 (10ng/ml) and bFGF (5ng/ml)(All R&D Systems, Abingdon, UK)) and maintained in culture until day 21 with media changes given every 2-3 days. Cells were passaged on day 7 and 14 with samples taken and pelleted for further investigations. On day 20, cells from one T25 flask were plated into two 12-well-plates (12-wp). Each row was coated in one of the following extracellular matrix proteins (ECM): PDL (4µg/cm^2), Laminin (2 µg/cm^{2,}), Fibronectin (5µg/cm^2, (All Sigma, Dorset, UK)), 0.1% Gelatin, Matrigel (diluted 1:3 in serum free basal media, BD Biosciences 354230) and one row left uncoated (blank). These 12-wp were then cultured in differentiation media for a further 6 days. It must be notes that for the investigation using Shef 3 cells, bFGF was omitted from the differentiation media.

3.5 Immunocytochemistry

All cells were fixed using 2ml 4% (w/v) paraformaldehyde (PFA) for 20 minutes at room temperature followed by several washes with DPBS and stored at 4^{o}C in DPBS. For intracellular staining, cells were permeabilised in permeabilisation solution (DPBS and 0.25% (v/v) Triton X-100 Sigma T8787) for 10 minutes at room temperature, followed by two washes with DPBS (note for extracellular staining the permeabilisation stage was omitted). Blocking solution (PBS, 0.25 % Triton and 2% Goat serum Sigma G9023) was then added to the cells and incubated at room temperature for 30 minutes. The blocking solution was then removed and the primary antibody (diluted in blocking solution) then added to the cells and incubated at 4^{o}C overnight.

The primary antibodies used were as follows: monoclonal mouse anti- SSEA1(1:200) , monoclonal mouse anti- SSEA3 IgM (1:200) (Both kindly donated by Peter Andrews, Sheffield), monoclonal mouse anti -OCT4 IgG (Invitrogen 1:400), B-III-Tubulin (Sigma, Dorset, UK), Chx10 (Millipore, Watford, UK), Pax6 (Millipore, Watford, UK). Cells were then washed several times with DPBS before the addition of the secondary antibody either Alexa Fluor 555 goat anti-mouse IgG (H+L) 2mg/ml, Alexa Fluor 488 goat anti-mouse IgG (H+L) (Both Invitrogen, Paisley, UK) and incubated at room temperature for 2 hours.

After several washes with DPBS, 4',6 Diamidino-2-phenyl-indole, dihydrochloride (DAPI) (Invitrogen, Paisley, UK) was then added to the cells and incubated for 2 minutes before being discarded. After a final wash with DPBS cells were then analysed using a fluorescence microscope.

3.6 RNA Extraction and cDNA Synthesis

All RNA extractions were achieved using the protocol by the Qiagen RNeasy kit (Qiagen, West Sussex, UK). In short, pelleted cells were resuspended in buffer RLT (guanidine thiocyanate buffer)and homogenized via aspiration through an RNase-free syringe using a 18G needle 5 times. Following the manufacturer's protocol the DNase digestion was also followed and finally the RNA was eluted with 40µl RNase-free water after centrifugation at 10,000 rpm for 1 minute. The concentration of the eluted RNa was measured using a spectrophotometer at 260nm (NanoDrop ND-1000, Thermo Scientific, Epson, UK).

cDNA synthesis was carried out following the Ambion 1st Strand cDNA synthesis kit (RETROscript®Ambion, Warrington, UK) using 1µg of RNA previously extracted. Briefly, using 1µg of RNA, random decamers and nuclease-free water was added to make up a volume of 12µl before centrifugation at 10,000rpm for 30 seconds. The mixture is then denatured at 80^{o}C for 3 minutes and cooled for up to an hour at 4^{o}C, after which they were centrifuged and placed on ice whilst the matermix containing dNTPs, RT buffer, RNAse inhibitor and MMLV-RT enzyme were added. The cDNA synthesis was then carried out at 42^{o}C for 1 hour followed by the inactivation of the enzyme at 92^{o}C for 10 minutes.

3.7 Real-time Quantitative Polymerase Chain Reaction (qPCR)

All qPCRs were carried out using the MESA Blue qPCR SYBR assay kit (Eurogentec, Hampshire, UK) following the manufacturers protocol. All primers were acquired from Qiagen and are listed in Table 3.1 and all reactions were set up using an Eppendorf Master cycler Realplex machine for reaction incubation and analysis. The total reaction volume was 20µl containing 1µl of cDNA and each measurement was taken in triplicates. The following PCR conditions were used: 95^{o}C for 5 minutes, followed by 40 cycles at 95^{o}C for 15 seconds and 60^{O}C for 2 minute. This was followed by another stage at 95^{O}C for 15 seconds followed by a cool down process at 60^{O}C for 15 seconds and incubation at 95^{O}C for 15 seconds. All samples were normalised to an endogenous housekeeping gene (β-actin) and relative quantification carried out using a protocol previously published (Pfaffl *et al.,* 2001). This equation uses expression levels of a housekeepiung gene as a standard to provide ratios of target gene expression, thus giving a fold increase or decrease of expression of target genes.

Table 3.1: A list of qPCR primers used for analysis.

Gene Name	Symbol	Transcript Detected	Catalogue Number
Actin, Beta	ACTB	NM001101	QT01680476
Orthodenticle homeobox 2	OTX2	NM021728	QT00213129
Six homeobox 3	SIX3	NM005413	QT00211897
Paired box 6	PAX6	NM000280	QT00071169
Visual system homeobox 2	VSX2 (CHX10)	NM182894	QT00221081
Retina and anterior neural fold homeobox	RAX (RX)	NM013435	QT00212667
Cone-rod homeobox	CRX	NM000554	QT01192632
Neuralretina leucine zipper	NRL	NM006177	QT01005165

4 Characterisation of Shef3 hESCs

4.1 Introduction

In 1998, Thompson and his group were the first to isolate the world's first hESC lines from the inner cell mass of the human blastocyst. The group also created essential characterisation criteria that would define a hESC. If a cell was able to maintain (i) in an undifferentiated state of proliferation for a prolonged period and (ii) was able to hold a stable potential to form derivatives of all three germ layers even after prolonged culture then this would characterise that cell as a pluripotent hESC (Thompson *et al.*,1998). These very properties of hESCs make them the ideal candidates for the development of novel cellular therapies, with the potential to treat a vast number of degenerative diseases as potentially, these cells could be directed to form any cell of the body.

1.7.1 4.1.1 Aim

The aim of this investigation was to identify whether human embryonic stem cells (Shef3-hESCs) fulfilled all the characteristics that governs a cell to be a pluripotent stem cell.

4.2 Morphology of undifferentiated Shef3-hESCs

Although numerous techniques are available in order to identify whether cells comply with the criteria described above, several classic cellular surface markers have been found to identify hESCs in the undifferentiated state. Stage-specific embryonic antigens (SSEA)-3, SSEA-4, TRA-160 and TRA-181 have all been found to be expressed in hESCs whilst they are in an undifferentiated state (Carpenter *et al.*,2003).

By raising antibodies against these markers, immunocytochemistry is commonly used to identify undifferentiated hESCs (Thompson *et al.*,1998). Similarly, transcription factors Oct 4, Nanog and Sox2 have been identified in the presence of pluripotent hESCs and thus using the same technique, whereby antibodies are raised against these markers, pluripotent hESCs can also be easily identified (Loh *et al.*, 2006).

Typically hESCs are cultured in the presence of a mouse embryonic fibroblast (MEFs) feeder layer, in order to aid with maintenance of cells in a pluripotent state in culture. As this process introduces the cross contamination of species it is not viable for use in a

clinical environment (Mallon *et al.*,2006). For this reason a range of feeder- free culturing systems have now become available whereby commercially available extracellular matrices (ECM) replace the need of MEF feeders as.

Human embryonic fibroblasts (HEF) have also now become available to maintain culture of hESCs on a feeder culture system that does not introduce cross contamination (Amit *et al*., 2003; Hernandez *et al.,* 2011).

In this investigation, Shef3 hESCs were co-cultured with MEFs, inactivated with Mytomycin C in order to maintain cells in an undifferentiated state. Within three days of culture cells were observed to be tightly compacted displaying the characteristic flat, rounded morphology of hESCs colonies (Figure 4.1).

The colonies were also found to abundantly express pluripotent and undifferentiated markers Oct4, TRA-160 and SSEA-3 (Figure 4.1). SSEA recognise defined carbohydrates on epitopes of lacto and globo-series glycolipids and are involved in the control of cell surface interactions during development (Zhao *et al.,* 2012). Both SSEA3 and SSEA4 are synthesised during oogenesis and thus is expressed in hESCs whilst they remain in an undifferentiated state (Zhao *et al.,* 2012). The TRA-1-60 antibody reacts with a part of a proteogylcan that is sensitive to neuraminidase (Zhao *et al.,* 2012). Neuraminidase is a group of enzymes which cleave glycosidic linkages in neuraminic acids.

TRA-160 and SSEA-3 are both cell surface markers and it is clearly visible from the immunocytochemistry results for these markers that cells express these markers abundantly across the whole population. Comparisons between the fluorescence exhibited by the markers and the DAPI staining are visually identical; suggesting that the expression observed is a true reflection of expression of these markers and not residual fluorescence from improper washing steps during the staining process.

Oct4, as the name suggests, is a member of the POU family of transcription factors and plays important roles in the regulation of pluripotency and differentiation in hESCs (Zhao *et al.,* 2012). The expression of Oct4 is maintained in the inner cell mass of the blastocyts and is restricted mainly to pluripotent and germ line cells (Zhao *et al.*, 2012).

In the case of transcription factor Oct4, results again exhibit a high expression of this marker throughout the population of cells suggesting that this population of hESCs is

truly pluripotent (Figure 4.1). Once again, results for Oct 4 expression is almost identical to that of the DAPI staining and phase image of cells, suggesting that all cells visible in this population are in fact also pluripotent. This clearly suggests that this population of cells were characteristic hESCs and therefore those cells used in other investigations also held the same properties as they were initially retrieved from this very population of cells.

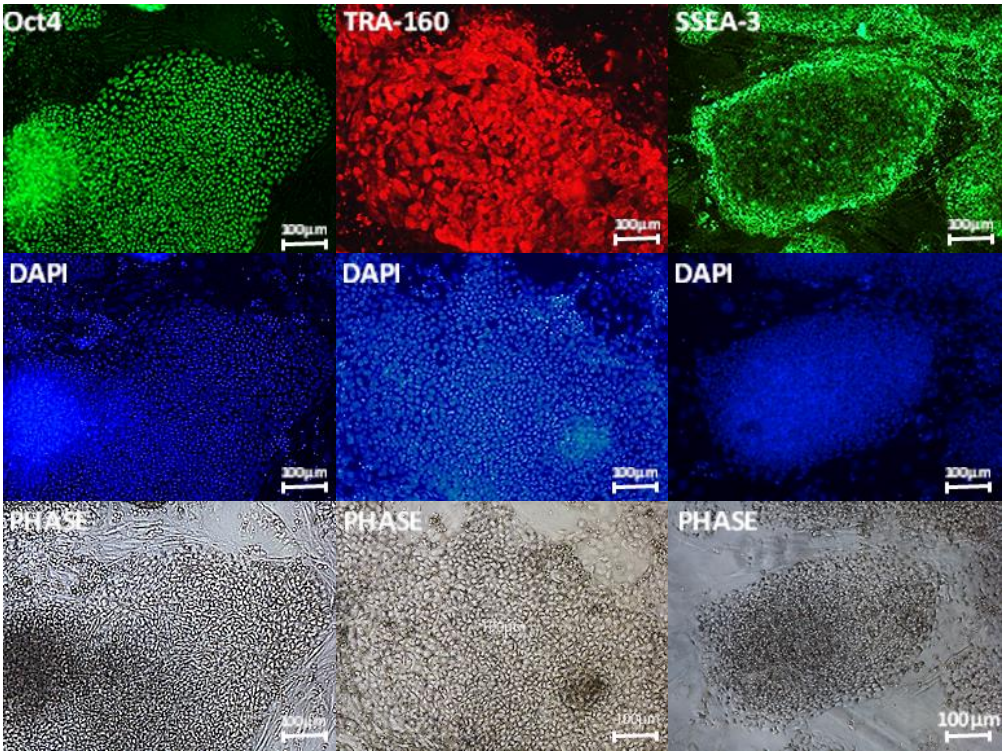

Figure 4.1: Immunocytochemistry results of pluripotency markers Oct4, TRA-160 and SSEA-3 for Shef3 hESCs. Top row shows expression of various markers of undifferentiation and pluripotency; second row shows nuclear staining with DAPI and bottom row shows phase constrast microscopic images of cells.

Once pluripotent hESCs are plated onto a MEF feeder layer, cells were found to attach to the MEF feeder layer. These cells then continued to proliferate in an undifferentiated manner. Morphologically these cells appear as well rounded cells, displaying a prominently large nucleus (Figure 4.2A). Occasionally in a population of undifferentiated cells, more than one prominent, dark structure is often visible in one cell. This is more than likely a result of a cell undergoing mitosis, whereby the cell

proliferates and divides into two cells and thus the number of organelles are doubled at this point (Figure 4.2A).

As cells proliferate within colonies, the peripheral edges of colonies appear phase-bright and distinct. Whilst colonies continue to grow, the feeder layer surrounding these colonies appears as whorls around these colonies (Figure 4.2B).

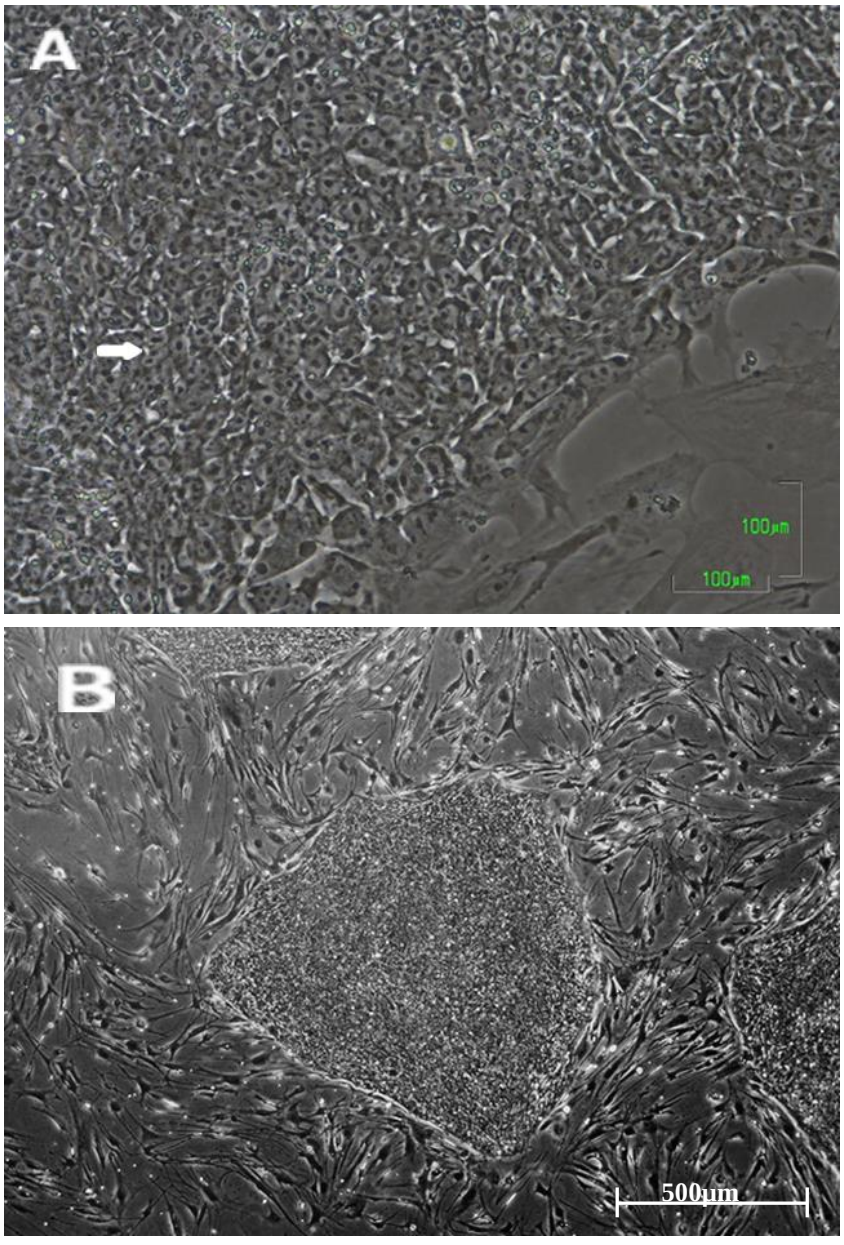

Figure 4.2: Morphology of healthy undifferentiated cells.A:A high magnification of undifferentiated Shef3 cells. Arrow indicates an example of a cell containing two dark structures most likely to be nuclei. This is an example of a cell most likely to be undergoing mitosis. B: A typical colony of undifferentiated hESCs.

4.3 Differentiation of Shef3 hESCs

As differentiation sets in this also results in the loss of the bright periphery of the colony (Figure 4.3A). Figure 4.3 A shows the morphology of undifferentiated Shef3 hESCs on the left of the image whilst differentiated cells, forming rosette like structures are visible towards the right of the same image. A change in shape in these cells is notable, with cells losing their characteristic well rounded shape as differentiation occurs. It is also difficult to identify the large nucleus in the centre of the cell, which usually appears as a very prominent structure in undifferentiated cells.

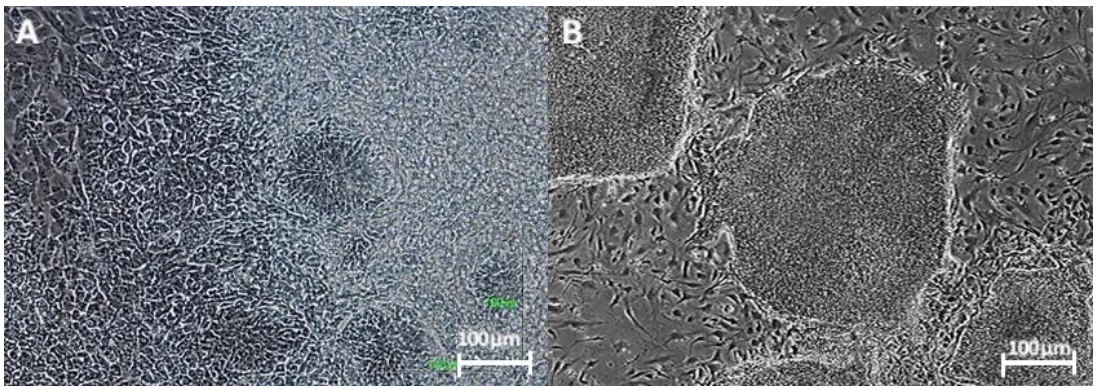

Figure 4.3: Morphology of Shef3 hESCs undergoing differentiation. A: Image of cells remaining in a state of undifferentiation (left) and differentiation (right) within a population of cells. B: Morphology of cells at the beginning of differentiation within a colony. Areas where a break in the phase-bright periphery are areas where differentiation is taking place.

With the onset of differentiation hESCs have been found to express a cell surface marker SSEA1, which is not expressed by hESCs in the undifferentiated state. Immunocytochemistry can be employed to identify cells undergoing differentiation (Figure 4.4). As is visible from the image below, cells within a population or colony of cells differentiate at various time periods. Some cells within the colony express a high intensity of SSEA1 whilst expression levels are very low in other parts of the cells. This suggests that, as expected, differentiation is not one uniform process that occurs within one population of cells, but instead individual cells undergo differentiation at various points. Once a particular cells starts differentiation however, it is also then capable of contributing in the direction of surrounding cells through the same process or encouraging surrounding cells to continue through the same process via inter cellular

signalling processes. This could be one explanation to the abundance of fluorescence emitted by single cells in a population surrounded by cells only emitting low levels of expression.

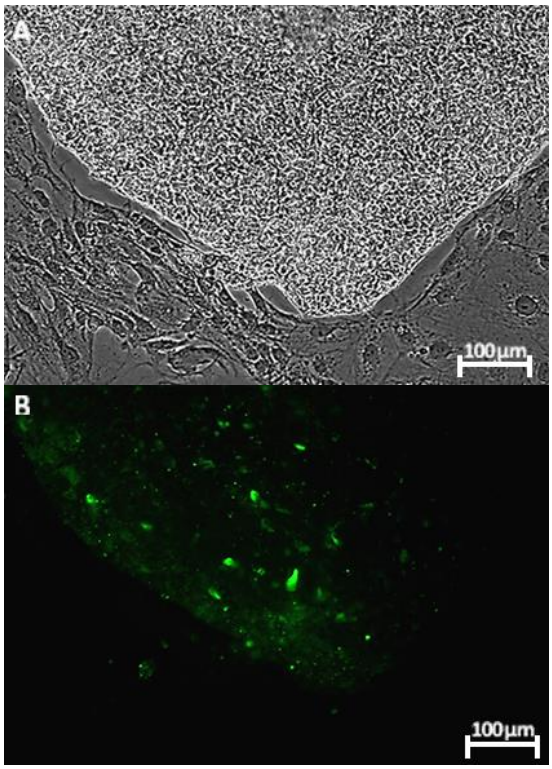

Figure 4.4: Immunocytochemistry results for cell surface marker SSEA1 on a population of hESCs. A: Microscopic image of cells. B: SSEA1 results for the same population of cells in image A.

4.4 Formation EBs from pluripotent Shef3 hESCs

One commonly used strategy to encourage undifferentiated hESCs down a specific lineage is through the formation of embryoid bodies (EBs) in suspension. Cells are dissociated from the monolayer and cultured in specific supplemented media in a suspended manner. These cells then make cell to cell adhesions in suspension via adhesion receptors and form small aggregates called EBs (Bratt-Leal *et al.,* 2009). These EBs are typically formed over a period of days or weeks and are found to form spheres of aggregated cells. Aggregates are usually well rounded in morphology. This process is often employed to initiate a specific differentiation route of cells and is often followed by a classic attachment culture system once the period of suspended culture has occurred. An example of EBs formed after 5 days of static suspended culture is shown below (Figure 4.5). As is evident from the image pluripotent hESCs form aggregates within the suspension. These 3D aggregates are darkened in colour when analysed under an electron microscope due to the dense makeup of cells within the aggregate. The size of aggregates are not uniform in this particular investigation as they are highly dependent on the number of cells which have come together in order to form the EB, which in this case, is dependent on location of the cells in suspension (the main reason for heterogeneous EB size and shape of is due to a limited control of the initial size of hESCs colonies at the beginning of suspension culture, not location of the colonies in suspension).

Technology has however progressed for this process, whereby culture plates with minute wells force equal numbers of single hESCs into EBs, making this process more uniform throughout investigations. One such culture plate is called the AggrWell produced by StemCell Technologies. As mentioned before in chapter 1.8.1 this plate has a number of micro wells built into the plate and as a single cell culture suspension is added to the plate, after centrifugations cells settle to the bottom of the micro well. Culturing of cells then proceeds as normal but allows the formation of EBs in a uniform and reproducible manner.

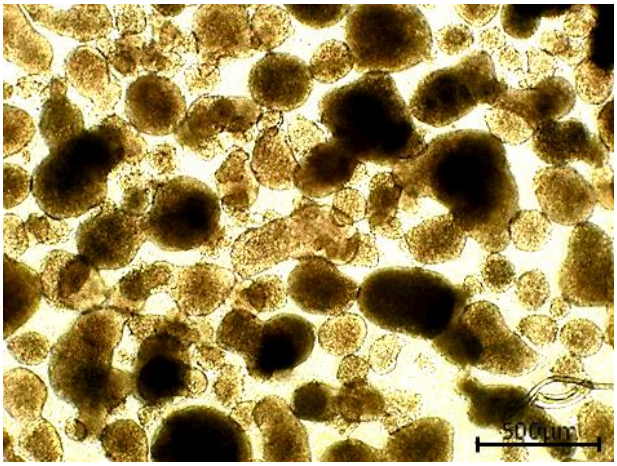

Figure 4.5: Image of EBs formed from Shef3 hESCs after 5 days of suspended culture.

4.5 Karyotype analysis of Shef3 hESCs

The ultimate goal for clinical therapy is to differentiate pluripotent stem cells into target cells which can then eventually be transplanted into humans to treat the disease that is deficient of those target cells.

Pluripotent stem cells have enormous potential as mentioned previously due to their potential to follow any lineage to become potentially any cell in the body. Whilst pluripotent hESCs are capable of remaining in an undifferentiated state for prolonged periods of time in culture, this leaves cells prone to genetic changes. This, for obvious reason poses a challenge for application in therapy as this has potential to lead to tumour progression (Loring *et al.*,2007).

Thus, it is very important to ensure that cells contain normal number and structure of chromosomes before any hESCs are used for investigative purposes. Cells with chromosomal abnormalities could lead to tumour progression if incorporated into regenerative medicine.

Karyotyping results for a sample of the pluripotent Shef 3 hESCs shows normal number and structure of chromosomes (Figure 4.6). The karyotype investigation was carried out by a third party.

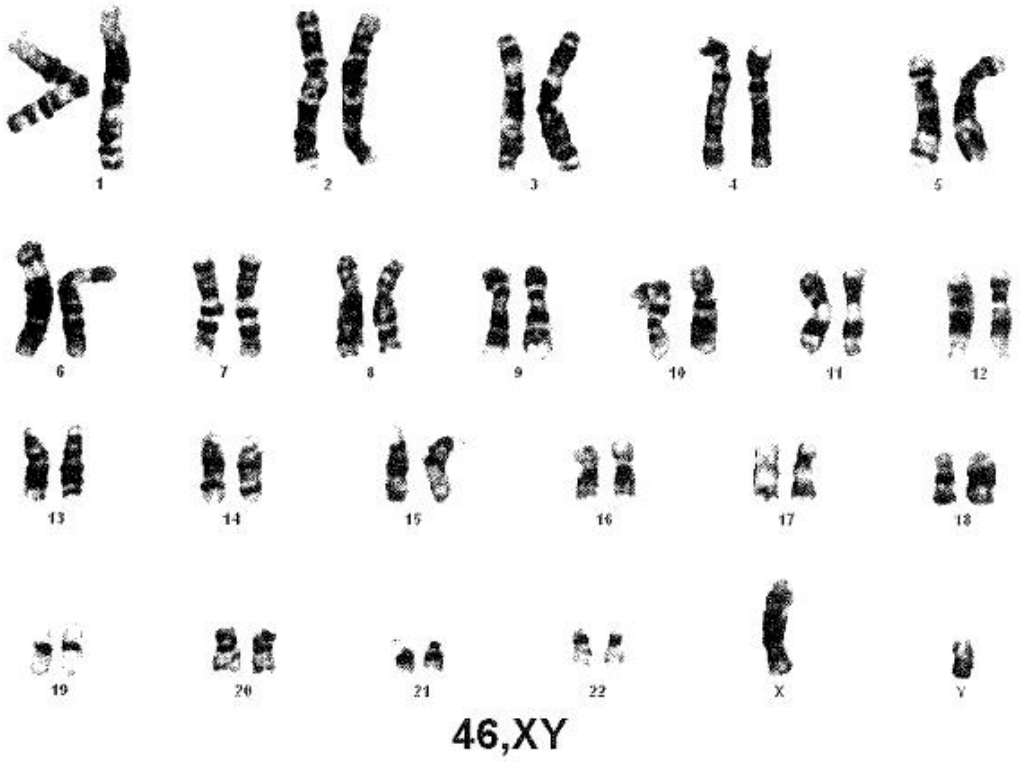

Figure 4.6: Cytogenetic analysis of Shef 3 hESCs. Image shows results of karyotyping of these cells.

5 Differentiation of Pluripotent Human Embryonic Stem Cells using the Lamba protocol

5.1 Introduction

The degeneration of rod and cone photoreceptors is a major cause of blindness, affecting millions of people around the world. Unfortunately, current treatment only aim to slow down the process of degeneration but no cure is presently available for ocular diseases that result in blindness. Human pluripotent stem cells (hESCs) have given new hope for some degenerative diseases such as Retinitis Pigmentosa (RP). The generation of retinal progenitor cells (RPCs) from these hESCs have been shown to integrate and function once transplanted into the sub-retinal space of mature mice (Lamba *et al.*, 2006; MacLaren *et al*., 2006).

A range protocols are now available, each using various combinations of growth factors which aid in inducing growth of primarily the forebrain. Some of these growth factors include: Dkk1 (Wnt signalling pathway anagonist), Lefty A (Nodal pathway anagonist) and Noggin (BMP pathway antagonist). Each protocol has varying time periods and efficiencies of target cells (Lamba *et al.*, 2006; Osakada *et al.*, 2008; Hirami, Osakada *et al.*, 2009; Meyer *et al.*, 2009).

Lamba *et al.*, generated over 80% of Pax6 expressing cells and over 70% of Chx10 expressing cells. A small percentage (~5%) of cells expressing the photoreceptor precursor gene Nrl was also recorded. This particular protocol included the shortest timeframe, to date, of 21 days. It should be noted that target yields can vary significantly depending on pluripotent stem cell lines (Osakada *et al.*, 2009).

The Lamba protocol was followed in this investigation. This was because after taking into consideration of timeframes, number of soluble factors required for the differentiation as well as target yields, this protocol provided the most efficient process. As this protocol involves the formation of EBs, the terms “EB differentiation” and “EB incorporated differentiation” have been widely used in this study in reference to the whole process of this differentiation method.

5.1.1 Aim

The aim of this investigation was to reproduce the Lamba protocol and generate RPCs. As this chapter contains the control data, any benefits of optimisations of the protocol are comparative to these results.

5.2 Differentiation of Shef 3 hESCs following the protocol devised by Lamba

In accordance with the Lamba protocol, Shef3 hESCs were mechanically dissected from the feeder layer with Collagenase IV. Cells were then cultured in suspension for a period of 3 days with media supplemented with the following growth factors: DKK1, Noggin and IGF-1. During this period of suspended culture, colonies began to form floating aggregates similar to EBs. These EB-like structures did not appear as well rounded spheres commonly reported in literature (Figure 5.1). By definition, an EB is an aggregate of cells, containing cells from all three germ lines. Visually cells appeared as aggregates, but verification that these aggregates were EBs would require a test confirming the presence of cells from all three germ lines.

After day 1 of suspended culture, large aggregates were observed with areas of densely populated cells. In some cases aggregates were observed to have combined to form very large sized aggregates (Figure 5.2). Although the mechanical dissection using Collagenase IV does not produce single cells, many single cells were observed in the suspension around the EB-like structures (Figure 5.2B). Many of these cells were observed to migrate and attach onto other cell aggregates. In some cases smaller EB-like structures were observed to migrate and attach to either bigger aggregates or form smaller aggregates (Figure 5.2B).

A small population of debris was also observed in the suspension appearing as small dark specks in comparison to live cells which exhibited a bright appearance.

By day 3 of the suspended culture, aggregates were observed to have become very densely populated with cells. This gave aggregates an extremely dark morphology. At this point in the investigation a visibly larger population of cell debris was also observed in comparison to that observed on day 1 of the suspension culture (Figure 5.2F).

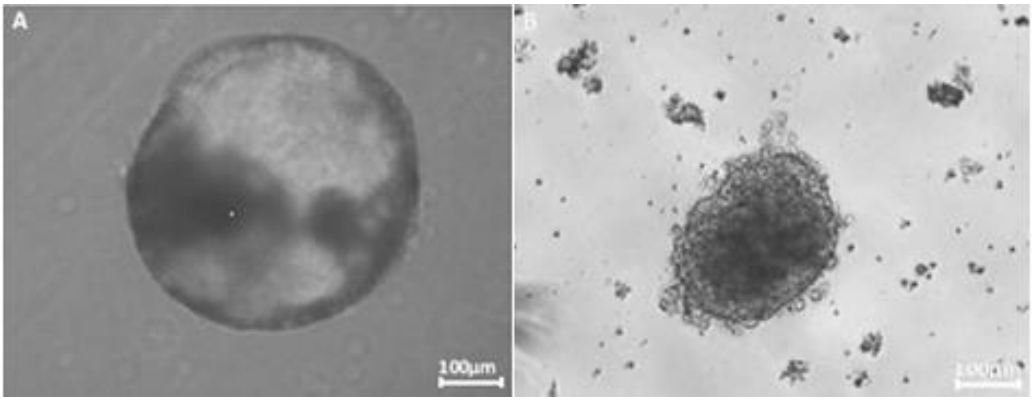

Figure 5.1: Morphology of EBs. A: Typical EB formed from suspension culture of WA09 hESC line. Image taken from Luzzani *et al.*, 2011. B: EB formed on day 3 of the differentiation protocol in this study.

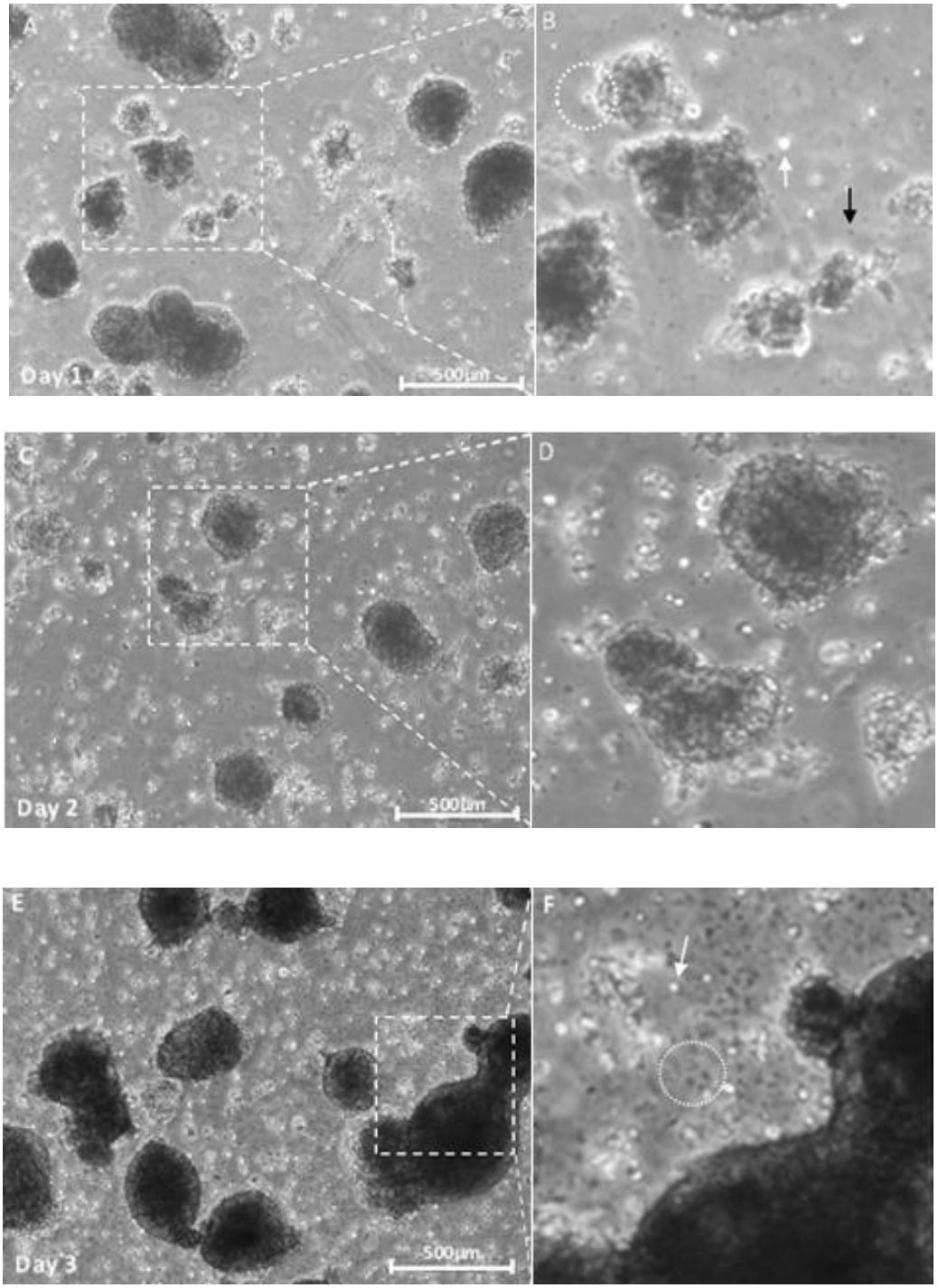

Figure 5.2: Morphology of cell aggregates formed from cells mechanically dissected with Collagenase VI at various time points in the differentiation process. A: Aggregates formed after day 1 of suspension culture. B: Enlarged image of the area indicated in image A. Image shows various sized aggregates migrating towards each other. White arrow indicates example of a live cell and the black arrow indicates an example of cell debris. C: EB-Like structures formed on day 2 of suspension culture. D: Enlarged image of area indicated in image C. E: EB-like structures formed on day 3 of the suspension culture. F: Enlarged image of area indicated in image E. Area indicates an example of cell debris which appear as black specks. The arrow indicates an example of a live cell.

After 3 days of suspended culture, EBs were plated down onto matrigel (day 4 of the differentiation process) coated 6-well plates and maintained in media supplemented with N2 supplement and bFGF (KOSR was omitted in this media) until day 21. Media changes were maintained every 48 hours.

Cells became adherent by day 5 and the point at which each cell aggregate had attached resulted in the formation of a colony of cells (Figure 5.3). Whilst cells located in the centre of the colony remained tightly compacted, those located on the edge of the colony exhibited signs of migration and differentiation (Figure 5.3B).

Several morphologies were observed. Some cells appeared more flattened with nodules sprouting out towards the surrounding (Figure 5.3 C & E). Others exhibited a more elongated morphology, with the elongation narrowing out into smaller elongations (Figure 5.3 F). These cells resembled the morphology of neural cells; the elongated centre was similar to an axon which progressed into smaller partitions resembling dendrites.

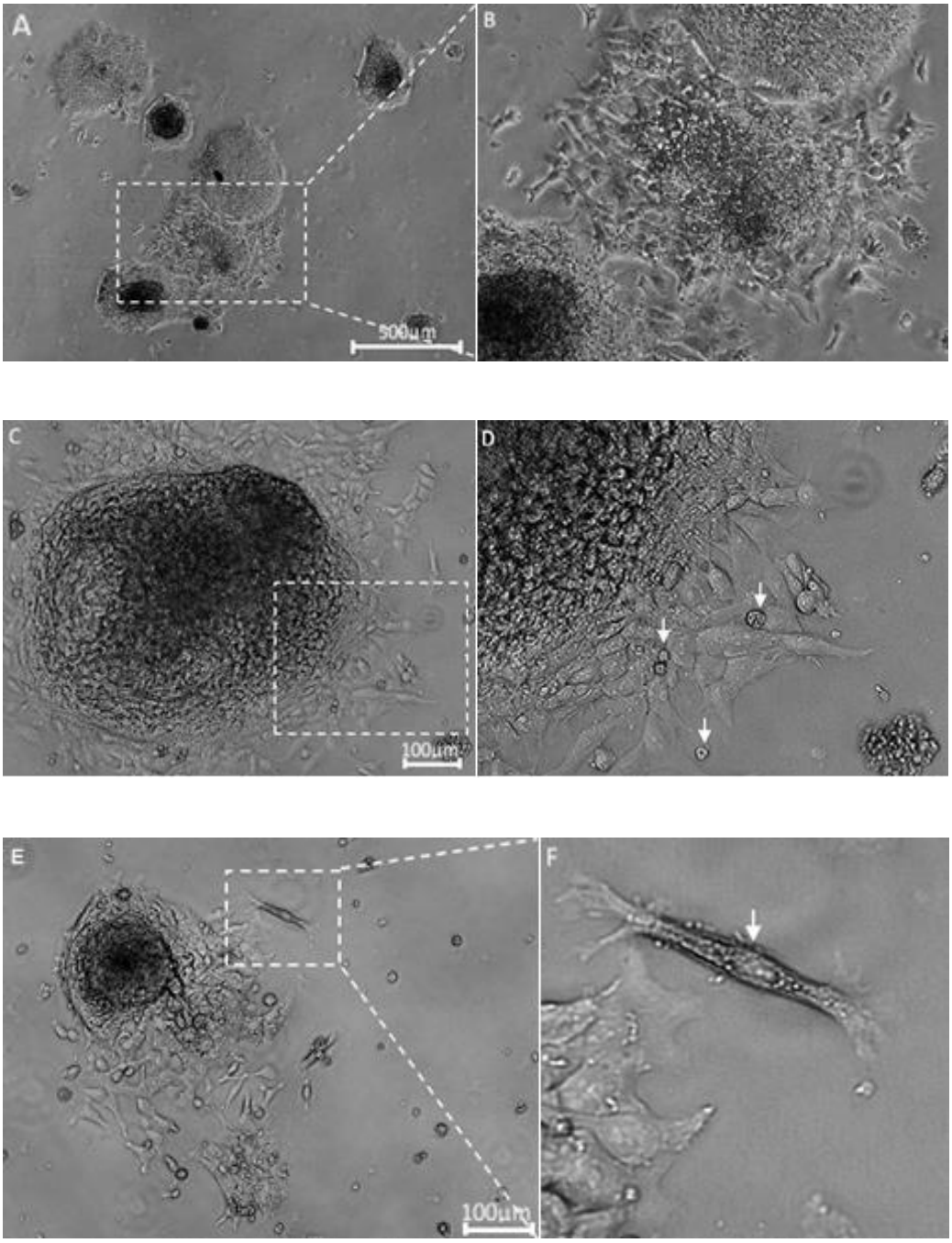

Figure 5.3: Morphology of cells on day 5 of the differentiation of Shef 3 hESCs. A: Colonies of cells. Area indicates a population of differentiating cells. B: Enlarged image of A. Morphology of flattened cells. C: Colony of cells with differentiating cells located on the edges of the colony. D: Enlarged image of indicated area on C showing morphology of differentiating cells. White arrows indicate example of circular cells. E: Colony of differentiating cells. Indicated area shows morphology of another cell type. F: Enlarged image of indicated area on E. Arrow indicates the presence of neural-like cells.

By day 6 of the differentiation process, cells had migrated outwards from their respective colonies although the reminiscence of the colonies was still visible (Figure 5.4 A). Cells located in the centre of these colonies still remained compacted but those located on the peripheral edges exhibited visual signs of differentiation. Amongst these tightly packed colonies of cells, populations of triangular cells were observed (Figure 5.4 B). These cells resembled epithelial cells in morphology (Nie *et al.*, 2008).

Some of these cells were more elongated in appearance than others whilst others exhibited small spindle-like structures. Cells containing spindle-like structures were mainly located on the edge of these populations of differentiated cells. Cells on the edge of these regions migrated and evolved to become more elongated by day 7 with the development of more spindle-like structures. Some cells displayed a star-like morphology common to astrocytes with small spindles sprouting out from a central body (Figure 5.4 D). These cells resembled fibroblast cells in appearance (Liu *et al.*, 2007).

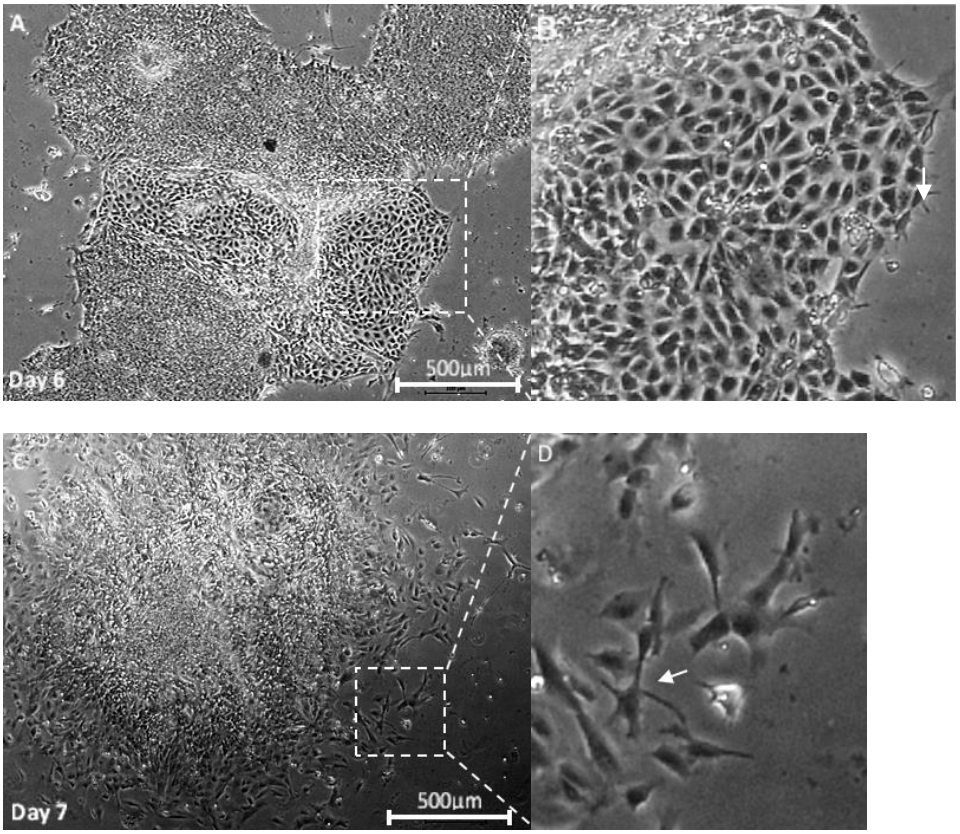

Figure 5.4: Morphology of cells on days 6 and 7 of the differentiation process. A: Cells on day 6 of the differentiation process. Area indicates example of triangular cells. B: Enlarged image of indicated area in image A. Epithelial-like cells. Arrows indicate an example of spindle-like structures. C: Cells on day 7 of the differentiation process. D: Enlarged image from indicated area on image C.

By day 10 of the differentiation process cells had become very compacted and had reached approximately 70% confluency. Amongst the compacted sheet of cells, colonies of epithelial-like cells were observed to have proliferated (Figure 5.5 A).

Larger numbers of these epithelial-like cells were observed. Some of these cells were found to have lost their triangular shape but remained as large cells in comparison to the compacted cells present in the overall population. Surrounding these regions of large cells, networks of intertwined spindle-like structures were observed (Figure 5.5B). Observations made using a higher magnification revealed that these spindle-like structures were beginning to pan over central regions of these large cells. These spindle-like structures were predominantly located on the edges of these cell groups (Figure 5.5 C).

By this point of the investigation, cells were observed to begin to proliferate and/or differentiate in multilayered structures in some areas of the culture vessel (Figure 5.5 A). This is often observed in the differentiation processes after attachment of EBs. Often as EBs attach, cells in the centre of the aggregate remain attached to other cells in the aggregate resulting in the formation of multi-layered structures after the attachment process.

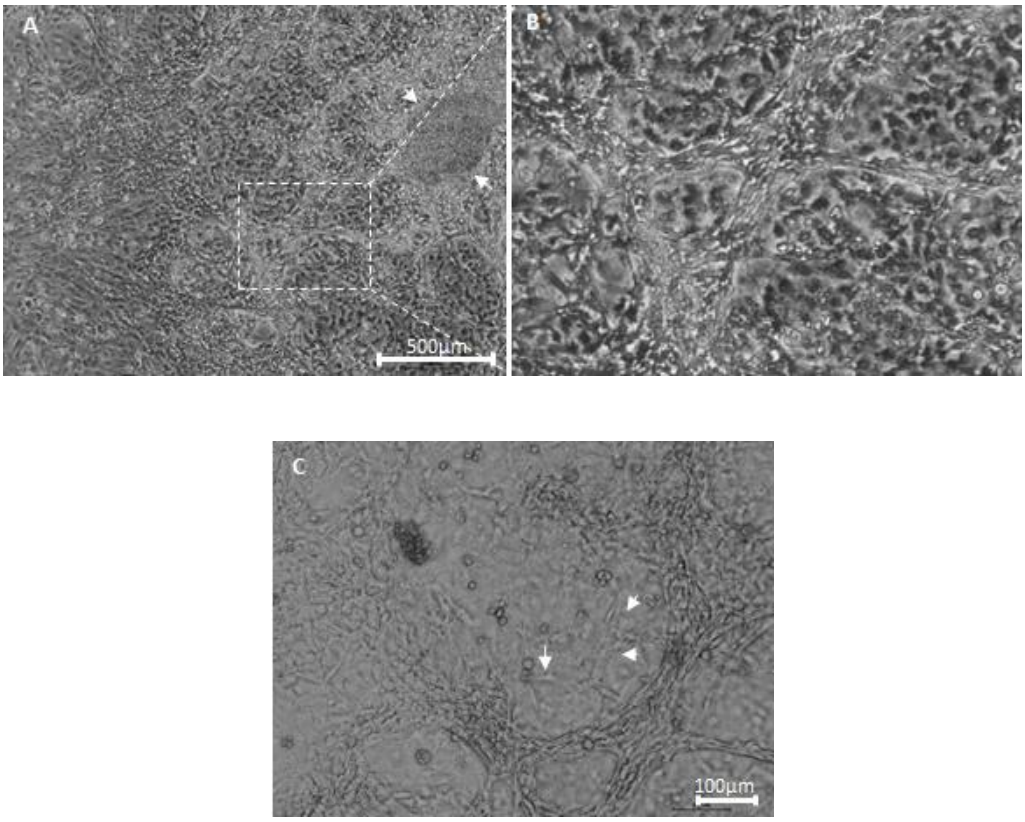

Figure 5.5: Morphology of cells on day 10 of the EB incorporated differentiation process (A). Area indicates a population of spindle-like structures. Arrows indicate a population of cells growing in multilayers. B: Enlarged image of indicated area in image A. C: Morphology of spindle-like structures.

By day 11 of the differentiation process, much of the same cell types were observed as mentioned above. Cells continued to migrate, proliferate and differentiate abundantly. Areas of compacted cells, were however, observed to have a change in morphology. Cells in these regions were so compacted that it was no longer possible to identify the morphology of single cells. All that could be visualised were a vast population of very small darkened specks (Figure 5.6 A). Magnified observations of these regions revealed the appearance of occasionally two darkened pigments in close proximity of each other and a vague shape resembling the number "8" in some cases (but not in all) (Figure 5.6 B).

An increase in small single cells was also observed in the cell population. Single cells appeared more distinct in areas of cells with a less defined morphology than cells with a triangular morphology. In some regions of large cells, cells were observed to have migrated, creating an appearance of more available space surrounding these cells (Figure 5.6 C) in comparison to the group of triangular cells observed previously. This migration of cells was not observed in all regions of large cells but only in some areas of these cells.

On day 12 of the investigation, these regions appeared larger in size with an increase of such cells. This suggested that these cells had proliferated during the 24 hours in culture (Figure 5.6 D). Some cells in these areas had also become more elongated and spindle-like structures were once again observed. Over the next 7 days of culture, cells became more compacted and formed multi-layered structures. Webs of spindle-like connections were observed across cell population in areas of large cells (Figure 5.6 E).

By day 19, cells had become extremely compacted with only a few regions containing large cells, the morphology of which was still vaguely evident amongst the mass of cells. In many areas, multi-layered structures had formed over the monolayer of cells and it was very difficult to identify specific cell types in the cell population (Figure 5.6 F).

By day 20, cells had become so over confluent that in some very densely compacted areas, the monolayer was observed to detach from the matrigel coating (Figure 5.7).

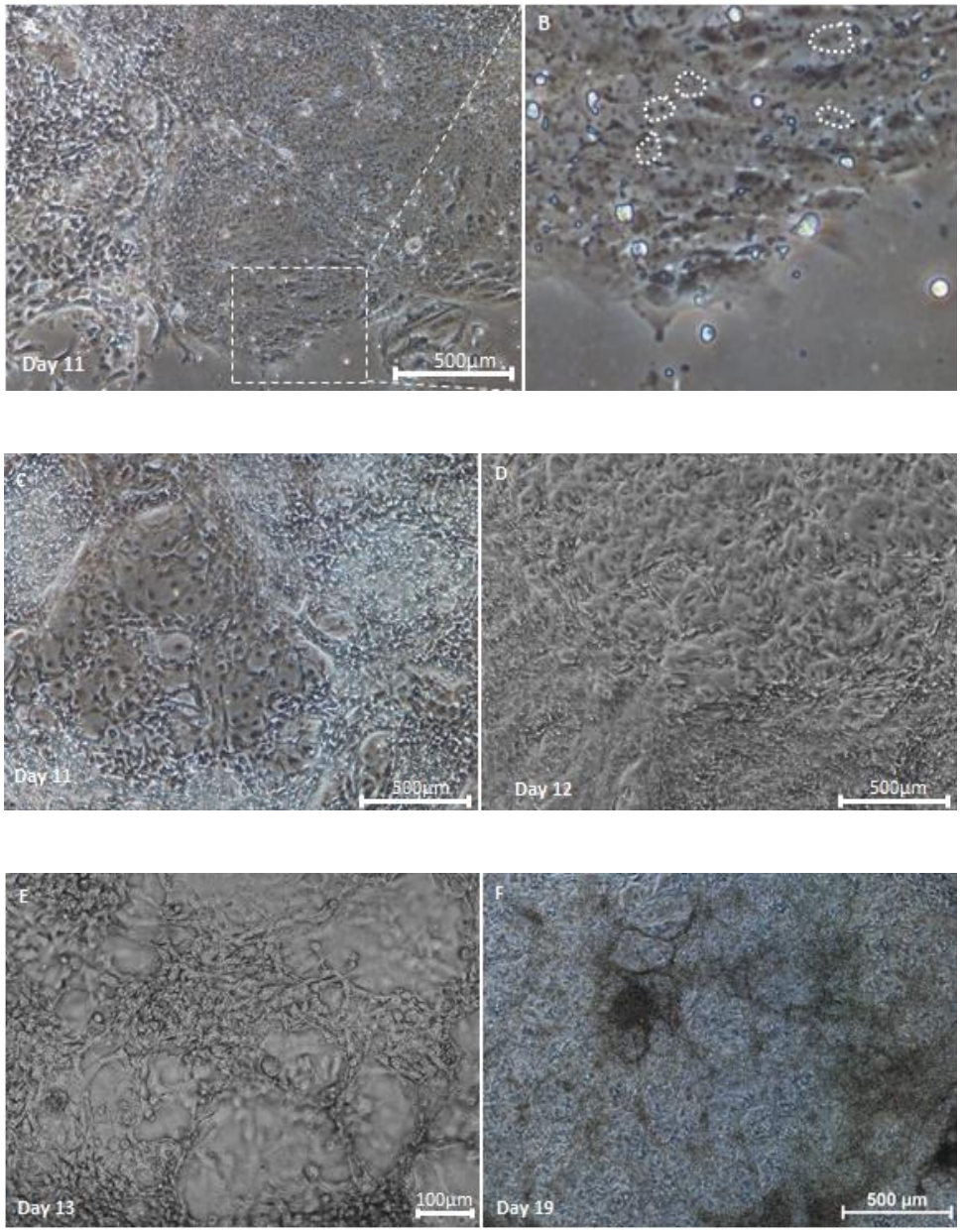

Figure 5.6: Morphology of cells during days 11, 12, 13 and 19 of the differentiation process. A: Image of cells on day 11 of the differentiation process. Area indicates example of compacted cells with mildly visible darkened specks. B: Enlarged image of area indicated in image A. C: Image of migrated, large cells on day 11. D: Cell morphology on day 12. E: Image of network of spindle-like structures on day 13 of the differentiation process. F: Cell morphology on day 19 of the differentiation process.

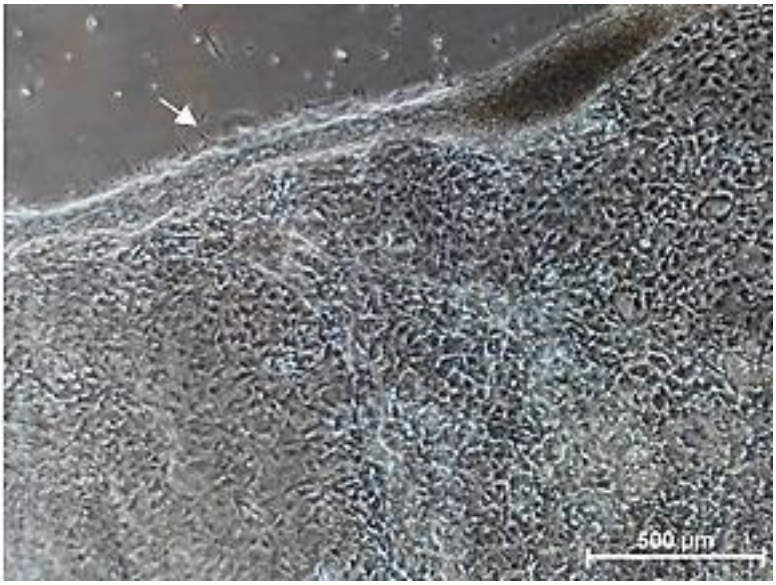

Figure 5.7: Cell monolayer detachment from the matrigel coating on day 20 of the differentiation process. White arrow indicates detachment of cells from the matrigel coating.

5.3 Generation of Early RPCs

Immunocytochemistry results revealed expression of neural retinal progenitor markers Pax 6 and Chx10 after 21 days of differentiation.

In the case of Pax6 expression, fluorescence was mainly observed in groups of compacted cells, although low levels were also observed in surrounding areas of these cells (Figure 5.8). Chx10 expression was observed to be more widespread in comparison to Pax6 (Figure 5.8).

The absence of Chx10 expression was most prevalent in areas where cells were not very compacted. Some of these Chx10 negative cells appeared fairly large and elongated. DAPI staining confirmed the presence of many cell nuclei in these areas providing further evidence that these cell types were negative in expressing Chx10. Additionally this also gives evidence that the fluorescence observed in these cells was specific.

After making comparisons between Pax6, Chx10 expression and DAPI staining, it was possible to conclude that this investigation was in fact successful in directing pluripotent hESCs down the retinal lineage.

This was because, as expected, not all areas where cells were present expressed a marker for retinal precursors. Additionally those areas exhibiting fluorescence coincided with the presence of differentiated cells suggesting this was a true display of cellular expression.

It must however be noted, that although retinal progenitor markers Pax6 and Chx10 were observed, overall, only low levels of expression were visualised. As ICC data only provides visual results thus quantitative PCR was used to confirm these findings (Figure 5.9).

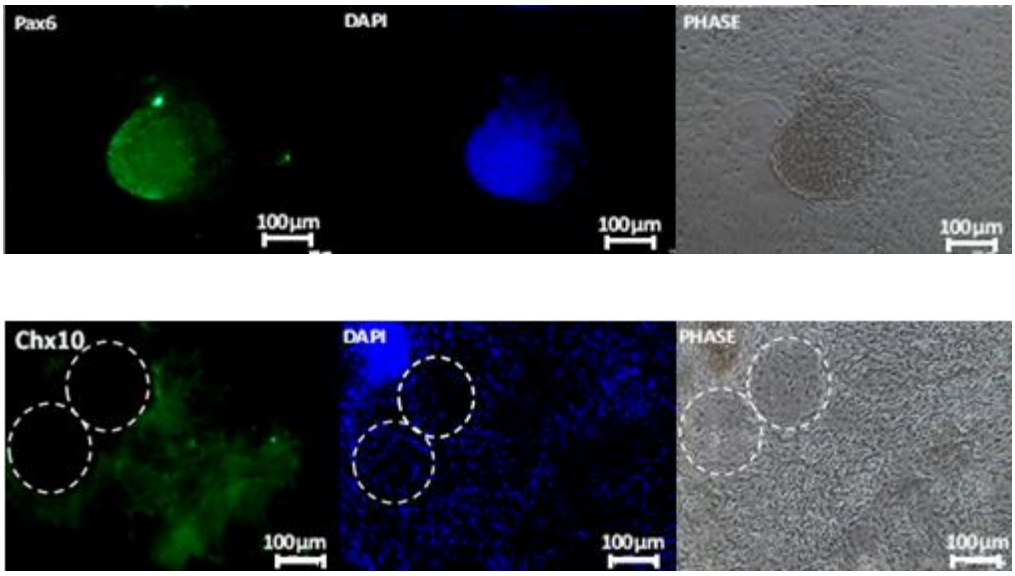

Figure 5.8: Generation of Pax6 and Chx10 positive cells from Shef3 cells differentiated using the EB incorporated differentiation protocol.

qPCR results confirmed low expression of early eye field genes Pax6, Six3 and Rx. Expression of Rx however, was found to be mildly more increased in comparison to Six3 and Pax6 (Figure 5.9).

In the case of Pax6 expression, this finding was in line with ICC data discussed above, as only low levels of fluorescence was observed for Pax6. Also in line with the ICC data, only low levels of Chx10 expression was observed although qPCR data revealed the expression of Chx10 was mildly more increased than Pax6. Only a 2 ½ fold increase of Chx10 expression was observed in comparison to the housekeeping gene β-actin (Figure 5.9).

Over a 5 fold expression of the later eye field gene, Nrl, was observed in comparison to the housekeeping gene (Figure 5.9). Nrl is a marker for photoreceptor precursor cells, confirming the presence of photoreceptor precursor cells in this differentiated population.

This confirms that this investigation was very successful in its aim in differentiating pluripotent Shef3 hESCs towards the retinal lineage. The significantly increased expression of Nrl, in comparison to other early eye field genes, is an indication that by the end of this differentiation process, a larger population of photoreceptor precursor cells was present than other early eye field cells.

In order to determine the efficiency of the protocol however, further investigations are required in order to calculate the percentage of eye field cells relative to the overall population of cells.

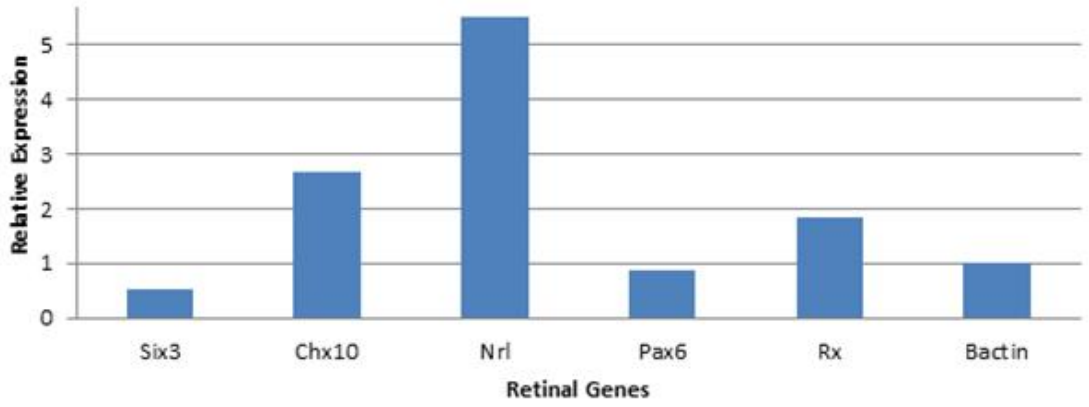

Figure 5.9: qPCR analysis of retinal gene expression of cells mechanically dissected with Collagenase IV. These cells were then differentiated into RPCs using the EB incorporated differentiation process.

5.4 Optimisation of the Lamba Differentiation Process

5.4.1 Aim

Although the protocol devised by Lamba and his group was successful in directing pluripotent hESCs into the retinal lineage, it was thought that optimisation of the protocol was still necessary in order to devise a more efficient and cost-effective protocol. As in most protocols, a vast numbers of avenues could be investigated as part of the optimisation. Such avenues included (but not exclusive): dissociation method type, cell seeding density, ECM protein coating type, buffer pH, oxygen percentage exposure amongst others.

In the first instance it was decided to investigate the method of dissociation of cells. This was because the dissociation of cells is involved right at the beginning of the process. If the method used to dissociate cell resulted in a negative effect on the differentiation capacity of pluripotent hESCs, then this would have a knock on effect on the retinal differentiation process. If pluripotent hESCs are damaged in the dissociation process at the beginning of the differentiation protocol, then this would result in a lower population of target cells at the end of the process. For this reason, Accutase and TrypLE Express were tested in order to investigate whether these methods of dissociation could impact the expression of RPC markers compared to the original mechanical dissection method with Collagenase IV.

5.4.2 Differentiation of Shef3 hESCs using dissociation enzyme Accutase and dissociation reagent TrypLE Express

In order to make precise comparisons the method of differentiation was followed as mentioned above (Chapter 5.2) with the exception of using Accutase or TrypLE Express in the cell dissociation stage. In short, cells were initially dissociated with either Accutase or TrypLE Express and maintained in suspension for a period of 3 days with media containing growth factors: DKK1, Noggin and IGF-1.

At this stage of the process both dissociation methods resulted in a high population of single cells in comparison to cells dissociated in the control investigation. Those dissociated enzymatically with Accutase were observed to produce a higher population of single cells than using TrypLE Express (Figure 5.10 A & C). TrypLE Express was found to have dissociated cells as a mixture of cells groups as well as single cells.

Both dissociation methods were observed to produce aggregates of cells during the period of suspension culture. Similar to what was observed in the mechanical dissection using Collagenase IV (the control), in this investigation aggregates were not well rounded EBs as often reported in literature.

After day 1 of the differentiation process, cells dissociated with TrypLE Express had formed fairly large aggregates in comparison to those formed by cells dissociated with Accutase (Figure 5.10). In the case of cells dissociated with Accutase, a large population of cell debris was observed. These appeared as small darks specks in the suspension, giving the appearance of a reduced population of cells in the wells.

Aggregates formed by cells dissociated with Accutase were observed to be visibly smaller in size than those formed by cells mechanically dissected with Collagenase IV and TrypLE Express, at the same time point. Aggregates formed by TrypLE Express had a very darkened appearance as these were very densely packed with cells in comparison to the smaller, lighter aggregates formed by cells dissociated with Accutase. In some cases, aggregates formed by cells dissociated with TrypLE Express were observed to attach to other aggregates (Figure 5.10).

By day 4, cells dissociated with TrypLE Express continued to form dark aggregates in comparison to cells dissociated with Accutase. In the later of these a larger population of single cells was observed to remain in the suspended culture (Figure 5.11).

Observations made at this point of the investigation found that of the three dissociation methods investigated, Accutase best favours cells to remain as single cells rather than in aggregates. In the case of Collagenase VI and TrypLE Express, these methods suited cells to remain in culture as aggregates. Although both Accutase and TrypLE Express produced a large population of single cells at the dissociation stage, cells dissociated with TrypLE Express continued to form many large aggregates whereas those dissociated with Accutase remained predominantly as single cells. Cells dissociated with Accutase also exhibited the largest population of cell debris in comparison to cells dissociated with TrypLE Express and mechanical dissection with Collagenase IV.

At this stage of the differentiation process it was unclear whether the formation of smaller aggregates or the presence of a high single cell population would have an effect on retinal gene expression at the end of the process. Although morphologically aggregates resembled EBs, in order to verify this cells would have to be tested in order to confirm the presence of cells from all three germ layers.

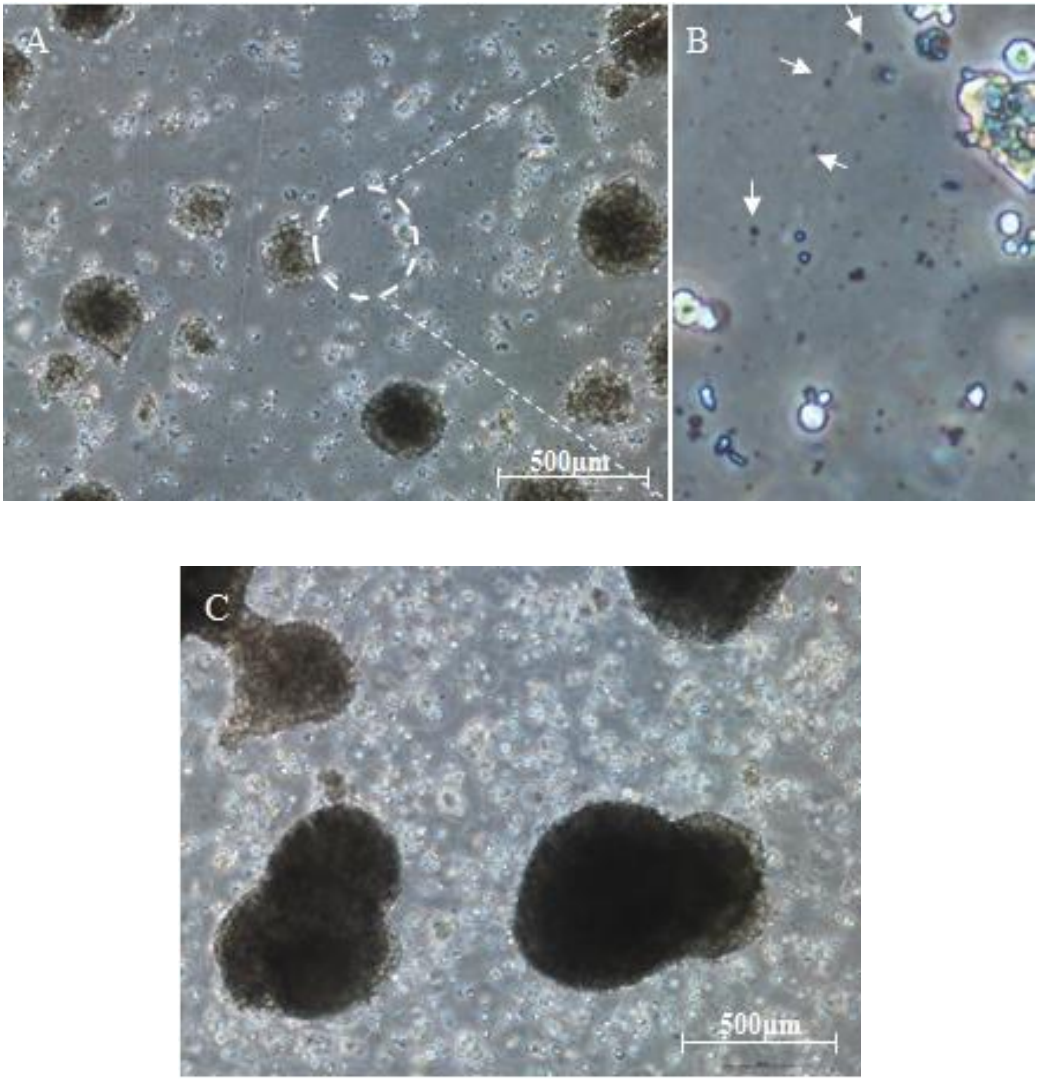

Figure 5.10: Morphology of day 1 aggregates formed from cells dissociated with Accutase and TrypLE Express. A: Aggregates formed by cells dissociated with Accutase. Area indicates area of cell debris. B: An enlargement of area indicated in image A. Arrows indicate examples of cell debris appearing as dark specks. C: Aggregates formed by cells dissociated with TrypLE Express.

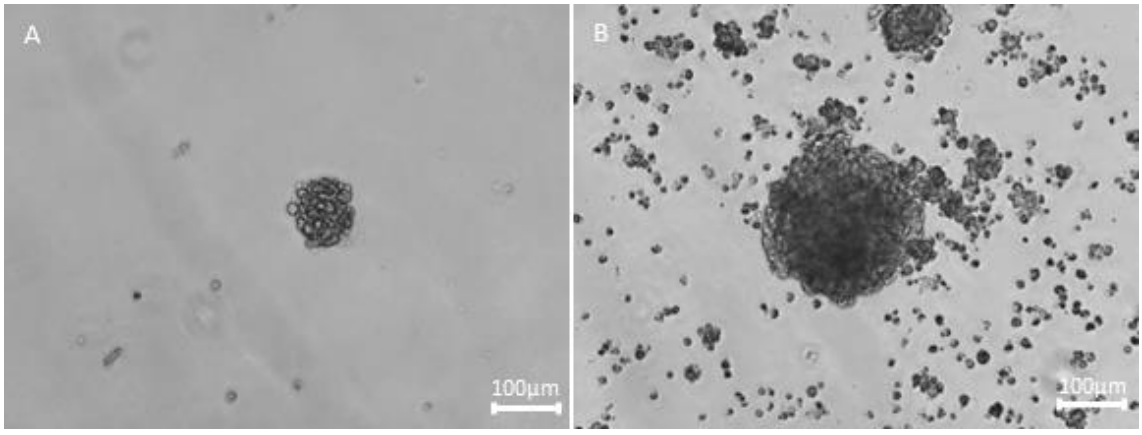

Figure 5.11: Morphology of day 4 aggregates. A: Aggregate formed from cells dissociated with Accutase. B: Aggregates formed from cells dissociated with TrypLE Express.

These cells were then transferred onto matrigel coated well plates and maintained in culture media supplemented with N2 supplement and bFGF until day 21 with media changes every 48hrs.

As a large population of single cells were present in cells dissociated with Accutase and TrypLE Express, care was taken to transfer all cells present from these cultures to ensure potential RPCs were not discarded.

As observed in the control investigation (mechanical dissection with Collagenase IV), cells dissociated with both Accuatse and TrypLE Express adhered and migrated well by day 5 of the differentiation process. In line with the control investigation, cells appeared to form colonies at the point at which the aggregate had attached to the coating (Figure 5.12A & C). Differentiation was also readily observed in cells dissociated with both TrypLE Express and Accutase. Cell appeared compacted towards the centre of the colonies whilst those located on the peripheral edges of colonies were observed to migrate outwards from the colony and differentiate (Figure 5.12). This was true for cells dissociated with both TrypLE Express and Accutase.

In the case of cells dissociated with Accuatse, differentiated cells were elongated but flattened in appearance, often with spindle-like structures sprouting out from the main body. These cells resembled fibroblasts (Figure 5.12B). Cells with the same morphology were also observed in cells dissociated with TrypLE Express. In addition to these cells, more cell types were observed in cells dissociated with TrypLE Express.

In some areas of the wells, very elongated, thin cells were observed with ends dividing into further spindle-like structures resembling dendrites. These cells also contained a cell body within the main elongation and resembled the morphology of nerve cells (Figure 5.12D). The nucleus was difficult to identify in these cell types.

As cells dissociated with Accutase only produced small aggregates in size, it was no surprise that the colonies of cells observed after the attachment were also small in size in comparison to those observed in cells dissociated with Collagenase VI and TrypLE Express.

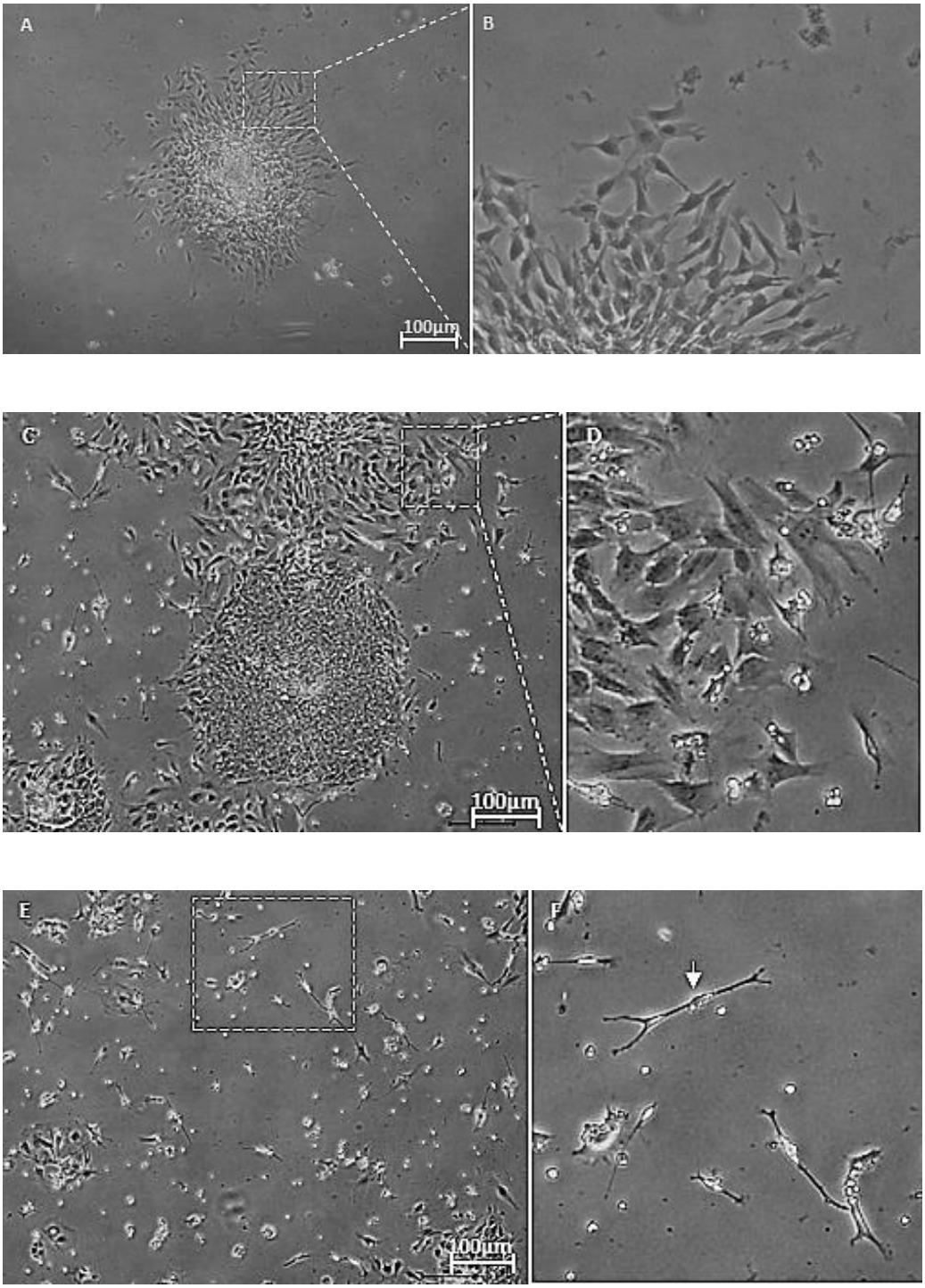

Figure 5.12: Morphology of cells on day 6 of the differentiation process. A: Morphology of cells dissociated with Accutase on day 6. Area indicates differentiated cells. B: Enlarged image of indicated area of differentiated cell from image A. C: Morphology of cells dissociated with TrypLE Express on day 6 of the differentiation process. Area indicated differentiated cells. D: Enlarged image of differentiated cells indicated in image C. E: Morphology of another cell type from cells dissociated with TrypLE Express. Area indicates cells with similar morphologies to neural cells. F: Enlarged image of indicated area in image E. Arrow indicates location of cell body-like structure.

By day 7, in both buffer types tested cells had continued to migrate and differentiate. In the case of cells dissociated with TrypLE Express, in some areas of the vessel cells were observed to form multi-layered structures. In some areas of compacted cells, large cell and spindle-like structures were observed. In these cells were located amongst compacted cells. The area surrounding these large cells appeared to have a cleared area around these cells (Figure 5.13). Occasionally these spindle-like structures were observed to connect with other cells. These cell types were also observed in the control investigation but were not observed in cells dissociated with Accutase.

By day 10, whilst cells continued to migrate, proliferate and differentiate some cells in compacted areas were observed to have become more visible. Cells located in these areas seemed to have migrated outward creating more space between cells. These cells appeared large with undefined peripheral edges. In some cases these cells appeared to be attached resembling the figure “8” (Figure 5.13D). Although only small colonies were observed in cells dissociated with Accutase by this point of the investigation cells were still observed to proliferate in multi-layered structures (Figure 5.13C).

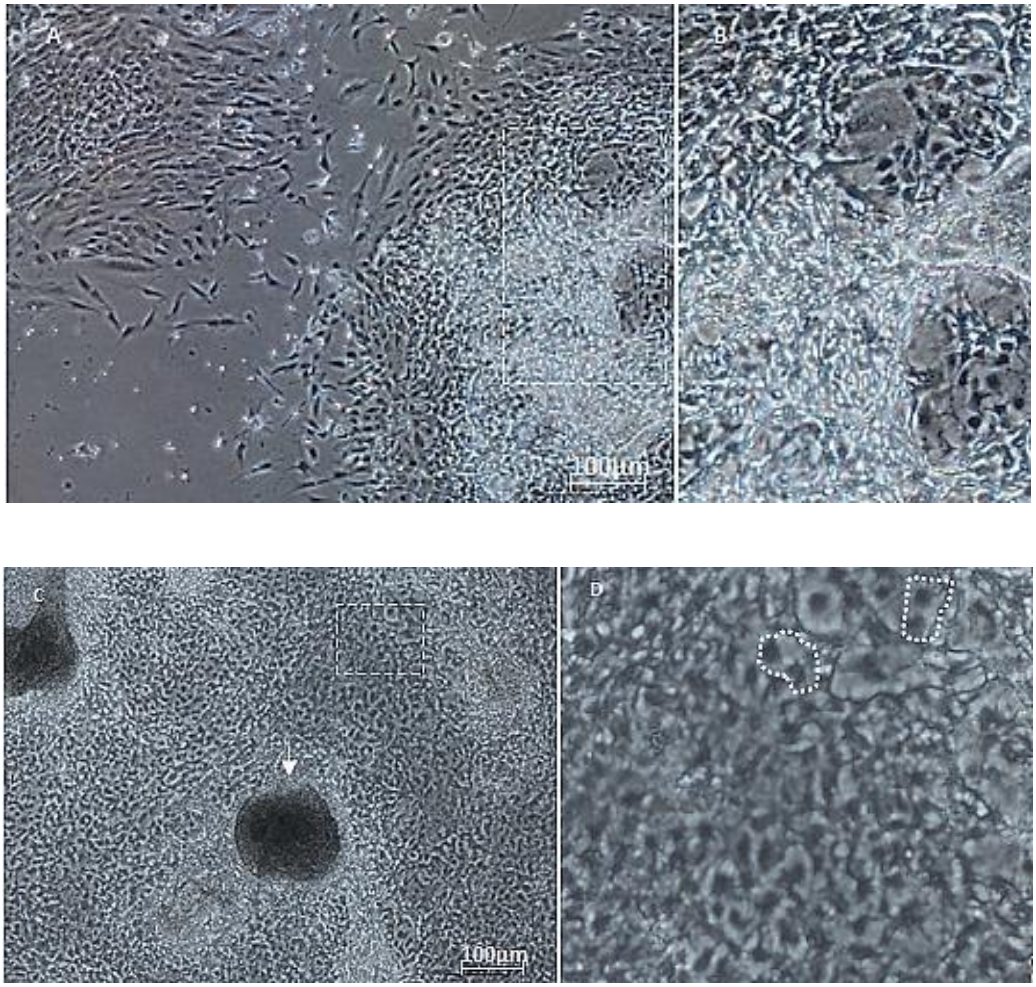

Figure 5.13: Morphology of cells during different time points of the differentiation process. A: Morphology of cells dissociated with TrypLE Express on day 7. Area indicates clearing around cells amongst compacted cells. B: Enlarged image of area indicated in image A. C: Morphology of cells dissociated with Accutase on day 7. Area indicates mitotic-like cells. White arrow indicates example of multi-layered structure. D: Enlarged image of indicated area on image C.

By day 11, large cells located within colonies of compacted cells were observed to have proliferated, in cells dissociated with TrypLE Express. These cells types were found to have expanded creating a large area occupied by these cells (Figure 5.14A). A closer analysis revealed a network of tubule-like structures spanning over the area of these large cells (Figure 5.14B). In addition to these tubule-like structures a web of smaller, spindle-like structures were also observed to interconnect cells within these regions of cells.

At this point of the investigation, proliferation of these large cells was observed in cells dissociated with Accutase (Figure 5.14C). In addition to this, cells from areas of compacted cells were observed to be more visible with some cells appearing more elongated. By day 12, an increase in population of these elongated cells were observed (Figure 5.14D). As was observed in those cells dissociated with TrypLE Express, in cells dissociated with Accutase, a network of spindle-like structures was not visualised. As a lower population of cells had attached to the matrigel coating at the initial stages of attachment, a larger surface area was still available to these cells to continue down the differentiation or proliferation route.

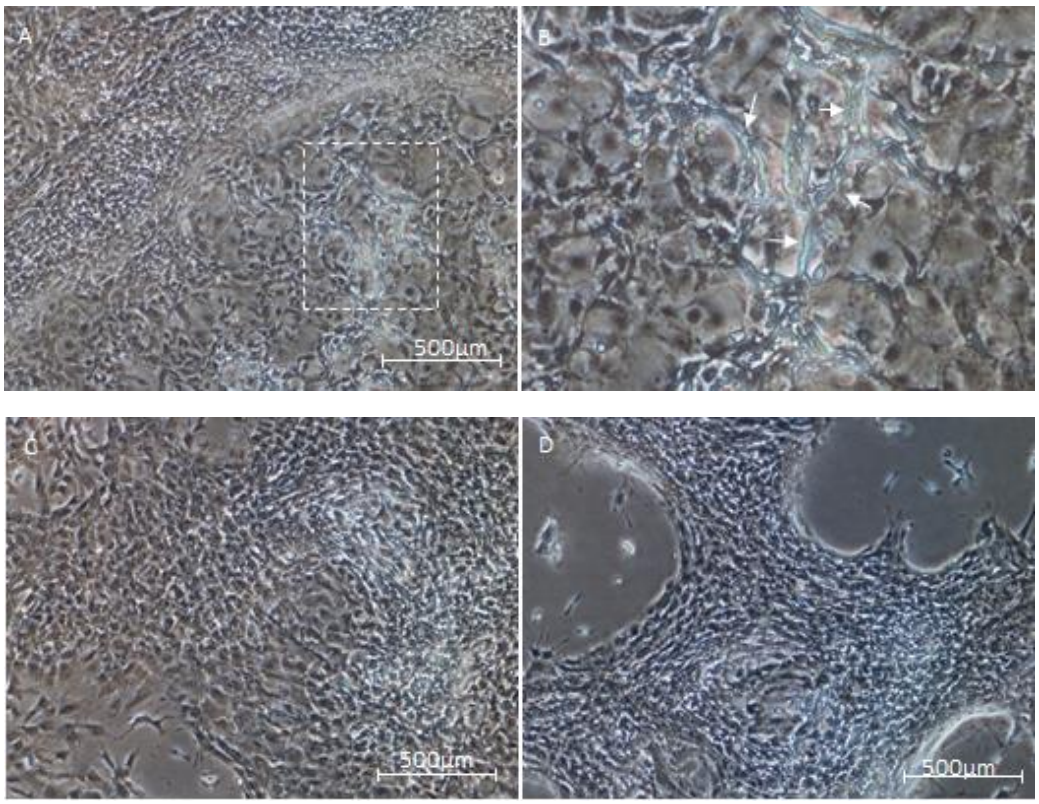

Figure 5.14: Morphology of cells dissociated with TrypLE Express and Accutase on days 11 & 12 of the differentiation process. A: Day 11 of cells dissociated with TrypLE Express. Area indicates region of tubule-like structures. B: Enlarged image of indicated are in image A. White arrows indicate examples of tubule-like structures. C: Image of cells on day 11 of the differentiation process of cells dissociated with Accutase. D: Morphology of cells dissociated with Accutase on day 12 of the process.

Cells continued to proliferate and differentiate until day 19; by this point of the investigation cells dissociated with TrypLE Express had become over confluent. Wells were observed to be extremely compacted. Many multi-layered structures were visible predominantly located in regions of compacted cells although some were also observed to be positioned in areas of elongated, neural-like cells (Figure 5.15A). As cells continued to proliferate cell detachment was also observed in some areas of the wells by day 20 (Figure 5.15B). These areas of detachment were mainly observed in peripheral regions of small compacted cells. The detachment resulted in a sheet of cells rolling towards the centre of the cell population.

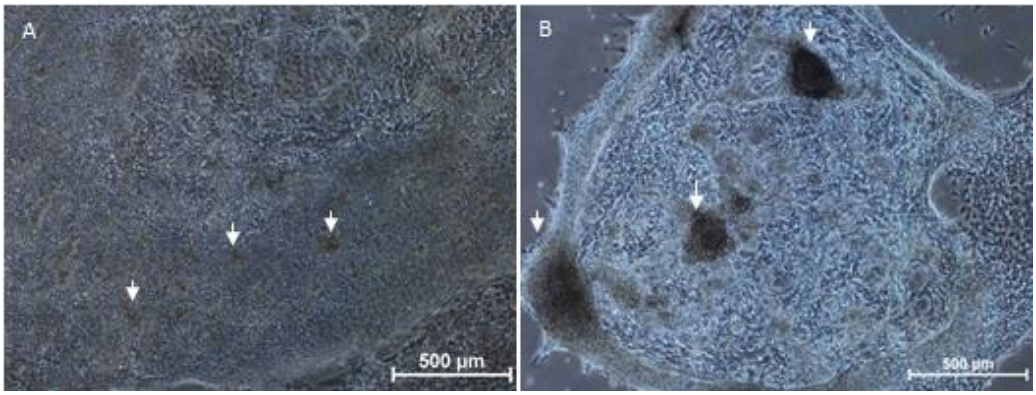

Figure 5.15: Morphology of cells dissociated with TrypLE Express on day 20 of the investigations. A: Morphology of cells on day 20 of the investigation, arrows indicates examples of multi-layered structures. B: Phase image of cell detachment on day 20 of the differentiation process, arrows again indicate examples of multi-layered structures.

5.4.3 Generation of early RPCs

On day 21 of the investigation cells were fixed with paraformaldehyde for immunocytochemistry investigations looking for expression of early eye field markers Pax6 and Chx10.

Immunocytochemistry results revealed low level expression of Pax6 in cells dissociated with Accutase, expression of Pax 6 was mainly observed in areas of multi-layered structures with almost no expression observed elsewhere in the wells (Figure 5.16). It was difficult to conclude whether this was a true reflection on Pax6 expression or whether the stain had become trapped between layers of the multi-layered structures resulting in an accumulation of the stain in these areas.

Pax6 expression was observed in cells dissociated with TrypLE Express and visually the intensity of expression was very mildly reduced in comparison to cells dissociated with Accutase. In cells dissociated with TrypLE Express, expression was mainly observed in areas of compacted cells in comparison to cells dissociated with Accutase and Collagenase where Pax6 positive cells remained in groups of cells.

Overall Pax6 expression was observed in both dissociation buffers investigated with those cells dissociated with TrypLE Express expressing slightly lower levels than cells dissociated with Accutase.

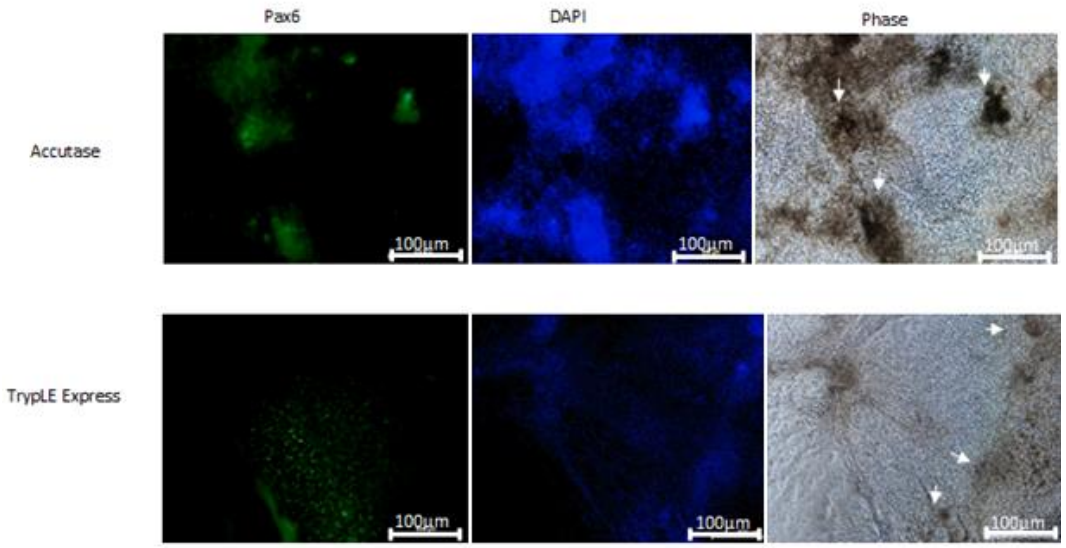

Figure 5.16: Pax 6 expression of cells dissociated with Accutase and TrypLE Express. Arrows indicate examples of multi-layered structures. First coloumn shows expression of Pax6, second coloumn shows nuclear staining with DAPI and third coloulm shows phase images of cells.

Similar to the immunocytochemistry results observed for Pax6, cells dissociated with Accutase exhibited very low levels of Chx10 expression with the majority, once again, observed in multi-layered structures (Figure 5.17). Whilst some expression was observed in areas of compacted cells, the intensity of expression was visibly lower in these cell types than that observed in areas of multi-layered structures. It is difficult conclude whether the intensity of fluorescence is a true reflection of Chx10 expression. In this case it is likely that the dye had become trapped between multi-layered structures leading to an excess of the stain resulting in the intense fluorescence but low intensity fluorescence observed in other cells may in fact be a reflection of on the Chx10 expression within the population of cells.

In cells dissociated with TrypLE Express a similar observation was made in that the intensity of fluorescence was greatly increased in areas of multi-layered structures (Figure 5.17). Again, this is more than likely not to be a true reflection of Chx10 expression in this population. Visually, expression of Chx10 was found to be more widespread across compacted cells in this population, in comparison to the population of cells dissociated with Accutase. This suggests the presence of a larger population of Chx10 expressing cells in cells dissociated with TrypLE Express than those dissociated by Accutase but qPCR results are required to confirm this statement.

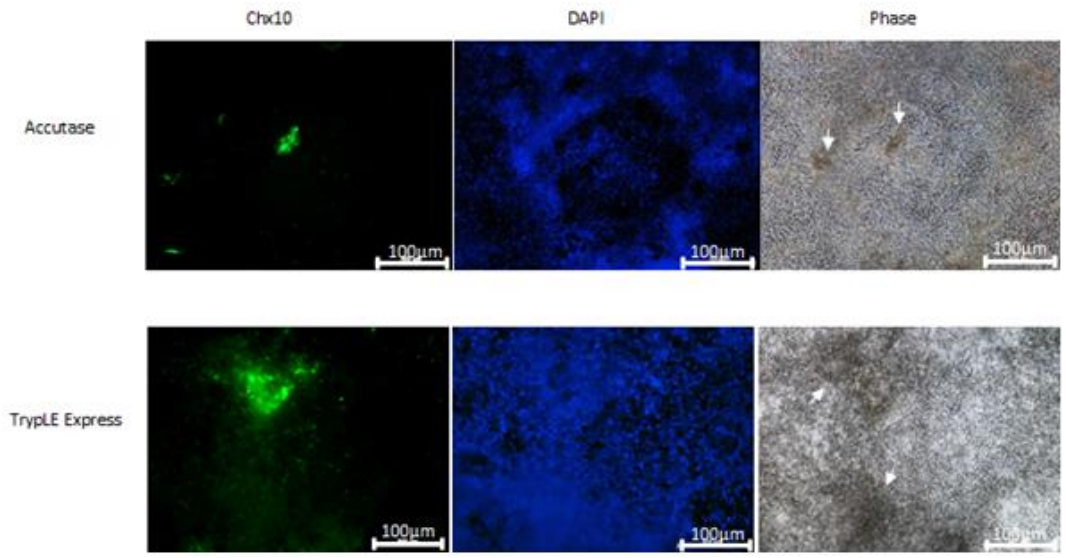

Figure 5.17: Immunocytochemistry results of Chx10 Express from cells dissociated buffers Accutase and TrypLE Express. Arrows indicate examples of multi-layered structures. First coloumn shows exoression of Chx10, second coloumn shows nuclear staining with DAPI and thirs coloumn shows phase images of cells.

Once qPCR results had been analysed, of all the dissociation methods tested, retinal gene expressions from cells dissociated with Accutase consistently produced the lowest expression. For this reason the expression of genes from these cells were set as a baseline to which the expression from cell dissociated with the remaining two methods could be compared against including results from the control investigation.

The expression of Six 3, a marker for eye field cells was recorded in cells dissociated with all three methods. In cells dissociated with TrypLE Express, a 20 fold increase in expression of this gene was noted in comparison to cells dissociated with Accutase (Figure 5.18). In cells mechanically dissected with Collagenase VI, Six 3 was found to express less than a 10 fold compared to those cells dissociated with Accutase (Figure 5.18). Although another early eye field marker, Rx1, was also investigated, no expression of this marker was noted in cells dissociated with Accutase and therefore it was not included in the qPCR data displayed in Figure 5.18. This was because comparisons of expressions could not be calculated for the remaining two buffer types. Expression of Rx1 was however recorded in cells dissociated with TrypLE Express and mechanical dissection with Collagenase VI.

In accordance with immunocyctochemistry results, Pax 6 expression was recorded in cells dissociated enzymatically and mechanically with Accutase and Collagenase IV respectively. No expression of this eye field marker was recorded from cells dissociated with TrypLE Express contrary to ICC analysis. This suggests that the fluorescence observed in the ICC analysis may be due to nonspecific staining. Together with Pax 6, Chx10 is a marker for neural retinal progenitor cells and expression of this marker was consistent to immunocytochemistry results.

qPCR analysis revealed an over 70 fold increase in expression for this neural retinal progenitor marker in cells dissociated with TrypLE Express, with the expression of the same marker only being recorded at less than 10 fold with those cells mechanically dissected with Collagenase VI in comparison to cells dissociated with Accutase (Figure 5.18).

One of the most exciting markers to be investigated was that of Nrl as this is a marker for photoreceptor precursor cells. It was interesting to note that over a 110 fold increase in expression for this marker was recorded from cells dissociated with TrypLE Express in comparison to those dissociated with Accutase. The mechanical dissection with the Collagenase VI control was only found to have a less than 10 fold increase in Nrl expression to those cells dissociated with Accutase.

qPCR data analysis clearly revealed that cells dissociated with TrypLE Express exhibited a significant increase in retinal gene expression in comparison to the other dissociation methods tested in this investigation.

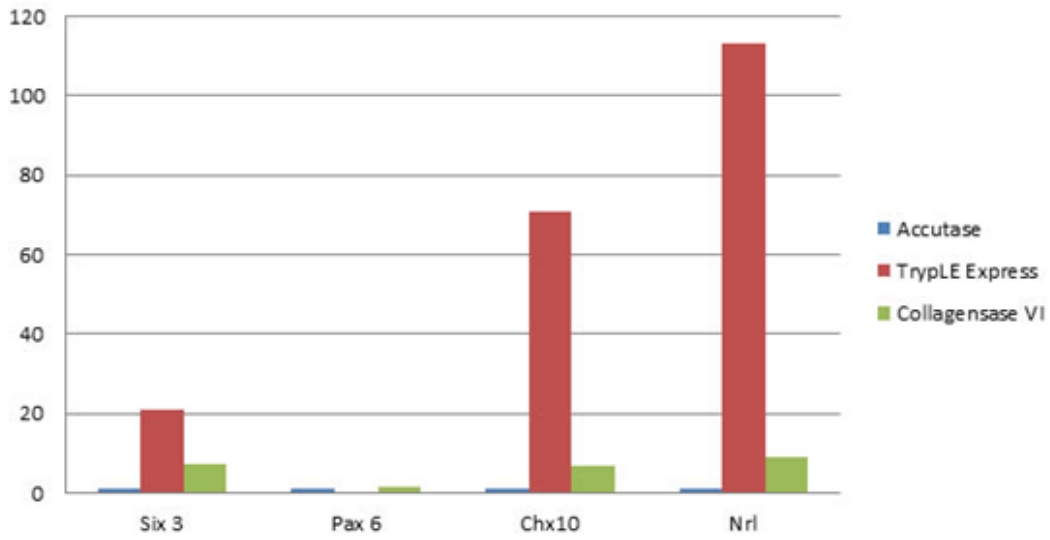

Figure 5.18: qPCR analysis of retinal gene expression in cells dissociated with Accutase, TrypLE Express and mechanical dissection with Collagenase. Gene expression in each condition was normalised to gene expression in the Accutase samples, as expression levels were lowest here and are therefore regarded as baseline values.

5.5 Discussion

Since the discovery of human pluripotent stem cells an array of protocols have been developed in order to exploit their properties to generate specific cell types for potential therapeutic treatment. The efficiency of protocols is however cell line dependant. Lamba and his group developed one of the first successful protocols to generate RPCs from the H1 cell line in 2006. This cell line was one of the first pluripotent human stem cells to be created by Thompson and his group in 1998. The protocol devised by Lamba involved a two-stage differentiation process consisting of a phase of suspended culture followed by a plated culture system for a period of 21 days in total.

The first phase of this protocol consisted of the formation of EBs in suspended culture in the presence of growth factors DKK1, noggin and IGF1- all of which have been found to hold important roles in the induction of forebrain development in early mammalian embryogenesis (Lamba *et al.,* 2006). The second phase of this protocol involves the attachment of the EBs formed and maintenance of culture in media supplemented with N2 and B27 in addition to the growth factors previously mentioned. Following the Lamba *et al.*, 2006 protocol, this group found ~70% of H1 hESCs to co-express retinal progenitor markers Pax6 and Chx10.

This chapter successfully followed the Lamba protocol to generate RPCs from a pluripotent Shef 3 cell line and also investigated the effect of Accutase, Collagenase VI and TrypLE Express on the differentiation process.

At the dissociation stage it was very apparent that both Accutase and TrypLE Express both dissociated cells as single cells in contrast to that of mechanical dissection with Collagenase VI. Although a large population of single cells was created by both Accutase and TrypLE Express, those cells dissociated with TrypLE Express were found to form large aggegrates. This was similar to those produced by the mechanical dissection of cells with Collagenase VI.

These aggregates were large and dark in appearance due to the presence of a large population of cells. In contrast to this, those cells dissociated with Accutase only formed small aggregates with a light appearance- again reflecting the size of the cell population present in these aggregates.

Although a large population of single cells were also visible in both groups of cells dissociated with TrypLE Express and Accutase, towards the end of the EB phase a lower population of these cells were observed in cells dissociated with TrypLE Express than that of Accutase. A higher population of cell debris was also observed in cells dissociated with Accutase in comparison to those dissociated with TrypLE Express and mechanical dissection with Collagenase VI. These were dark in appearance with a less apparent cell membrane.

Common to all dissociation buffer types investigated, all aggregates formed did not have a typical well rounded appearance commonly reported as EBs. Although in appearance aggregates formed resemble EBs, in order to confirm this further tests are required to ensure cells from aggregates are capable of forming cells from all three germ lines.

After the initial phase of the differentiation process it was evident that the enzyme Accutase was more suited to dissociating cells as a single cell population but was not the preferred method of dissociation in order to create cell aggregates in suspension. This may be a factor which contributed to the increase in cell debris.

Cell to cell signalling plays a vital role in cell maintenance especially the case of suspension culture. When cells aggregate these signalling systems are undisturbed

aiding cellular functions to continue as usual. When cells do not form aggregates and remain as single cells in suspension, inter-cell signalling pathways are disturbed which then in turn could have a knock-on effect on the intra-cell signalling system. This could result in the diversion of the differentiation or proliferation process of the cell into apoptosis. In mouse stem cells especially it has been found that the location of cells within aggregates play important roles in the direction of cellular process taken such as differentiation and apoptosis (Murray and Edgar, 2004).

Both conditions where cells had formed large cell aggregates, in this investigation, contained a lower population of cell debris in comparison to those cells which remained predominantly as single cells. Additionally, only cells that remained as single cells progressed into cell debris.The control of EB size and shape could have a significant impact on retinal differentiation. Some studies have found a controlled EB method to increase the production of photoreceptor precursor cells (Yanai *et al.*, 2013). Briefly, the study carried out by Yanai and his group focussed on size controlled EB differentiation of hESC into retinal cells. This group found that by controlling EB size to 1000 cells, Crx positive cells (photoreceptor precursor cells) could be recorded as early as day 17.

In the second phase of this differentiation, cells from all conditions tested were observed to adhere well onto the matrigel coated vessels. Cells were observed to adhere within a colony at the location where the attachment of the aggregate had occurred and this was common to all conditions investigated. Another common factor to all cells investigated was the appearance of these colonies of cells. Those cells located in the centre of these colonies were observed to be very compacted whilst those located on the outer boundaries were found to migrate and differentiate. As expected those cells dissociated with Accutase were only found to display small colonies in comparison to cells dissociated with TrypLE Express and those mechanically dissected with Collagenase VI. This was no surprise as these cells also produced small aggregates of cells and therefore as only a small population of cells were present in these aggregates a large colony after attachment was not expected.

By day 5 of the investigation, all cells tested were found to display signs of differentiation. Commonly to all dissociation methods investigated, cells with an elongated, flattened morphology with spindle-like structures were observed in all cells investigated. In those cells mechanically dissected with Collagenase VI, cells

resembling astrocytes were also observed in addition to those cells mentioned previously. In cells dissociated with TrypLE Express very thin, elongated cells resembling neural cells were recorded.

By day 10 cells has become very confluent, more common to those cells mechanically dissected with Collagenase VI and dissociated with TrypLE Express. Those cells dissociated with Accutase appeared to have a lower population of live cells, this again was no surprise. Towards the middle (Day 12) of the differentiation process, cells were observed to form multi-layered structures presumably due to the lack of space available. It was interesting to note that although space had become very limited due the vast population of cells, proliferation and differentiation was still taking place. By this point of the investigation, cells mechanically dissected with Collagenase VI and dissociated with TrypLE Express were found to also display a network of tubule-like structures interconnecting areas of cells. This network of tubules was not observed in cells dissociated with Accutase. As cells had become over crowded by the end of the investigation cell detachment was observed in some areas of over confluency.

It was evident that those cells dissociated with Accutase displayed less varied cell morphologies in comparison to the other two dissociation buffers investigated. It was also interesting to find that, although initially dissociation with TrypLE Express produced a fairly high population of single cells this did not in any way hinder the formation of aggregates or differentiation in these cells as was the case in cells dissociated with Accutase.

Overall qPCR results revealed a clear advantage to using TrypLE Express as a dissociation buffer for the purpose of this investigation in comparison to both Accutase and Collagenase VI. The latter of which was used to mechanically dissect cells in the original protocol produced by Lamba and his group in 2006. Cells dissociated with TrypLE Express produce an exceptionally high expression of RPC genes in comparison to cells dissociated with Accutase and Collagenase VI. Dissociation with Accutase consistently produced very low level expression of all RPC genes investigated with no expression of Rx detected although expression of this gene was detected in cells dissociated with TrypLE Express and mechanical dissection with Collagenase VI.

The qPCR results of Pax 6 and Chx10 expression of cells dissociated with Accutase was consistent with the immunocytochemistry results as only very low levels of these genes

were detected. This was also the case with those cells dissociated with TrypLE Express as it was difficult to confirm the presence of Pax6 expression from the immunocytochemistry results but this was confirmed from the qPCR results as no expression was present for this gene in these cells.

As over a 100 fold expression of Nrl, a marker for photoreceptor precursor cells was observed in cells dissociated with TrypLE Express it was clear that those cells contained a larger population of cells that had been directred towards the retinal lineage.

A high population of cell loss as a result of the formation of EBs was observed in this investigation. This prompted the investigation of a monolayer differentiation system, in order to reduce the population of cells lost during this process.

5.6 C**onclusion**

The aim of this investigation was initially to follow the protocol produced by Lamba and his group in 2006 to generate cells expressing RPC genes and was successful in its aim.

Secondly, it aimed at optimisation of the protocol whereby three dissociation methods: (mechanical dissection) Collagenase VI, Accutase and TrypLE Express were investigated in order to detect whether the dissociation methods could have a significant effect on directing pluripotent Shef 3 cells into RPCs. The results of this investigation were again successful in its aim and found cells treated with TrypLE Express to consistently have a significant increase in RPC gene expression. The results also confirmed Accutase was not favourable to direct pluripotent Shef3 cells into RPCs as these cells consistently produced very low levels of RPC gene expression. In accordance with the results from this investigation using TrypLE Express to dissociate cells at the start of the differentiation process can aid significantly to direct Shef 3 cells down the RPC lineage.

6 Monolayer Differentiation of Human Pluripotent Stem Cells

6.1 Introduction

One of the key hurdles that exist in introducing pluripotent hESCs clinically is the efficiency of the differentiation protocols. Without an efficient protocol, production and maintenance of cells would not be clinically viable. Current protocols rely on the EB differentiation system in order to direct pluripotent hESCs into the retinal lineage. This method cannot be used to create a highly efficient differentiation system as a large population of cells are lost during the EB stage at the early stages of the process.

A monolayer differentiation protocol was first devised by Lamba and his group in 2010 to direct iPSCs into retinal cells with successful results. Within three weeks over 70% of cells were found to express the early eye field marker Pax6, with over 11% of cells expressing the photoreceptor precursor marker Crx (after two months of induction). These results show clearly that a monolayer differentiation could be successful in directing iPSCs towards the retinal lineage and that differentiated cells incorporate well after induction. The advantage of this protocol is that a reduction is made to the number of cells lost during the initial stages as cells no longer have the need to aggregate for survival before once again attaching onto the monolayer.

The difference in cell type and differentiation success varies greatly as mentioned previously but if this protocol could be used to direct the differentiation of pluripotent hESCs, omitting the EB stage of the protocol, it could provide a step in the right direction for cell maintenance and productivity for clinical trials.

6.2 Aim

This chapter aims at directing pluripotent Shef 3 hESCs into RPCs following the protocol established by Lamba *et al.,* (2010).

6.3 Monolayer Differentiation of Shef-3 hES cells

Following routine cell culture of pluripotent Shef 3 hESCs using Collagenase VI for mechanical dissection, cells were transferred onto Mef feeder cells. For a period of 3 days cells were maintained in media supplemented with growth factors noggin, Dkk1

and IGF-1, in accordance with the protocol established by Lamba and his group in 2006.

By day 1, cells had adhered well to the MEF feeder layer and remained in small colonies at the point of attachment. Cells appeared to be well rounded with many large nuclei observed, characteristic of undifferentiated hESCs (Figure 6.1). A low population of un-attached cells were also observed. By day 3 of the protocol cells had proliferated well covering approximately 60% of the surface (Figure 6.1). Cells appeared very compacted and in some cases were losing the characteristic well rounded morphology of undifferentiated cells, especially on the peripheral areas of smaller colonies (Figure 6.1D).

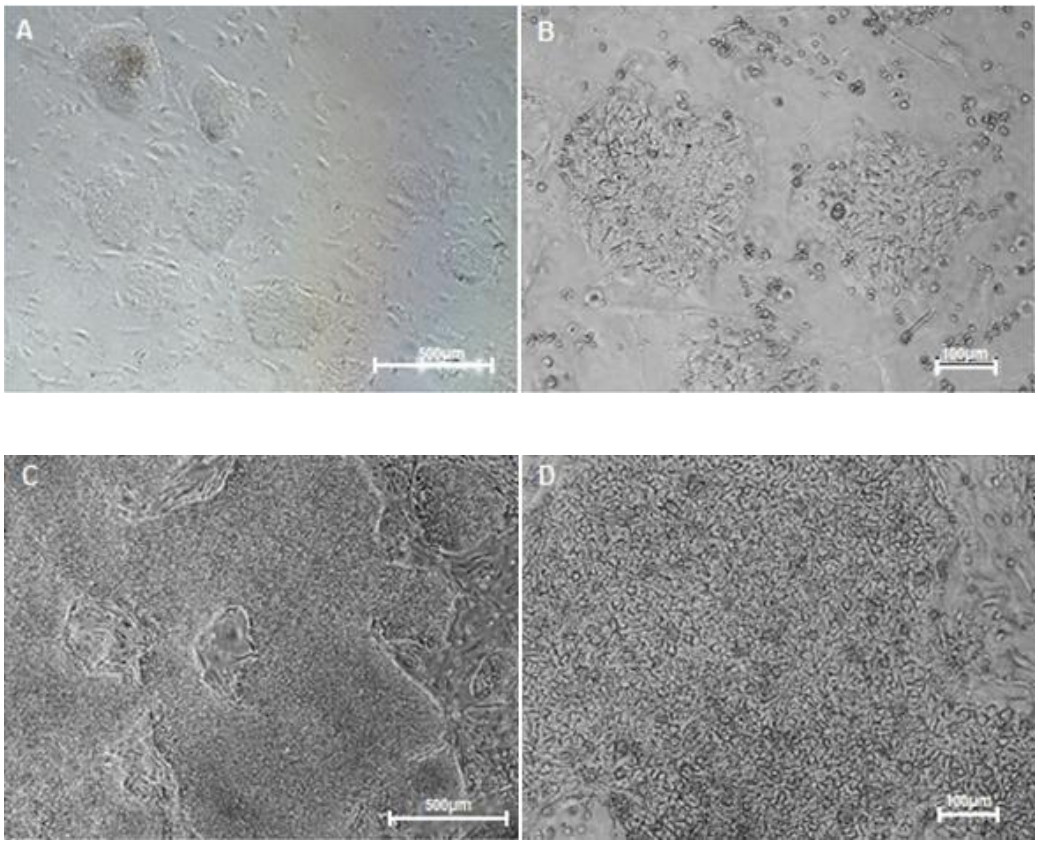

Figure 6.1: Morphology of Shef-3 hESCs on day 1(A & B) and day 3 (C & D) of the monolayer differentiation.

By day 4 of the differentiation process, cells had become over confluent with cells appearing to be extremely compacted (Figure 6.2). In some areas of the vessels, cells were observed to have formed multi-layered structures due to the lack of space available and appeared dark in colour. Some cells appeared to have an elongated morphology showing signs of differentiation (Figure 6.2). These cells were prominently visible in peripheral areas of colonies as the centre of colonies was often too compacted to distinguish individually differentiated cells. By this point of the investigation feeder cells were becoming increasingly difficult to distinguish within the population of migrating cells. A high population of compacted cells were also found to contain large cells (Figure 6.2B).

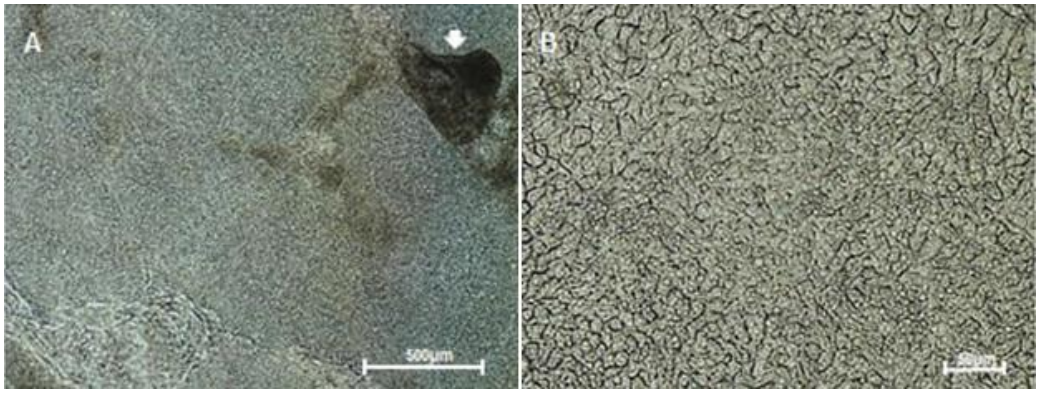

Figure 6.2: Morphology of differentiated Shef 3 hESCs on day 4. A: Image of compacted cells with a lower magnification (x4). Arrow indicates example of multi-layered structure. B: A magnified image of differentiated Shef3 cells on day 4 of the process (x20).

By day 5 and 6 cells had become extremely compacted and over confluent. This made it very difficult to both distinguish specific cells and also to clarify whether cells were continuing to undergo differentiation and proliferation (Figure 6.3). The presence of multi-layered structures was also observed to have increased and it was very apparent that the lack of space was going to be detrimental to the differentiation process. Although there were some signs of differentiating cells, these cells would not be able to continue to their full potential if left in this state (Figure 6.3). For this reason on day 7 on the differentiation process, cells were cultured so that a lower density of cells were replated on a new layer of MEF cells using mechanical dissection with Collagenase VI, and maintained in the same supplemented media as mentioned above. During culture, a portion of the cells was pelleted for further analysis.

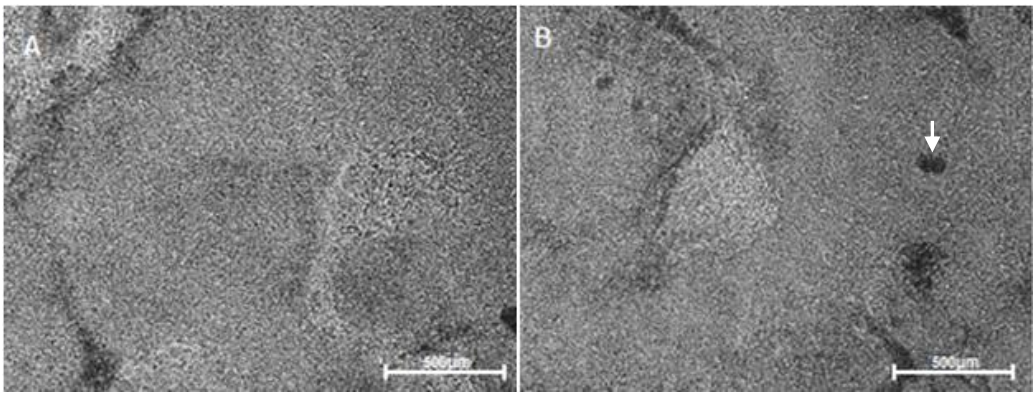

Figure 6.3: Shef-3 hESCs at various points of the monolayer differentiation. A: Image of cells taken on day 5 of the differentiation process. B: Image of Shef3 hESCs take on day 6 of the process. Arrow indicated example of areas containing multi-layer structures.

On day 10 of the process, cells were found to still be recovering from the culture process to reduce the cell population. Although a large population of cells had attached well onto the monolayer and an abundance of space was now available for differentiation to take place by this point in the investigation, a healthy population of undifferentiated, well rounded cells with a strong cell membrane and large nucleus were not observed. A large population of cells appeared small and dark in colour with no prominent cell membrane or morphology (Figure 6.4A). These small cells were located across the monolayer and were also observed to be suspended in the media.

Cultured cells were observed to have again formed colonies at the point of attachment and differentiation of cells within these colonies was observed once again (Figure 6.4 B). Generally differentiated cells had a flat and elongated morphology occasionally with protrusions (Figure 6.4 C). A large population of large cells with a rounded appearance were also observed. Some of these cells contained a large dark structure whilst other did not.

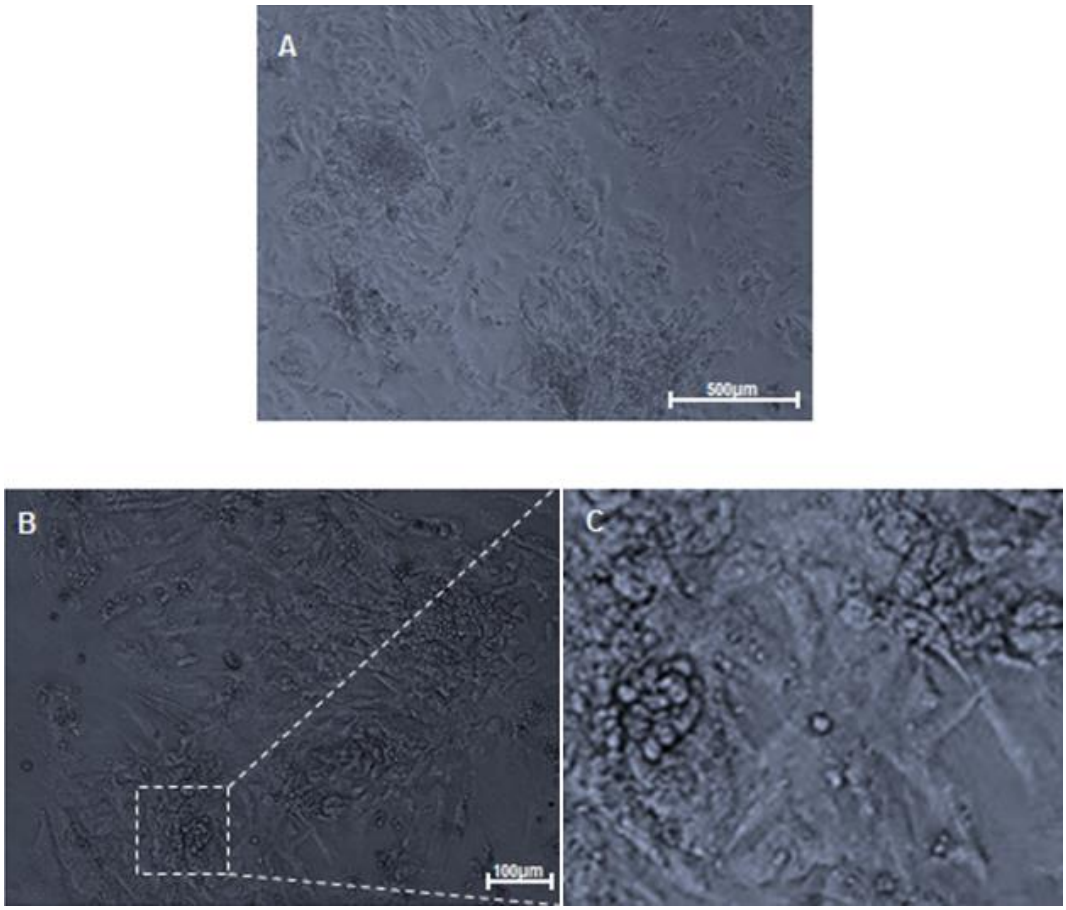

Figure 6.4: Images of Shef 3 hESCs on day 10 of the monolayer differentiation process. A: Image at a lower magnification of cells taken on day 10. B: A high magnification of cells taken on day 10. Area indicates an area of differentiate cells. C: Enlarged image of area indicated in image B. This image shows the morphology of differentiated cells on day 10.

Notable changes in morphology of cells were observed on day 11 of the differentiation process. An obvious decrease in the population of small, dark, cell debris was visible and various other morphologies were also exhibited. Overall cells had a much less defined cell membrane giving the appearance of a mass of amalgamated cells (Figure 6.5A). In addition to the cell morphologies described above, more elongated cells were also observed. A closer analysis revealed a number of very small protrusions similar in morphology to spindles, inter-connecting cells creating a web-like network were observed on these cells (Figure 6.5B). These networks of tubules were observed to pan across the whole population of cells (Figure 6.5C).

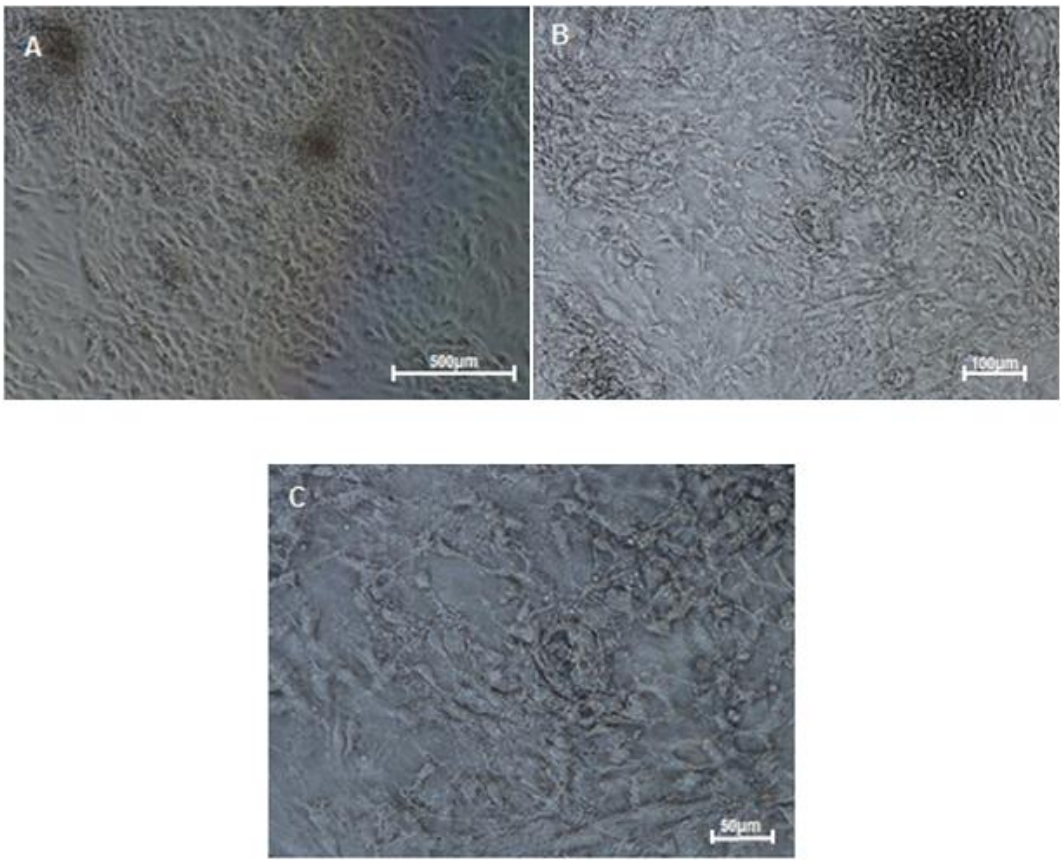

Figure 6.5: Images of Shef3 hESCs on day 11 of the differentiation process. A: A low magnification image of Shef3 cells. B: A higher magnification image of Shef3 hESCs on day 11 of the differentiation process. The network of tubules is clearly visible. C: A higher magnification of the network of tubules observed in these cells.

During days 12 and 13 much of the same cell morphologies described previously were observed (Figure 6.6A). Very occasionally rounded cell morphology was also observed; these cells appeared to have a very large dark structure prominently located into the centre of the cell, almost like a cell nucleus. These cells were found to be slightly increased in size in comparison to all other cells observed in the population (Figure 6.6B). Cells were also found to have become fairly compacted by day 13 with many colonies observed to be tightly surrounded by highly differentiated cells with a network of tubules (Figure 6.6C).

By day 14 cells were once again observed to have become over confluent with no vacant area available for further differentiation and development. Colonies of cells were very compacted and appeared dark in colour as cells predominantly formed multi-layered structures over areas of the colonies. In general, cells within colonies appeared

very compacted making it very difficult to identify individual cells. In the areas between these colonies a mass of differentiated cells without a prominent cell membrane were observed (Figure 6.6D). Generally these cells had a darkened structure which morphed into an elongation.

The outermost edges of the colonies were also observed to be slightly brighter in colour almost like an outline. A magnified image analysis of this region revealed the presence of cells with a very thin elongated morphology surrounding these colonies (Figure 6.6E). As there were still a number of days remaining for the investigation to be completed, it was once again decided that it would be in the best interest of the investigation to dissociate cells mechanically with Collagenase VI in order to reduce the density of cells for the remaining of the investigation. The culture was carried out in the same way as previously explained with a small portion pelleted for further analysis. Whilst a vast majority of cells were observed to have attached onto the monolayer, a large population of cells were also observed to remain in suspension a day after the process was carried out.

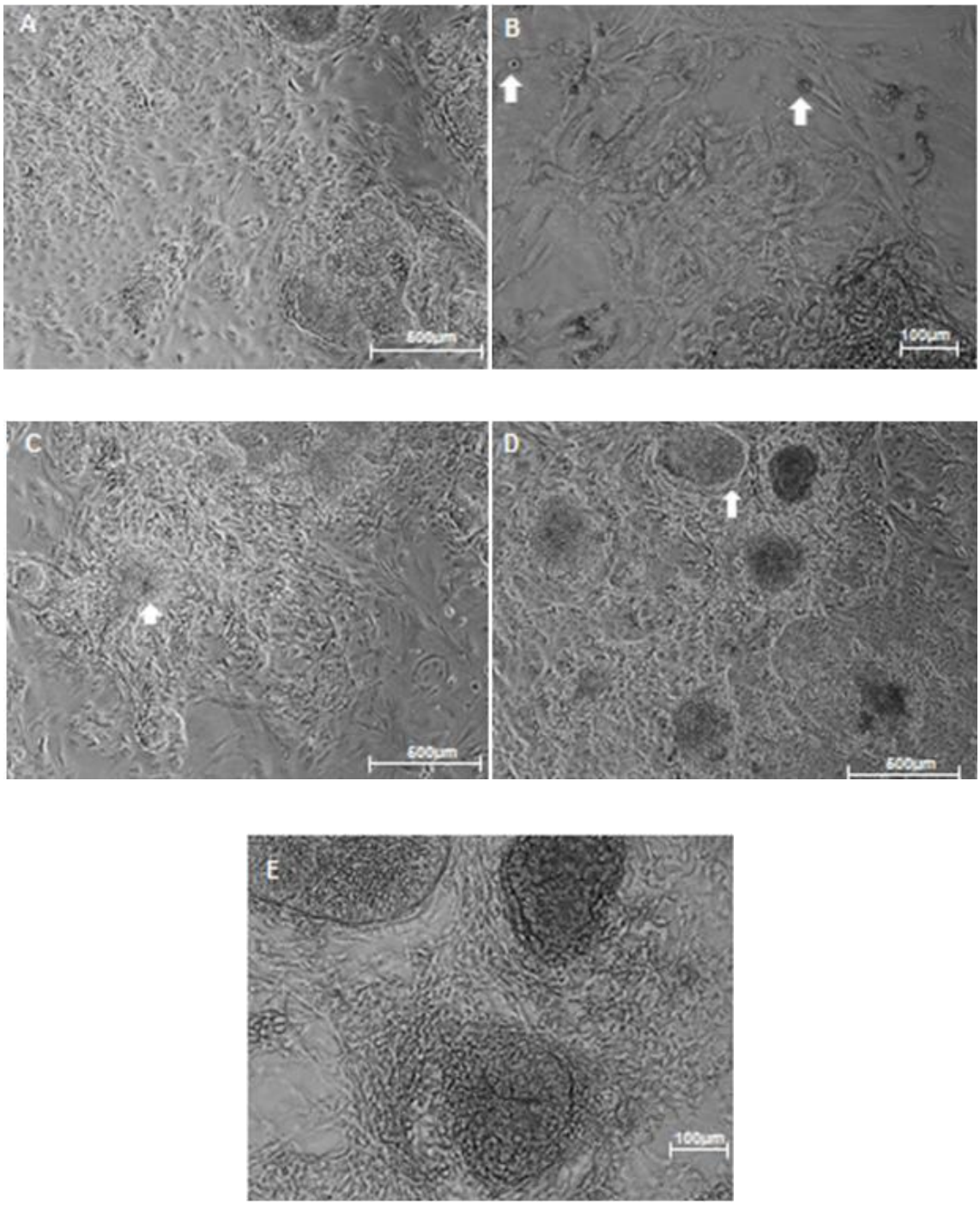

Figure 6.6: Images of Shef3 hESCs at various time points of the differentiation. A: Image of Shef3 hESCs on day 12 of the differentiation process. B: A magnified image of Shef3 hESCs on day 12 of the differentiation process. Arrows indicate examples of rounded cells with a darkened structure located in the centre of the cell. C: Image of Shef3 hESCs on day 13. Arrow indicates example of compacted colonies surrounded by a high population of differentiated cells and tubular network. D: Image of Shef3 hESCs on day 14 of the differentiation process. White arrows indicate example of brightened edges of colonies. E: Magnified image of cells located on the periphery of colonies on day 14 of the differentiation process.

By day 17 cells had adhered well onto the monolayer. Cells located between colonies, those with less prominent cell membranes, were observed to have migrated well giving the appearance of more available space around each cell. The spindle-like elongations of these cells were also more prominent (Figure 6.7 A). A closer analysis of these cell types revealed the presence of yet more network-like connections panning across the monolayer (Figure 6.7B). Cells within colonies became more apparent with individual cells becoming more visible. Within these colonies some large cells with a less prominent cell membrane were recorded.

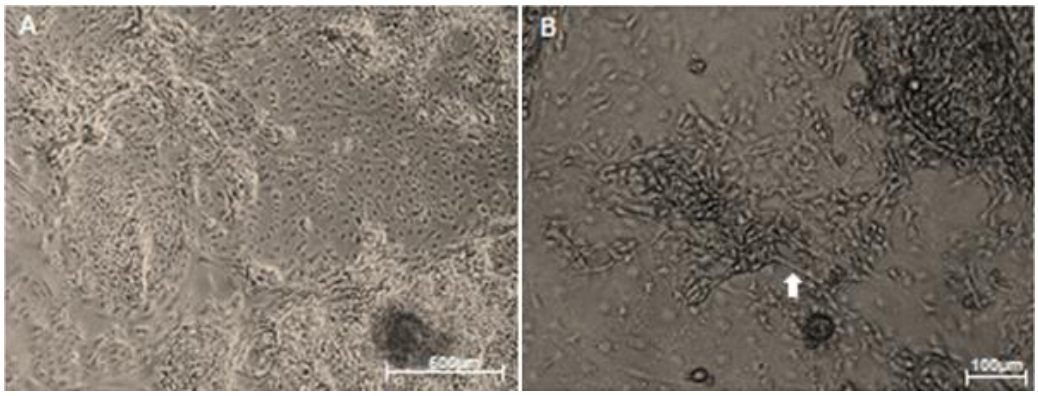

Figure 6.7: Image of Shef3 hESCs on day 17 of the differentiation process. A: Image of cells at a lower magnification on day 17. B: Magnified image of cells on day 17 of the differentiation process. Arrows indicates example of tubular network.

By day 18 cells had become very confluent with some areas of the vessel observed to be darker in colour in comparison to other areas of the vessel. These areas had a growth of cells in multi-layered structures (Figure 6.8A). In contrast to the availability of space between cells observed the day before, by this point of the investigation cells were observed to have once again become very compacted. Networks of tubule-like structures were also visible across the monolayer of cells but due to the vast number of compacted cells it was difficult to identify individual cells (Figure 6.8A).

By day 19 only one type of cell morphology was observed as cells were very compacted (Figure 6.8B). These cells were elongated with spindle-like structures. A closer analysis revealed cells to have a darkened bulb like mass which narrowed into an axon or spindle-like structure (Figure 6.8C). As expected, cells were observed to have become very compacted towards the end of the investigation although on day 20, some parts of the vessel were observed to display a darkened structured within the cells. These large

cells with a less prominent cell membrane were located within the reminiscence of colonies whilst those cells surround these colonies appeared to have a less defined cell membrane as described before (Figure 6.8D).

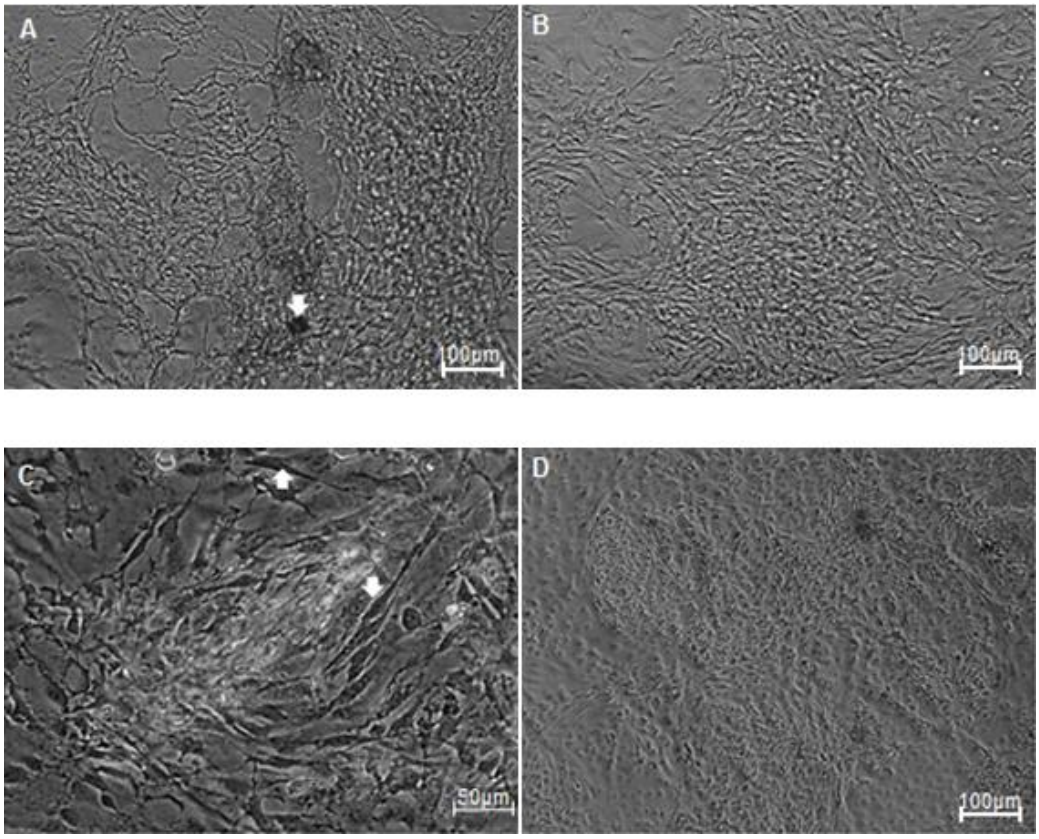

Figure 6.8 Images of Shef3 hESCs at various time points of the differentiation process. A: Cells on day 18 of the differentiation. Arrow indicates example of cell growing in multi-layered structures. B: Cells on day 19 of the investigation. C: A magnified image of cells taken on day 19 of the differentiation. Arrows show example of cells containing a morphology similar to axons sprouting from a bulb-like mass D: Image of cells on day 20 of the investigation.

6.4 Differentiation of Retinal cells on various ECMs

On day 21 cells were pelleted for further analysis and cultured onto plates coated with the following extracellular matrix proteins (ECM): laminin, matrigel, fibronectin, gelatin and Poly-D-Lysine (PDL) with one left uncoated. Cells were then passaged onto these plates and maintained for a further 6 days in differentiation media with media changes given every 2-3 days in order to identify any ECMs that may benefit the differentiation process

Cells were found to have attached well onto the various ECM coatings with the exception of PDL. Cells were also found to have adhered well onto the uncoated vessel, although a high population of cells were also observed in suspension. A higher population of multi-layered structures were also observed in uncoated vessel (Figure 6.9A). In the case of those cells located in the PDL coated vessel, cells had the appearance similar to cell debris. These cells appeared very small with an undefined cell membrane and more than 90% of the population of cells were in suspension (Figure 6.9B). A few larger aggregates were also observed in this vessel again in suspension, these aggregates were not in a rounded formation as are EBs but instead took various formations most likely dependant on the number of cells and location where cells had become attached to the aggregate.

In general, the population of cells observed in gelatin were visibly lower in comparison to all other coated vessels. Cells contained in the PDL coated vessels had an unhealthy morphology but the population of cells in these vessels still remained high as the majority of the population remained in suspension. With exception of cells cultured in PDL coated vessels, all other ECM contained cells, were of the same morphology and in fact were also the same as those observed during the initial differentiation process for the first 21 days.

In summary the morphology of cells was flat and elongated with long tubule-like structures. A closer analysis also revealed the presence of a network of tubule-like structures interconnecting cells. These cells also maintained the same morphology as those observed during the initial differentiation process. A large population of cells with a very prominent structure in the centre of the cell (possibly a nucleus) were also observed but these cells did not have a distinctive cell membrane (Figure 6.9D). In comparison to these cell types described above, a smaller population of cells with a faint

structure located in the centre of the cell (again, possibly a nucleus) and a faint cell membrane were also observed (Figure 6.9F). Cells cultured in the gelatine coated vessels were found to hold a large population of elongated cells without any tubule or spindle-like structures and differing slightly in morphology to those elongated cells described previously (Figure 6.9H).

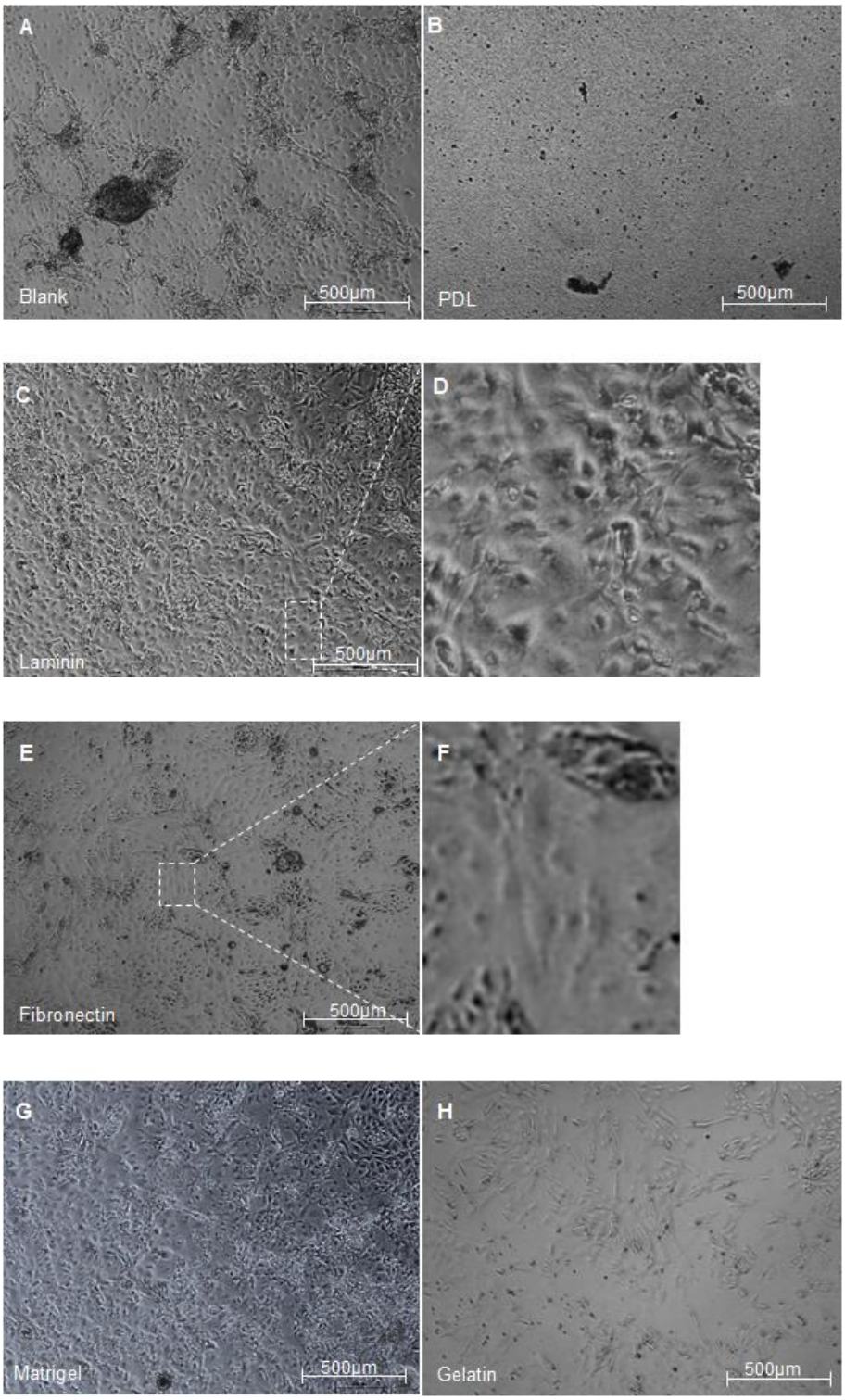

Figure 6.9: Image of cells on day 25 of the differentiation process on various ECM coatings. A: Image of cells cultured on the uncoated surface. B: Cells cultured on the PDL coated surface. C: Cells cultured on the laminin coated surface. Area indicates example of large cells. D: Enlarged image of indicated areas shown in image. C. E: Cells cultured on fibronectin. Area indicates example of large cells. F: Enlarged image of indicated area in image E. G: Cells cultured on Matrigel coated surface. H: Cells cultured on gelatin coated surface.

6.5 Generation of Early RPCs Using a Monolayer Differentiation

On day 27 of the investigation, cells were fixed in paraformaldehyde in order to identify the presence of early RPCs using immunocytochemistry.

β-III Tubulin plays an important role in neuronal development and is heavily involved in the health and maintenance of neuronal circuits (Tischfield and Englel, 2010). It is thus a marker for the presence of neurons and neurites.

Immunocytochemistry results for β-III tubulin showed good expression of the marker within cell cultures on the uncoated vessel, with expression also found in both the main body of cells as well as the network of tubules present in this population (Figure 6.10). A high expression of β-III tubulin was also observed in cells cultured on fibronectin and gelatin coated vessel (Figure 6.10). A closer analysis of these cells revealed the morphology of positive cells to predominantly be exhibited in large cells with a faint cell membrane (Figure 6.10).

Visually a lower intensity of fluorescence was observed in cells cultured on laminin and matrigel coated vessels, but the DAPI staining reveals the presence of a high population of cells suggesting that it is more than likely that the fluorescence was not a true reflection of the expression of β-III-tubulin in these cells.

Although only low levels of expression was observed in cells cultured on matrigel in comparison to those cells cultured on laminin, visually matrigel cultured cells had a slightly increased population of positive cells (Figure 6.10). Cells cultured on uncoated vessels were also found to have low levels of β-III-tubulin positive cells with the exception of areas of heavily aggregated cells (Figure 6.10A). The intensity in surrounding areas was similar to that displayed by cells cultured on laminin. In comparison to intensities displayed by cells cultured on fibronectin and gelatin, cells cultured on the uncoated vessel only exhibited low levels of β-III-tubulin expression.

Although on most ECMs investigated, cells expressed at least low levels of β-III tubulin, cells cultured on PDL coated vessels displayed extremely low levels of expression although in some cases specks of expression could faintly be matched to the presence of a cell from the DAPI staining (Figure 6.10). The expression exhibited by these cells was so low that visually it was very difficult to identifiy whether any

expression was present at all. Even expression in aggregated areas was of only low intensity in these cells.

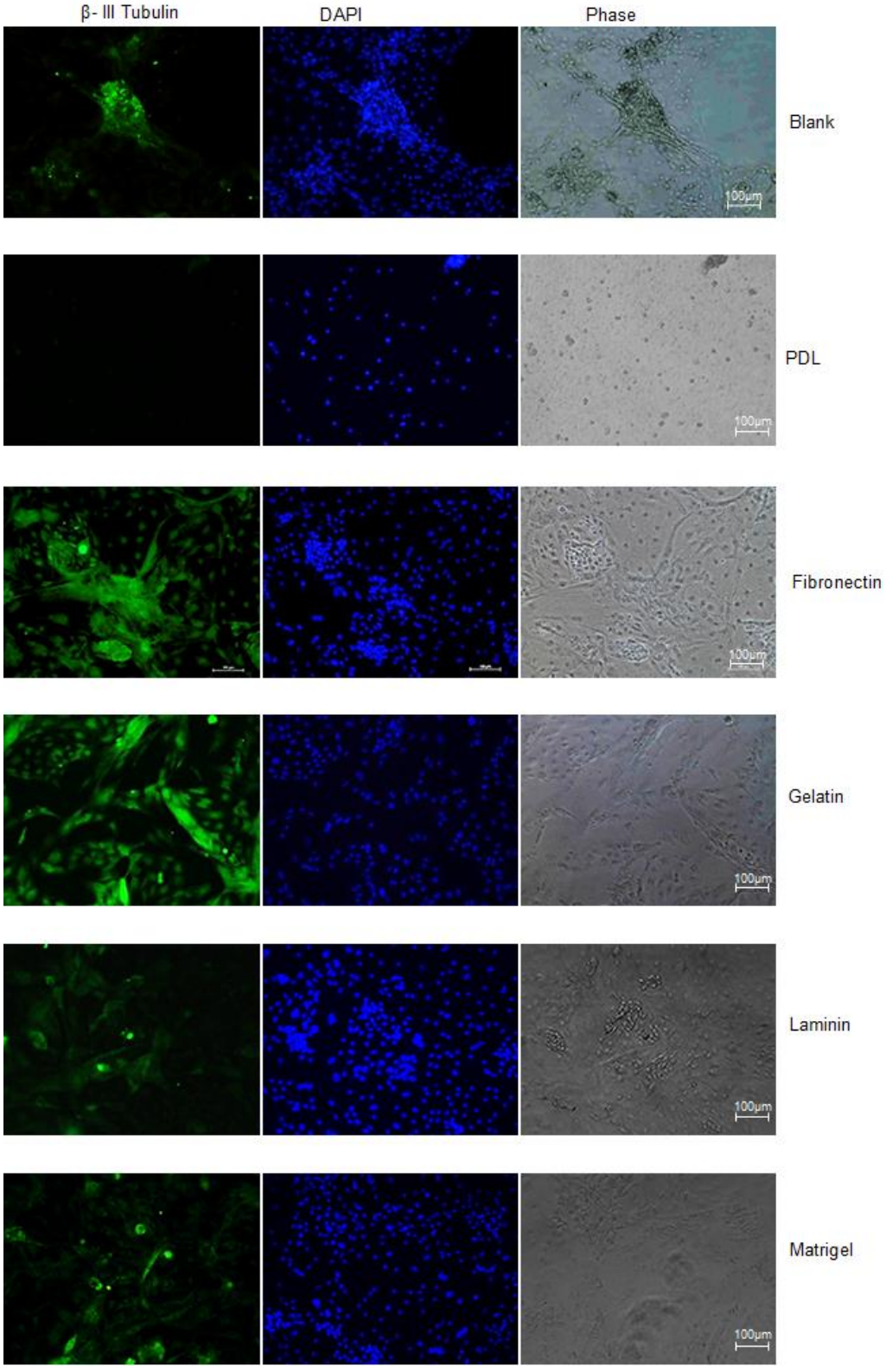

Figure 6.10: Immunocytochemistry for β-III-Tubulin, DAPI Staining and phase images for cells cultured on various ECMs.

Overall, expression of early eye field marker Pax6 was only observed at low levels on all ECM coatings investigated with the exception of the uncoated vessel where no expression was recorded (Figure 6.11). Cells cultured on the PDL coated vessel were observed to express extremely low levels of Pax6 but as the intensity of expression was so low and visually very difficult to identify whether the fluorescence was in line with the location of cells displayed by the DAPI staining. This is highly likely to be a result of non-specific expression (Figure 6.11). Although low Pax6 expression was observed on all other ECMs investigated a particularly low intensity of expression was found in cells cultured on gelatin coated vessels in comparison to all other cells investigated (with the exception of PDL and the uncoated cultured cells) (Figure 6.11).

True to all ECMs tested in this investigation, Pax6 expressing cells were predominantly observed in small groups of attached cells rather than single cells (Figure 6.11). These groups of Pax6 positive cells took a morphology that was visibly similar to grapes emitting a strong intensity of Pax6 expression within the group of cells making a clear distinction between positive and negative cells (Figure 6.11).

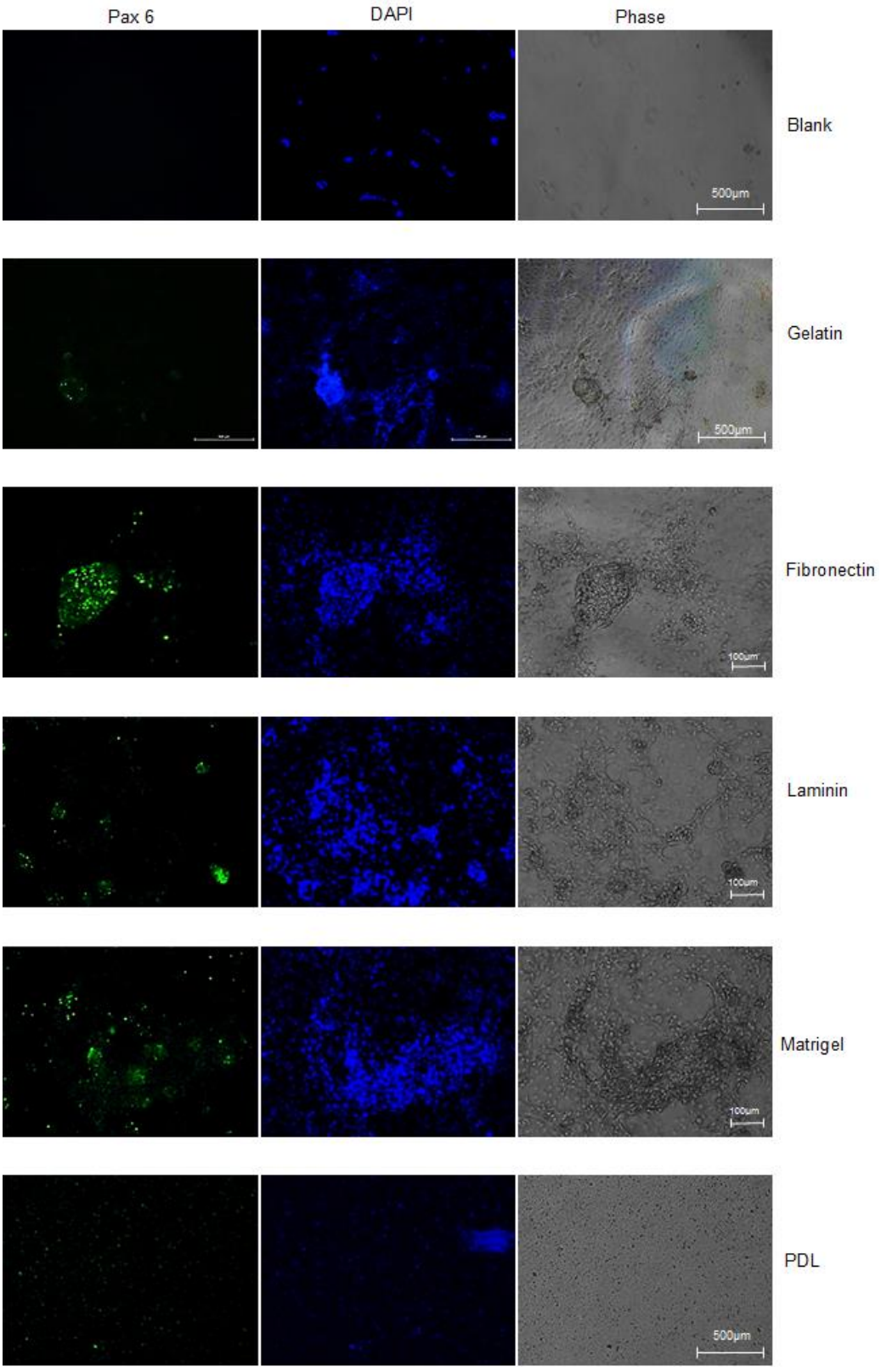

Figure 6.11: Immunocytochemistry for Pax6, DAPI staining and phase images for cells cultured on various ECMs.

As was observed with Pax6 expression, in general, only low levels of neural retinal progenitor marker Chx10 was recorded. This was true of all cells tested in this investigation (in all culture vessels) with the exception of those cells cultured on gelatin coated vessels.

In the case of cells cultured on gelatin, a widespread expression of Chx10 was observed across the vessel with a high intensity of expression (Figure 6.12). Expression was not limited to specific aggregates of cells or specific cell types as was observed previously with Pax6 positive cells. Instead expression was found to be more widespread. DAPI staining revealed the presence of a high population of cells in these vessels the location of which was consistent with Chx10 expression (Figure 6.12).

Some expression was also observed in cells cultured on uncoated surfaces although this expression was mainly confined to groups of compacted cells with very low expression surrounding these areas in comparison to the expression observed in gelatin cultured cells (Figure 6.12). Expression exhibited by cells cultured on fibronectin coated vessels was observed to be extremely low; so low, that it was difficult to visually estimate whether expression was present at all (Figure 6.12). This was also true in the case of cells cultured on both laminin and matrigel coated vessels (Figure 6.12). The expression of Chx10 exhibited by cells cultured on PDL coated vessels was again so low that it was very difficult to commit to whether fluorescence was present at all (Figure 6.12). A closer analysis revealed the location of Chx10 positive cells to mimic the location of cells exhibited by the DAPI staining.

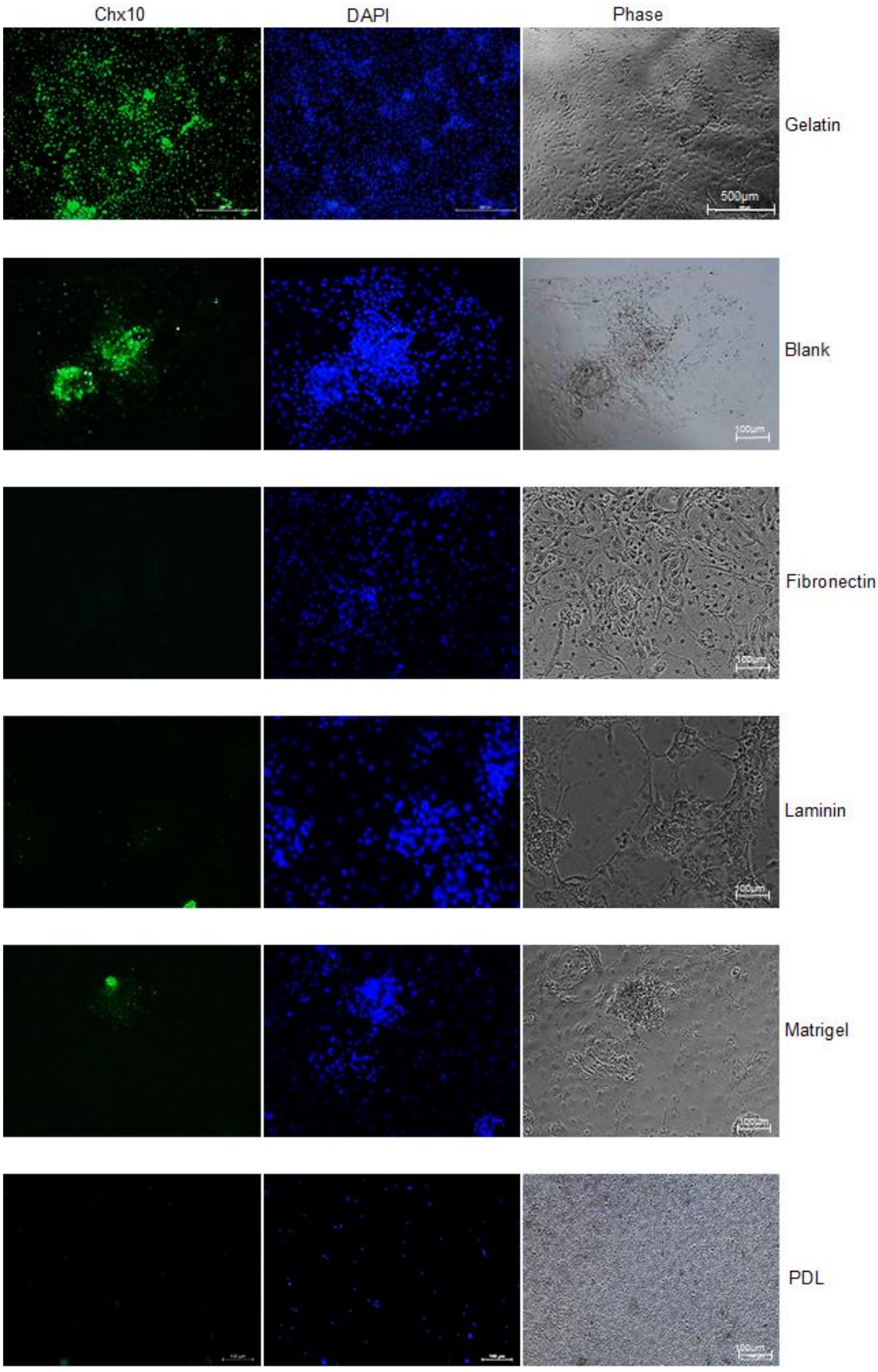

Figure 6.12: Immunocytochemistry results for Chx10 for monolayer differentiated Shef3 cells cultured on various ECM coatings.

qPCR results were supportive of immunocytochemistry results in that Pax6 and Chx10 expression was also found to be low in this investigation.

qPCR results revealed that on day 7 of the differentiation period, very low Pax6 expression was observed and in fact was found to be visually almost half of that of the control on the same day (Figure 6.13). On day 7, Chx10 expression was very slightly improved in that expression was found to remain slightly increased in comparison to the control (EB differentiation).

Expression of photoreceptor precursor marker Crx was in fact observed to be increased by over 10 fold in comparison to that of the control on day 7. qPCR analysis of samples taken on day 14 of the differentiation process revealed a very slight increase in Pax6 expression in comparison to day 7 with expression remaining lower than that of the control sample (Figure 6.13). Chx10 expression was also observed to be increased on day 14 with an increase of over 2 fold in comparison to that of the control. Differing to the pattern of expression of Pax6 and Chx10 on days 7 and 14, Crx expression was found to be greatly reduced on day 14 (Figure 6.13).

In comparison to the excess of 10 fold increase in expression observed on day 7 of Crx, on day 14 this had reduced to only a ~6 fold increase in expression in comparison to the control. Within 7 days of differentiation a decrease of over 4 fold in expression had been recorded. qPCR results for expression of all retinal markers investigated was found to be even more greatly reduced on day 21.

On day 21, both Pax6 and Chx10 expression was found to be less than half the expression of that of the control with the greatest reduction in expression exhibited by Crx; where expression was found to drop to lower than that of the control (Figure 6.13). In comparison to the Crx expression levels observed on day 7, expression was found to have reduced by over 10 fold standing just under that of the expression exhibited by the control sample.

In general qPCR results revealed a decrease in expression of retinal markers over time in this investigation.

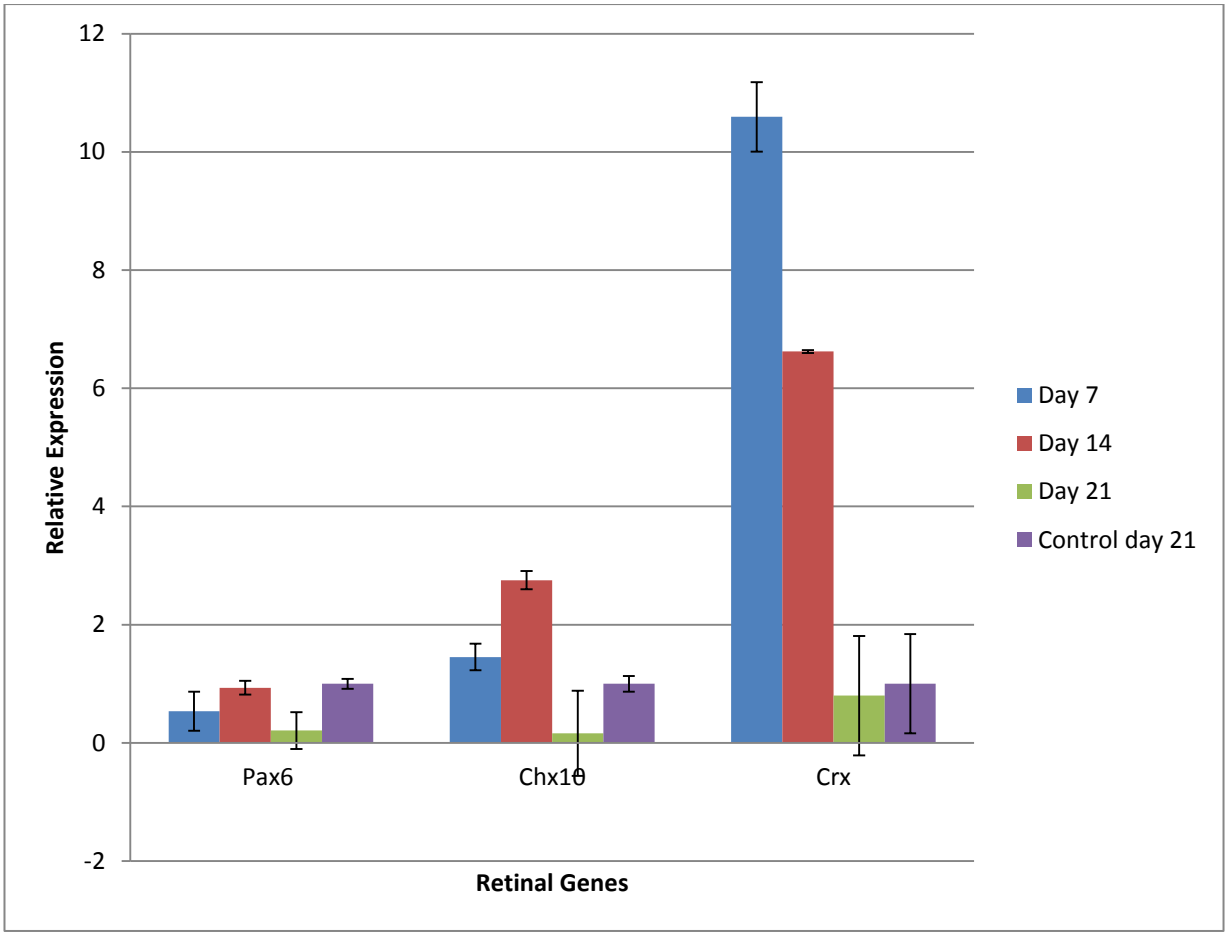

Figure 6.13: qPCR results for monolayer differentiation of pluripotent Shef 3 hESCs samples taken at various time points during the differentiation process.

6.6 Discussion and Conclusion

A major issue in the differentiation of photoreceptors from pluripotent stem cells is that predominantly the process is carried out in two stages, where initially EBs are formed which are then transferred to the second stage of the process. This process however immediately disposes off a high population of cells with the potential to differentiate into target cells. This can be a limiting factor, a bottleneck for the success of differentiation techniques, as the efficiency of any protocol is dependent on the time and yield of the process.

Whilst Lamba and his group were successful in eliminating this EB stage of the differentiation of photoreceptor cells in 2010 with their monolayer differentiation technique using iPS cells, this technique has not yet been completely investigated using

other pluripotent cell lines such as the Shef 3 cell line. Adult somatic cells can be reprogrammed into pluripotent iPS cells with the induction of Oct3/4, Sox2, c-Myc and Klf4 (Takahashi and Yamanaka, 2006). As characteristically iPS cells are in fact cells that have been reprogrammed to become pluripotent stem cells, as is the case with any cell line, they vary in differentiation efficiencies.

The first day of the differentiation process where pluripotent Shef3 hESCs were exposed to the initial supplemented media, cells were found to have adhered well forming many healthy colonies at the point of attachment as would be observed in any healthy population of cells. As days progressed it was evident cells were proliferating and differentiating and were found to become compacted and reached confluency by day 3. Following the over confluent nature of these cells, cells were sub-cultured in order to provide more available space and nutrients as a long period of differentiation was still ahead. After the initial culture maintenance, although a high population of cells remained to be healthy and found to adhere onto the monolayer a large population of cells were also found to be suspended in the media. This was an initial sign that the whole population of cells did not recover well from the initial maintenance procedure as suspended cells had a less rounded morphology as well as a darkened appearance. Cells were then found to have recovered and differentiation was observed amongst these cells with mainly an elongated and flat morphology observed at this point of the investigation. Some rounded cells with a large prominent nucleus were also observed in this population of cells whilst some others with a less prominent nucleus were also observed. A large nucleocytoplasm ratio is characteristic of pluripotent stem cells and as a result of this the presence of a large nucleus is also characteristic of undifferentiated pluripotent hESCs (Oh *et al.,* 2005). Therefore the observation of those cells with large nucleus is more than likely to be undifferentiated hESCs.

By day 11 cells were observed to have visually recovered from the initial cell maintenance process as the proportion of cell debris had visibly decreased and the remaining population had a healthy morphology.

Various other cell morphologies were also observed suggesting that a high population of cells were in fact undergoing differentiation. Although the exact lineage of the differentiation taking place was not predictable at this stage of the investigation, the fact that differentiated cells were displaying spindle-like protrusions and interconnecting

web-like tubule networks were observed across the monolayer was encouraging as these are similar in morphology to other neuronal cells- a step in the right direction .

Cells were observed to continue to proliferate and differentiate as by day 13 space had once again become restricted leading to another maintenance process on day 14. After the process visually cells were found to have adhered well onto the monolayer and continue down the differentiation and proliferation process with cellular morphologies displaying spindle-like outgrowths and interconnecting tubules as described previously.

qPCR results revealed an increase in Pax6 and Chx10 expression after this process. This suggests that the maintenance process may in fact have aided early eye field cells. This is because in comparison to the expression of these markers on day 7 as expression was found to be slightly improved on day 14. As cells were extremely compacted this may have limited the proliferation and differentiation of Pax6 and Chx10 positive cells resulting in the lower expression of these markers observed on day 7. The maintenance process may have however aided in the proliferation and differentiation of these particular cells resulting in the increase of Pax6 and Chx10 expression on day 14.

In the case of Crx expression however, qPCR results revealed a reduction in expression on day 14 in comparison to day 7. This shows that a small population of cells had in fact differentiated into photoreceptor precursor cells by day 7 from pluripotent Shef3 hESCs. It also suggests that the mechanical dissection with Collagenase IV may have been detrimental to the differentiation of these cells as a reduction in expression of Crx was observed. This also suggests the reduction in photoreceptor precursor cells. Mechanical dissection of cells is a harsh process and at this stage cells could not be individually isolated. This would have therefore resulted in the distortion and breakage of many cells in the population. This breakage may have disrupted intercellular signals which hold an important role in cellular differentiation. As inter-cellular signalling processes were disrupted this may have had a knock on effect on the proliferation of these cells as well as other cells differentiating into these cell types. This may have resulted in the reduction of these photoreceptor precursor cells as cells no longer have the initial communication between cells to progress down the same lineage. Breakage of cells could have also resulted in cell death of these cells again reducing the population of Crx positive cells.

The increase in expression of Pax6 and Chx10 positive cells after day 7 and the reduction of Crx positive cells after the same day suggests that early eye field cells may have been less prone to disruption than late eye field cells or photoreceptor precursor cells. It may be a fact that late eye field cells may rely more heavily on inter-cell signalling processes than early eye field cells. Additionally, further investigations to isolate Crx positive and early eye field positive cells may give a clearer understanding to the likelyhood of late eye field cells to be physically more prone to damage during manual culturing methods. For example if Crx positive cells were found to have a morphology possessing a large number of tubule-like connections intertwined within other cells in comparison to early eye field cells then these cells would most definitely be more prone to physical damage during mechanical dissection in comparison to other cells with less/no protrusions.

Although visually cells were found to recover well from the maintenance processes carried out in this investigation and continued to differentiate, proliferate and migrate this process was detrimental to the differentiation process. qPCR results clearly revealed a reduction in eye field marker expression with time and it is highly likely that the maintenance process contributed highly to this. Although early eye field marker Pax6 and Chx10 were initially observed to have a slight increase, expression was found to be heavily reduced over time.

Additionally cell recovery may have been prolonged over time either due to cell age or due to the time weakened cells takes to recover. Recovery of cells could be reduced depending on the number of times cells have been exposed to environmental and possibly physical stress, in the case of this investigation. If cells had not recovered fully this could also affect the differentiation status and thus again limit the differentiation and proliferation potential. If cells were affected in this way early on in the process then this would have resulted in a limitation of eye field positive cell proliferation reducing the population of target cells. As pluripotent cells continue to differentiate the repetitive manual maintenance process could have affected these cells in the same way again limiting cell differentiation towards the retinal lineage and possibly directing cells down a different lineage.

It is well known that ECMs can play a large part in many cellular processes including differentiation offering various forms of support to various cell types. Therefore the

ECM type on which cells are cultured during a differentiation process has the potential to play a large role in directing pluripotent cells down a specific lineage.

Visually it was very apparent that PDL did not support the growth of differentiated cells in this investigation. Cells cultured on this ECM where mainly found to be very small in appearance. Additionally the majority of cells were found to remain in suspension, suggesting that PDL did not support adherence of cells to the monolayer. It is accepted that if the coating process with PDL is not carried out efficiently with all washing steps carried out efficiently any residues left could be toxic to cells. In this investigation however it is not clear whether this may have been the underlying issue for the lack of cell support on this matrix.

A population of cells were also found to have adhered onto the uncoated surface although a fairly high population were also observed to remain in suspension. This suggests that a small population of cells did not in fact require an ECM coating to aid adherence to continue to differentiate and proliferate. As these cultures require regular media changes to maintain the health of the culture, any cells in suspension were lost during the process immediately reducing the efficiency of the process. For this reason, it is clear that an ECM coating is in fact required.

Cells cultured on all other ECMs were found to have adhered well onto the monolayer and continued along the cellular paths. The population of cells cultured on gelatine coated surfaces were found to visually have a lower population of cells in comparison to all other cells cultured. Overall visually the growth of cells was most supported by laminin, matrigel and fibronectin, as cells cultured on these ECMs were found to have adhered well on the monolayer as well as maintain a high cell population. In general the morphology of cells observed in these cultures were similar to those mentioned previously. Various cell types were observed in each culture system.

In the case of cells cultured on gelatine coated surfaces, visually a high population of elongated cells with no tubule-like protrusions were observed in comparison to all other cells investigated. Cells cultured on this system were also found to exhibit high expression of β-III-Tubulin and chx10 in comparison to all other ECMs investigated.

Although an extension of 7 days was added to the initial differentiation process it was interesting to find that this had no real effect on the expression of early eye field

markers Pax6 and Chx10. In line with the results exhibited by qPCR results, immunocytochemistry results also revealed, generally, a low expression of Pax6 and Chx10. This suggests the extension period did not have a large impact on early eye field cells already present in the population to proliferate. This is because qPCR results were carried out on cells samples taken on day 21, whilst immunocytochemistry analyses were carried out on cells at the end of day 28. In this period if there were a large increase in early eye field cells, then a large increase in fluorescence for these markers would have been observed. As this was not the case in this investigation, this suggests that there was a lack in support in directing cells down the retinal lineage. One reason behind this issue may have been the mechanical dissection carried out on day 21. As mentioned previous it is clear that this process is harsh on cells introducing cell breakage and cell death into the population of differentiated cells. Additionally, it must be taken into consideration that a very large population of cells which continued to differentiate on various ECMs had already be processed through the maintenance process twice. Therefore these cells may have had to go through the recovery period following this process several times. As mentioned previously, the recovery time of cells after the maintenance period may increase with the number of processes cells have undergone as it may have "weakened" the ability to recover.

qPCR results have clearly revealed the maintenance process to be detrimental to cells undergoing differentiation in this investigation. In light of this, it may be the case that the final maintenance process had resulted in a particularly increased recovery time of cells resulting in the lack of progression of cells down the retinal lineage despite the time extension given to these cells. It was also interesting to observe that although Pax6 expression may have only been observed at low levels, expression was mainly located in groups of aggregated cells. A number of repetitions and further investigations are however required in order to conclude whether the morphology of Pax6 cells is in fact confined to these cell types.

Although early eye field markers were found to be expressed at low levels it was encouraging to note that a high expression of β-III-tubulin was exhibited by these cells. This is encouraging as β-III-tubulin is a marker of neuronal cells and plays an important role in the health and maintenance of these cells suggesting that the remaining population of cells held a high population of neuronal cells which is a step in the right direction.

Although a high efficiency of RPCs were not observed, this investigation was still successful in mimicking the Lamba *et al.,* 2010 protocol using pluripotent Shef3 hESCs to produces early RPCs. Detection of early eye field markers Pax6 and Chx10 along with photoreceptor precursor marker Crx is evidence of the presence of pluripotent hESCs being differentiated down the retinal lineage using the monolayer differentiation protocol.

Although this investigation has proved that a monolayer differentiation system is feasible to produce RPCs the efficiency of the protocol is still too low to use in clinical supply.

A major issue brought to light by this investigation is the initial seeding density which may play a large role in the optimisation of this particular protocol. This investigation clearly shows the detrimental effects of mechanical dissection of cells during the differentiation process which may be omitted if the optimal seeding density is calculated. This seems to be the downside of this investigation. If mechanical dissection had not been employed during the differentiation process, cells may have had the opportunity to differentiate efficiently into RPCs and a reduction in expression of retinal markers may have not been observed.

It was exciting to note that detection of photoreceptor precursor marker Crx was recorded as early as day 7. If optimal conditions were met, there may be an opportunity to reduce the photoreceptor differentiation protocol by a vast number of days. In terms of use in therapy, this could hold a major advantage as this immediately has the potential to increase efficiency of the protocol by reducing cost of production.

As overall, no particular ECM type had profound advantages for the purpose of this investigation, this may also be another optimisation route to investigate as various combinations may contribute to the differentiation efficiency. This investigation however concludes that neither PDL nor an uncoated surface is optimal for the differentiation of Shef3 hESCs into RPCs.

Overall, this investigation shows that a monolayer differentiation protocol could be successful provided initial seeding densities of cells could be calculated. Along with other optimal conditions the time period of the protocol may also be heavily reduced. A

complete optimisation of the protocol could give better scope for cells to be used in regenerative medicine.

7 Concluding Remarks and Future work

7.1 Summary of results

Investigations into the following areas were made during this study: i) the characterisation of the Shef3 hESC line, ii) the differentiation of Shef3 hESCs into RPCs following a pre-existing protocol, iii) the effect of different dissociation buffers on the pre-existing protocol, iv) the effect of a monolayer differentiation system on RPC production and v) the effect of different ECMs on RPC maintenance.

In chapter 4, this study sought to characterise the Shef3 hESC line. The ability of the cells to remain undifferentiated and pluripotent for a prolonged period of *in vivo* culture was investigated. Expression analysis of intercellular (Oct4) and surface (TRA-1-60 and SSEA-3) pluripotent markers revealed that a large proportion of these cells remained pluripotent over a long period of time (refer to Figure 4.1).

Additionally, karyotyping was employed to ensure no abnormalities were present at the genetic level. This is important as chromosomal abnormalities could potentially lead to tumourigenesis once cells are injected into the patient. As discussed in chapter 4, the Shef3 line was shown to have a normal karyotype.

In chapter 5, the ability of Shef3 hESCs to differentiate into RPCs was investigated, using a protocol devised by Lamba and colleagues in 2006. Following this established protocol, it was demonstrated that Shef3 hESCs could successfully generate RPCs. Immunocytochemistry results revealed the expression of neural RPC marker Chx10 in these cells after 21 day of differentiation (refer to Figure 5.8).

Having confirmed the ability of Shef3 hESCs to generate RPCs using the Lamba protocol, the protocol was then further optimised through an investigation of the impact of dissociation buffers on RPC production. It was shown that the TrypLE Express dissociation buffer was by far the best buffer for use in this differentiation protocol. In comparison to cells dissociated with Accutase, cells dissociated with TrypLE Express

revealed an approximate 110-fold increase in photoreceptor precursor marker Nrl. In comparison to cells dissociated with Collagenase VI, as used in the Lamba protocol, the expression of Nrl was also increased by approximately 100-fold, in those cells dissociated with TrypLE Express (refer to Figure 5.18). This investigation highlighted the importance of process optimisation, and revealed a clear advantage for using the TrypLE Express dissociation buffer in the production of RPCs. There was however, a high degree of cell death observed during the EB investigation, and, thus, an alternative monolayer differentiation protocol was investigated in the following chapters.

In chapter 6, the effect of a monolayer differentiation protocol was investigated on the ability of Shef3 hESCs to produce RPCs. This protocol had been established by Lamba and colleagues in 2010, whereby iPSCs were successfully differentiated into RPCs. This study revealed that a monolayer differentiation protocol could be successful in directing Shef3 hESCs into RPCs. Indeed, qPCR analysis revealed more than a 10-fold increase in expression of photoreceptor precursor marker Crx, compared to the standard EB protocol (refer to Figure 6.13). This increased expression was observed as early as day 7.

This study revealed a decrease in retinal markers over time and highlighted the importance of not carrying out mechanical dissection of cells during the differentiation process. This reduction in retinal gene expression is most likely to be a result of cell degeneration due to damage and stress caused from the breaking up of cells during maintenance procedures.

The study also investigated the impact of the ECM on the growth and differentiation of RPCs. Visually, immunocytochemistry results indicated that cells cultured on gelatin exhibited higher Chx10 expression in comparison to all other ECMs investigated.

In conclusion, this study has been successful in its aim to contribute to the optimisation of the photoreceptor differentiation protocol. Results from this investigation have demonstrated a clear advantage to using TrypLE Express for the dissociation stage of this protocol. Additionally, it has also been shown that the differentiation period could potentially be vastly reduced, with expression of photoreceptor precursor cells detected as early as day 7 in the optimised protocol. In light of research that has found the successful integration of precursor cells for the treatment of blindness this hold great potential. The study has also provided some evidence that the differentiation of cells on

gelatin, could also have a positive impact on protocol with the presence of slightly increased RPC markers.

7.2 Future Work

Although this study has successfully investigated its initial aims, there are further investigations that could be carried out to support these findings.

A more comprehensive characterisation of the Shef3 cell line could further benefit investigations. Although important aspects of Shef3 characterisation were carried out, the majority of this concentrated on immunocytochemistry analysis for markers of pluripotency and the undifferentiated state. In addition to this, it would be prudent to allow cells to undergo spontaneous differentiation as EBs to confirm their multi-lineage potential. Markers such as Nestin (ectoderm marker), Brachyury (mesoderm marker) and Sox17 (endoderm marker), could then have been utilised to identify cells from all three germ layers.

A more rigorous method of confirming pluripotency is the transplantation of hESCs into immunodefficient (SCID) mice which form teratoma-like structures. These structures can then be analysed for multi-lineage differentiation.

Due to ethical reasons and limitation within the lab, this process was not employed in this study.

Many studies have reported the successful differentiation of hESCs into RPCs (Lamba *et al.,* 2006; Osakada *et al.,* 2008; Hirami *et al.,* 2009; Meyer *et al.,* 2009; Osakada *et al.,* 2009). Although success has been widely reported, a major hurdle remains the target cell yield, which has been consistently very low. With such low efficiencies, the process will not be clinically or financially viable for the treatment of patients.

Therefore a major hurdle is present at the very beginning of this differentiation process. In order to rectify this issue, optimisation of initial stages of the protocol is clearly required. Optimisation of initial processes in the differentiation system would increase efficiencies of target yield.

The EB differentiation system was shown to successfully direct Shef3 hESCs into retinal cells, as shown by qPCR analysis of gene expression (refer to Figure 5.18). Dissociating cells with TrypLE Express was shown to be extremely favourable over other buffers in this study, as indicated by increased retinal gene expression. A more comprehensive analysis of this effect could be obtained through the measurement of actual numbers of cells expressing retinal cell markers. By using flow cytometry, the precise proportion of the cell population expressing the various eye field genes could be established and compared. This would give increased support to the evidence for using TrypLE Express as a dissociation buffer for this differentiation. Additionally repetitions of this investigation would also give further supportive evidence. Repeating these investigations in another cell line would also add strength to the data set, whilst providing evidence for both generic and specific optimisation requirements for each cell line. Such investigations could also give insight into specific cell lines that may be more efficiently differentiated into RPCs.

This study observed a high degree of cell loss during the initiation of differentiation through EBs. This is likely to contribute to the low target efficiencies reported, and, thus, the potential loss of target cells at this stage must be minimised.

A monolayer differentiation system would be an ideal alternate solution to the EB system, aimed at combatting the high cell losses.

The results of this study showed the potential for the employment of a monolayer differentiation system. For monolayer system to be beneficial, optimisation of initial cell densities is required. Initial seeding densities used in this investigation heavily impacted the outcome of the result. It was clear that a lower seeding density would have been more beneficial to this study. The seeding density used in this investigation resulted in an over-confluency of cells early on in the differentiation period. An attempt to reduce this density of cells manually, during the differentiation process, had detrimental effects on the expression of retinal genes.

A more comprehensive investigation would involve the optimisation of the seeding density for the monolayer differentiation. Care would have to be taken not to dissociate cells for maintenance during the differentiation period. Allowing cells to remain in culture, undisturbed, may hold the key to greater efficiencies of target cells. By establishing optimal initial seeding densities the timeframe for the differentiation of

hESCs into RPCs could potentially be significantly reduced. Additionally, this could also aid in the isolation of target cells. Over-confluent cells, having formed multi-layered structures, cannot be physically separated without causing damage to cells. This can lead to cell death, as exhibited in this study. An optimal seeding density could allow for the use of FACS (Fluorescence Assisted Cell Sorting), whereby markers for target cells could be identified to sort cells from a single cell solution. The original protocol produced by Lamba and colleagues in 2006, set a timeframe of 21 days for the production of RPCs. In this study, photoreceptor precursor marker Crx was observed as early as day 7.

In terms of production of RPCs for therapy, a considerable reduction in the timeframe could greatly aid the formation of a cost effect production line.

Photoreceptor development can be separated into a number of stages which include: 1) the withdrawal of progenitor cells from the cell cycle to adopt a photoreceptor cell fate; 2) physical changes resulting in the morphology of inner and outer segments; 3) production of synapses with interneurons of the retina; 4) maintenance of photoreceptors (Hunter *et al.,* 2004). This process is highly organised with intrinsic controls monitoring the various developmental stages.

The retinal microenvironment is thus comprised of a range of factors which all play a part in the fine control of photoreceptor development (amongst other functions). One such set of components are the ECMs, secreted macromolecules which play vital roles in directing many aspects of photoreceptor development including: 1) the initiation, continuation and stop of cell division; 2) the timing of differentiation; 3) the location of migration; 4) locations at which synapses should be formed (Hunter *et al.,* 2004).

One type of retinal ECM is Laminin, which plays important roles in retinal differentiation. There are several members of the Laminin family but those containing the β2 chain have been found to play key roles in the maintenance of rod photoreceptor phenotype and bipolar cells (Hunter *et al.,* 2004).

Another component of the retinal ECM is Wnt- inhibitory factor 1 (WIF-1). WIF-1 has been found to be bound by many molecules including Wnt and LPR6, the Wnt pathways have been discussed in further detail in chapter 1.9.2.

Other small, soluble molecules can also interact with ECMs to promote or demote specific roles. For example FGF-2 has been found to promote rod photoreceptor generation whilst TGFβ has been found to inhibit this process (Hunter *et al.,* 2004). Acidic FGF (αGF) and basic FGF (βFGF) receptors have been found to be present in optic vesicles (Ramsden *et al.,* 2013).

There are many pathways that are vitally important for various development stages in the retina, which can be impacted by a range of ECM components. Notch signalling is involved in axis determination and appears later in retinal developmental (Ramsden *et al.,* 2013). Nodal signalling determines left-right determination. Whilst sonic hedgehog (SHH) is involved in the division of the eye field; SHH knockout results in cyclopia, a congenital disease characterised by the incomplete division of eye orbitals into both cavities of the eye (Ramsden *et al.,* 2013). The importance of ECMs in mimicking the retinal environment may hold the key to a successful RPC differentiation process.

This study investigated the impact of several ECMs on the maintenance of potential RPCs. Of those ECMs investigated, this study found gelatin to be the most advantageous to the differentiation process of RPCs. These results were based on visual assessment of immunocytochemistry results. The use of qPCR gene expression analysis would provide a quantitative measurement of the effect of ECM components on RPC production, providing a more robust and conclusive data set to reinforce the ICC results. Additionally, this study investigated the impact of ECMs during an extension period of the differentiation protocol. In light of the fact that photoreceptor precursor cells were observed as early as day 7, an investigation whereby ECMs were studied during the differentiation process would have been more beneficial to the optimisation process. For example, a study could have been set up with various ECMs, following the same monolayer differentiation protocol, omitting the culture maintenance stage of the protocol observed in this study. Following the end of the process, qPCR analysis of expression of various retinal markers would have given a more robust result set exploring the advantage of specific ECM type for the production of RPCs.

It is evident that the retinal microenvironment is tightly controlled, with various ECM components all playing significant roles in photoreceptor development. In light of this, once preliminary investigations of the most beneficial ECMs have been established, further studies could be employed to investigate optimal ECM combinations. Many

current protocols have used Matrigel for the production of RPCs, but the disadvantage of this is that Matrigel is not a well-defined matrix (Hughes *et al.*, 2010). This poses variability issues in research. Additionally, the use of Matrigel for therapeutic use immediately flags numerous safety issues. For these reasons, optimal ECM combinations, omitting Matrigel, would be highly beneficial for creating an efficient RPC differentiation protocol.

The key to creating an optimal RPC differentiation protocol, lies within mimicking the retinal microenvironment during embryogenesis. One factor that has been researched greatly in this process is oxygen concentration. It has been found that a state of hypoxia is present during embryogenesis. In ambient air approximately 20% of oxygen is present in comparison to the 2% of oxygen present during embryogenesis (Bae *et al.*, 2012). A study carried out by a group from our laboratory showed that Pax6 and Chx10 expression is increased in hESCs differentiated in hypoxia (2% Oxygen) (Figure 7.1). Results from the study carried out by Bae *et al*, 2012 could be incorporated into the optimisation of the RPC differentiation protocol.

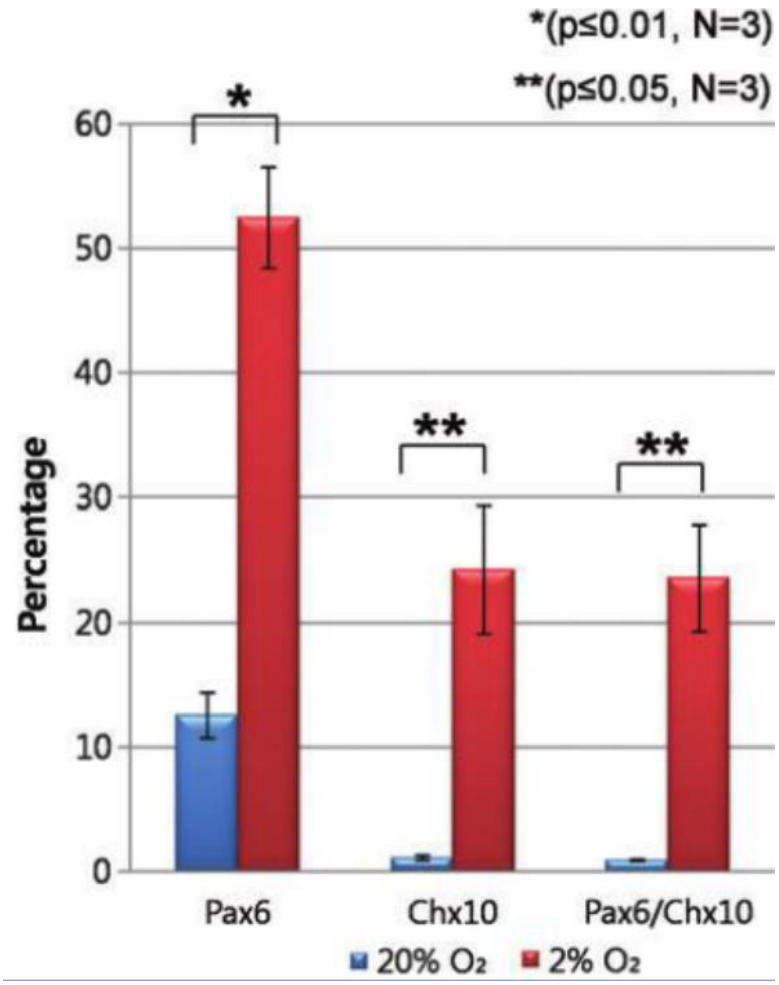

Figure 7.1: Quantification using flow cytometry for the differentiation of hESCs under normal and hypoxic conditions. Figure taken from Bae *et al.*,2012.

In conclusion, an optimisation strategy for production of RPCs firstly requires the establishment of optimal seeding densities. Once this has been achieved, cells should be dissociated using TrypLE Express, as use of this buffer has been shown to increase efficiencies of target cell production. Next the optimal combinations of ECMs could be investigated and once established, the differentiation process could be carried at hypoxia in a monolayer differentiation process. Once the optimisation of these critical factors has been achieved, attention could be turned towards the addition of various soluble components, such as growth factors and small molecules that may further improve the protocol as a whole.

An optimised protocol such as this could then be tested in a number of cell lines to identify those lines with an increased propensity for RPC differentiation. Additionally

qPCR and flow cytometry should be employed for quantitative analysis of marker expression. Once a fully optimised protocol has been identified target cells could be isolated using FACS, and then a secondary optimisation process could be investigated in order to identify ideal conditions to promote proliferation and growth of these RPCs.

Photoreceptor progenitor cells could then undergo transplantation studies to investigate the functionality and integration of these cells. If cells are found to integrate well and mature into functional photoreceptors then the process would be successful in its aim and could then be used for therapy.

A monolayer protocol would be highly beneficial in the scale-up process for supply in a clinical environment. Current strategies that employ EBs to initiate differentiation would result in a two-stage process. If cells were to be supplied for use as therapy currently, two set of machinery would have to be employed. For the initial EB stage a bioreactor system would have to be employed for example the DASGIP Parallel System or Cellmate (Tap Biosystems) for the maintenance of a suspended culture system. After this stage of the process another system for an attachment culture system could have to be employed such as for example SelecT (Tap Biosystems).

By establishing a monolayer culture system, scale-up for clinical use would only require one system such as the SelecT (Tap Biosystems) to carry out the whole differentiation process. This process intensification would be a more cost-effect method of production, which also has the added benefit of standardising production lines. Cost-effective and efficient methods for the production of photoreceptor precursor cells would greatly aid in the treatment for the many sufferers of ocular diseases.

Bibliography

1. Adewumi O, Aflatoonian B, Ahrlund-Richter L, Amit M, Andrews PW, Beighton G, Bello PA, Benvenisty N, Berry LS, Bevan S,Blum B, Brooking J, Chen KG, Choo AB, Churchill GA, Corbel M, Damjanov I, Draper JS, Dvorak P, Emanuelsson K, Fleck RA, Ford A, Gertow K, Gertsenstein M, Gokhale PJ, Hamilton RS, Hampl A, Healy LE, Hovatta O, Hyllner J, Imreh MP, Itskovitz-Eldor J, Jackson J, Johnson JL, Jones M, Kee K, King BL, Knowles BB, Lako M, Lebrin F, Mallon BS, Manning D, Mayshar Y, McKay RD, Michalska AE, Mikkola M, Mileikovsky M, Minger SL, Moore HD, Mummery CL, Nagy A,Nakatsuji N, O'Brien CM, Oh SK, Olsson C, Otonkoski T, Park KY, Passier R, Patel H, Patel M, Pedersen R, Pera MF, Piekarczyk MS, Pera RA, Reubinoff BE,Robins AJ, Rossant J, Rugg-Gunn P, Schulz TC, Semb H, Sherrer ES, Siemen H, Stacey GN, Stojkovic M, Suemori H, Szatkiewicz J, Turetsky T, Tuuri T, van den Brink S, Vintersten K, Vuoristo S, Ward D, Weaver TA, Young LA, Zhang W. 2007. Characterization of human embryonic stem cell lines by the International Stem Cell Initiative. Nat Biotechnol 25(7): 803-16.

2. Alberts, B.,Johnson, A.,Lewis,J., Raff M.,Roberts,K. and Walter, P. 2002. Molecular biology of the cell 4th edition. New York, Garland Science.Chapter 15.

3. Amit M, Margulets V,Segev H, Shariki K, Laevsky I, Coleman R, Itskovitz-Eldor J. 2003. Human feeder layers for human embryonic stem cells. Bio Reprod 68:2150-2156.

4. Anasagasti A, Irigoyen C, Barandika O, López de Munain A, Ruiz-Ederra J.2012. Vision Research 75 (2012) 117–129

5. Bae D, Mondragon-Teran P, Hernandez D, Ruban L, Mason C, Bhattacharya S, Veraitch F. 2012. Hypoxia Enhances the Generation of Retinal Progenitor Cells from Human Induced Pluripotent and Embryonic Stem Cells. Stem Cells and Dev 21:(8).

6. Barber AC, Hippert C, Duran Y, West EL, Bainbridge JW, Warre-Cornish K, Luhmann UF, Lakowski J, Sowden JC, Ali RR, Pearson RA. 2013. Repair of the degenerate retina by photoreceptor transplantation. Proc Natl Acad Sci U S A. 2;110(1):354-9.

7. Boughman, J. A., M. Vernon, Shaver, K. A. 1983. Usher syndrome: definition and estimate of prevalence from two high-risk populations. J Chronic Dis 36(8): 595-603.

8. Braude, P., Bolton, V., Moore, S. 1988. Human gene expression first occurs between the four- and eight-cell stages of preimplantation development. Nature 332(6163): 459-61.

9. Bratt-Leal1 AM,. Carpenedo1 LR, McDevitt TC. 2009. Engineering the Embryoid Body Microenvironment to Direct Embryonic Stem Cell Differentiation. Biotechnol Prog. 25(1): 43–51.

10. Brimble, S. N.,Sherrer, E.S., Uhl, E.W., Wang, E., Kelly, S., Merrill, A.H Jr., Robins, A.J., Schulz, T.C. 2007. The cell surface glycosphingolipids SSEA-3 and SSEA-4 are not essential for human ESC pluripotency. Stem Cells 25(1): 54-62.

11. Burdon, T., Smith,A., Savatier, P. 2002. Signalling, cell cycle and pluripotency in embryonic stem cells. Trends Cell Biol 12(9): 432-8.

12. Carpenter MK, Rosler E, Rao MS. 2003. Characterization and differentiation of human embryonic stem cells. Cloning Stem Cells. 5(1):79-88.

13. Carr AJ, Vugler AA, Hikita ST, Lawrence JM, Gias C, Chen LL, Buchholz DE, Ahmado A, Semo M, Smart MJK, Hasan1 S, Cruz L, Johnson LV, Clegg DO, Coffey PJ. 2009. Protective Effects of Human iPS-Derived Retinal Pigment Epithelium Cell Transplantation in the Retinal Dystrophic Rat. PloS One. 4(12): e8152.

14. Cavodeassi F, Carreira-Barbosa F, Young R.M, Concha M.L, Allende, ML, Houart C, Tada M, Wilson SW. 2005. Early stages of zebrafish eye formation require the coordinated activity of Wnt11, Fz5, and the Wnt/beta-catenin pathway.Neuron 47(1): 43-56.

15. Chang S1, Vaccarella L, Olatunji S, Cebulla C, Christoforidis J. 2011. Curr Genomics. Jun;12(4):267-75

16. Conley BJ, Young JC, Trounson AO, Mollard R. 2004. Derivation, propagation and differentiation of human embryonic stem cells. Int J Biochem Cell Biol 36(4): 555-67.

17. Esteve P1, Lopez-Rios J, Bovolenta P. 2004. SFRP1 is required for the proper establishment of the eye field in the medaka fish. Mech Dev 121(7-8): 687-701.

18. Ferrari S, Iorio1 ED, Barbaro1 V, Ponzin1 D, Sorrentino FS, Parmeggiani F. 2011. Retinitis Pigmentosa: Genes and Disease Mechanisms. Current Genomics 12, 238-249

19. Hamel, C. 2006. Retinitis pigmentosa. Orphanet J Rare Dis 1: 40.

20. Hanna J, Wernig M, Markoulaki S, Sun C, Messiner A, Cassady PJ, Beard C, Brambrink T, Wu L, Townes TA, Jeanisch R. 2011. Treatment of Sickle Cell Anemia Mouse Model with iPS Cells Generated from Autologous Skin. Science, New Series, Vol. 318.

21. Heller-Stilb B1, van Roeyen C, Rascher K, Hartwig HG, Huth A, Seeliger MW, Warskulat U, Häussinger D. 2002. Disruption of the taurine transporter gene (taut) leads to retinal degeneration in mice. FASEB J 16(2): 231-3.

22. Hernandez D, Ruban L, Mason C. 2011. Feeder-free culture of human embryonic stem cells for scalable expansion in a reproducible manner Stem Cells Dev.20(6):1089-98.

23. Hidalgo-Bastida, L. A. and S. Cartmell. 2010. Mesenchymal Stem Cells, Osteoblasts And Extracellular Matrix (ECM) Proteins: Enhancing Cell Adhesion And Differentiation For Bone Tissue Engineering. Tissue Eng Part B Rev.

24. Hirami Y1, Osakada F, Takahashi K, Okita K, Yamanaka S, Ikeda H, Yoshimura N, Takahashi M. 2009. Generation of retinal cells from mouse and human induced pluripotent stem cells. Neurosci Lett 458(3): 126-31.

25. Hiyama, E. and K. Hiyama. 2007. Telomere and telomerase in stem cells. Br J Cancer 96(7): 1020-4.

26. Hughes CS, Postovit LM, Lajoie GA.2010. Matrigel: a complex protein mixture required for optimal growth of cell culture. Proteomics. 10(9):1886-90.

27. Hunter DD1, Zhang M, Ferguson JW, Koch M, Brunken WJ. 2004. The extracellular matrix component WIF-1 is expressed during, and can modulate, retinal development. Mol Cell Neurosci. 27(4):477-88

28. Hwang YS1, Chung BG, Ortmann D, Hattori N, Moeller HC, Khademhosseini A. 2009. Microwell-mediated control of embryoid body size regulates embryonic stem cell fate via differential expression of WNT5a and WNT11. Proc Natl Acad Sci USA. 6;106(40):16978-83.

29. Ikeda H1, Osakada F, Watanabe K, Mizuseki K, Haraguchi T, Miyoshi H, Kamiya D, Honda Y, Sasai N, Yoshimura N, Takahashi M, Sasai Y. 2005. Generation of Rx+/Pax6+ neural retinal precursors from embryonic stem cells. Proc Natl Acad Sci U S A 102(32): 11331-6.

30. Ishikawa, T. and E. Yamada. 1969. Atypical Mitochondria in Ellipsoid of Photoreceptor Cells of Vertebrate Retinas. Investigative Ophthalmology 8(3): 302-16.

31. Iwasaki, M. and H. Inomata. 1988. Lipofuscin granules in human photoreceptor cells. Invest Ophthalmol Vis Sci 29(5): 671-9.

32. Kanno C1, Kashiwagi Y, Horie K, Inomata M, Yamamoto T, Kitanaka C, Yamashita H. 2009. Activin inhibits cell growth and induces differentiation in human retinoblastoma y79 cells. Curr Eye Res 34(8): 652-9.

33. Kaufman DS1, Hanson ET, Lewis RL, Auerbach R, Thomson JA. 2001. Hematopoietic colony-forming cells derived from human embryonic stem cells. Proc Natl Acad Sci U S A 98(19): 10716-21.

34. Kehat I, Kenyagin-Karsenti D, Snir M, Segev H, Amit M, Gepstein A, Livne E, Binah O, Itskovitz-Eldor J, Gepstein L. 2001. Human embryonic stem cells can differentiate into myocytes with structural and functional properties of cardiomyocytes. J Clin Invest 108(3): 407-14.

35. Kelley MW, Turner JK, Reh TA. 1994. Retinoic acid promotes differentiation of photoreceptors in vitro. Development 120(8): 2091-102.

36. Kerov V, Chen D, Moussaif M, Chen YJ, Chen CK, Artemyev NO. 2005. Transducin activation state controls its light-dependent translocation in rod photoreceptors. J Biol Chem. 9;280(49):41069-76.

37. Kibschull M, Mileikovsky M, Michael IP, Lye SJ, Nagy A. 2011. Human embryonic fibroblasts support single cell enzymatic expansion of human embryonic stem cells in xeno-free cultures. Stem Cell Res. 1:70-82.

38. Lamba DA, Karl MO, Ware CB, Reh TA. 2006. Efficient generation of retinal progenitor cells from human embryonic stem cells. Proc Natl Acad Sci U S A 103(34): 12769-74.

39. Lamba DA, McUsic A, Hirata RK, Wang PR, Russell D, Reh TA. 2010. Generation, purification and transplantationof pluripotent stem cells. PLoS One.5(1).

40. Levenberg S, Golub JS, Amit M, Itskovitz-Eldor J, Langer R. 2002. Endothelial cells derived from human embryonic stem cells. Proc Natl Acad Sci U S A 99(7): 4391-6.

41. Li L, Clevers H. 2010. Coexistence of Quiescent and Active Adult Stem Cells in Mammals. Science 327, 542.

42. Liu Y1, Suwa F, Wang X, Takemura A, Fang YR, Li Y, Zhao Y, Jin Y. 2007. Reconstruction of a tissue-engineered skin containing melanocytes. Cell Biol Int. 2007 Sep;31(9):985-90.

43. Liu Y, Fox V, Lei Y, Hu B, Joo KI, Wang P. 2013. Synthetic niches for differentiation of human embryonic stem cells bypassing embryoid body formation. J Biomed Mater Res B Appl Biomater. Dec 10.

44. Loh1 YH, Wu1 Q, Chew JL, Vega VB, Zhang W, Chen X, Bourque G, George J, Leong B, Liu J, Wong KY, Sung KW, Lee CWH, Zhao XD, Chiu KP, Lipovich L, Kuznetsov VA, Robson P, Stanton LW, Wei CL, Ruan Y, Lim B, Ng H. 2006. The Oct4 and Nanog transcription network regulates

45. pluripotency in mouse embryonic stem cells. Nature Gen. 38(4).

46. Loring JF, Wesselschmidt RL, Schwartz P.H. 2007. Human Stem Cell Manual: A Laboratory Guide, Academic Press is an imprint of Elsevier.Chapter 2 & 5.

47. Luzzani C1, Solari C, Losino N, Ariel W, Romorini L, Bluguermann C, Sevlever G, Barañao L, Miriuka S, Guberman A. 2011. Modulation of chromatin modifying factors' gene expression in embryonic and i nduced pluripotent stem cells. Biochem Biophys Res Commun. 15;410(4):816-22

48. MacLaren RE, Pearson RA, MacNeil A, Douglas RH, Salt TE, Akimoto M, Swaroop A, Sowden JC, Ali RR. 2006. Retinal repair by transplantation of photoreceptor precursors. Nature 444(7116): 203-7.

49. Maguire AM, High KA, Auricchio A, Wright JF, Pierce EA, Testa, Federico F, Mingozzi, Bennicelli JL, Ying G, Rossi S, Fulton A, Marshall KA, Banfi S , Chung DC, Morgan JIW, Hauck B, Zelenaia O, Zhu X, Raffini L, Coppieters F, De Baere E, Shindler KS, Volpe NJ, Surace EM, Acerra C, Lyubarsky A, Redmond M, Stone E, Sun J, McDonnell JW, Leroy BP, Simonelli F, Bennett J. 2009. Age-dependent eff ects of RPE65 gene therapy for Leber's congenital amaurosis: a phase 1 dose-escalation trial. Lancet 374: 1597–605

50. Maguire G, Friedman P. 2014. Enhancing spontaneous stem cell healing (Review). Biomed. Rep 2: 163-166

51. Mallon BS, Park KY, Hamilton RS, Mckay RDG. 2006. Toward xeno-free culture of human embryonic stem cells. Int J Biochem Cell Biol 38:1063-75

52. Mansergh FC, Millington-Ward S, Kennan A, Kiang AS, Humphries M, Farrar GJ, Humphries P, Kenna PF.. 1999. Retinitis pigmentosa and progressive sensorineural hearing loss caused by a C12258A mutation in the mitochondrial MTTS2 gene. Am J Hum Genet 64(4): 971-85.

53. Martini F, Nath J L. 2009. Fundamentals of anatomy & physiology. San Francisco ; London, Pearson/Benjamin Cummings.Pg500-700.

54. Masland, R. H. 2001. The fundamental plan of the retina. Nat Neurosci 4(9): 877-86.

55. Masli S, Vega JL. 2011. Ocular immune privilege sites. Methods Mol Biol. 677:449-58.

56. Méndez-Vidal C, Pozo MG, Vela-Boza A, Santoyo-López J, López-Domingo FJ, Vázquez-Marouschek C,Dopazo J, Borrego S, Antiñolo G. 2013. Whole-exome sequencing identifies novel compound heterozygous mutations in USH2A in Spanish patients with autosomal recessive retinitis pigmentosa. Mol Vis. 19: 2187–2195

57. Mesples A, Majeed N, Zhang Y, Hu X. Med Sci Monit. 2013. Early immunotherapy using autologous adult stem cells reversed the effect of an ti-pancreatic islets in recently
diagnosed type 1 diabetes mellitus: preliminary results. Med Sci Monit. 14;19:852-7

58. Meyer JS, Shearer RL, Capowski EE, Wright LS, Wallace KA, McMillan EL, Zhang SC, Gamm DM.. 2009. Modeling early retinal development with human embryonic and induced pluripotent stem cells. Proc Natl Acad Sci U S A 106(39): 16698-703.

59. Mundra V1, Gerling IC, Mahato RI. 2013. Mesenchymal Stem Cell-Based Therapy. Mol Pharm. 7; 10(1): 77–89

60. Nag TC, Wadhwa S.2012. Ultrastructure of the human retina in aging and various pathological states. Micron. 43(7):759-81

61. Nie Y1, Cui D, Pan Z, Deng J, Huang Q, Wu K. 2008. HSV-1 infection suppresses TGF
beta1 and SMAD3 expression in human corneal epithelial cells. Mol Vis. 3;14:1631-8.

62. Nishikawa S, Goldstein RA, Nierras CR. 2008. The promise of human induced pluripotent stem cells for research and therapy. Nat Rev Mol Cell Biol. 9(9):725-9.

63. NHSBT (2013). Cornea transplantation. http://www.uktransplant.org.uk/ukt/newsroom/fact_sheets/ cornea_transplantation_fact_sheet.jsp. Accessed 15th March 2013.

64. Oh SK, Kim HS, Ahn HJ, Seol HW, Kim YY, Park YB, Yoon CJ, Kim DW, Kim SH, Moon SY. 2005. Derivation and characterization of new human embryonic stem cell lines: SNUhES1, SNUhES2, and SNUhES3. Stem Cells. 23(2):211-9

65. Osakada F, Ikeda H, Mandai M, Wataya T, Watanabe K, Yoshimura N, Akaike A, Sasai Y, Takahashi M. 2008. Toward the generation of rod and cone photoreceptors from mouse, monkey and human embryonic stem cells. Nat Biotechnol 26(2): 215-24.

66. Osakada F, Jin ZB, Hirami Y, Ikeda H, Danjyo T, Watanabe K, Sasai Y, Takahashi M. 2009. In vitro differentiation of retinal cells from human pluripotent stem cells by small-molecule induction. J Cell Sci 122(Pt 17): 3169-79.

67. Pearson RA1, Barber AC, Rizzi M, Hippert C, Xue T, West EL, Duran Y, Smith AJ, Chuang JZ, Azam SA, Luhmann UF, Benucci A, Sung CH, Bainbridge JW, Carandini M, Yau KW, Sowden JC, Ali RR. 2012. Restoration of vision after transplantation of photoreceptors. Nature. 3; 485(7396): 99–103

68. Petrs-Silva H, Linden R. 2013. Advances in gene therapy technologies to treat retinitis pigmentosa. Clin Ophthalmol. 2014;8:127-136

69. Pfaffl MW.2001. A new mathematical model for relative quantification in real-time RT-PCR. Nucleic Acids Res. 1;29(9)

70. Prockop DJ, Gregory CA, Spees JL. 2003. One strategy for cell and gene therapy: harnessing the power of adult stem cells to repair tissues. Proc Natl Acad Sci U S A. Suppl 1:11917-23.

71. Ramsden CM, Powner MB, Carr AJF, Smart MJK, Cruz L,Coffey P. 2013. Stem cells in retinal regeneration: past, present and future. Development. 140(12).

72. Reubinoff BE, Pera MF, Fong CY, Trounson A, Bongso A. 2000. Embryonic stem cell lines from human blastocysts: somatic differentiation in vitro. Nat Biotechnol 18(4): 399-404.

73. Sakamoto K, McCluskey M, Wensel TG, Naggert JK, Nishina PM. 2009. New mouse models for recessive retinitis pigmentosa caused by mutations in the Pde6a gene. Hum Mol Genet 18(1): 178–192

74. Sernagor E. 2006. Retinal development. Cambridge, Cambridge University Press.Chapter 1& 2.

75. Shinya M[1], Eschbach C, Clark M, Lehrach H, Furutani-Seiki M. 2000. Zebrafish Dkk1, induced by the pre-MBT Wnt signaling, is secreted from the prechordal plate and patterns the anterior neural plate. Mech Dev 98(1-2): 3-17.

76. Siemiatkowska AM[1], Astuti GD, Arimadyo K, den Hollander AI, Faradz SM, Cremers FP, Collin RW. 2012. Identification of a novel nonsense mutation in RP1 that causes autosomal recessive retinitis pigmentosa in an Indonesian family. Mol Vis. 2012;18:2411-9

77. Snell R S., Lemp M A. 1998. Clinical Anatomy of the Eye, Blackwell Science. Ch1.

78. Solter D, Knowles B B. 1978. Monoclonal antibody defining a stage-specific mouse embryonic antigen (SSEA-1). Proc Natl Acad Sci U S A 75(11): 5565-9.

79. Stadtfeld M, Nagaya M, Utikal J, Weir G, Hochedlinger K. 2008. Induced Pluripotent Stem Cells Generated Without Viral Integration. Science 322(5903): 945–949.

80. Takahashi K, Yamanaka S. 2006. Induction of pluripotent stem cells from mouse embryonic and adult fibroblast cultures by defined factors. Cell. 25;126(4):663-76

81. Takahashi K, Yamanaka S. 2013. Induced pluripotent stem cells in medicine and biology. Development 140, 2457-2461.

82. Thomson JA, Itskovitz-Eldor J, Shapiro SS, Waknitz MA, Swiergiel JJ, Marshall VS, Jones JM. 1998. Embryonic stem cell lines derived from human blastocysts. Science 282(5391): 1145-7.

83. Tischfield MA, Engle EC. 2010. Distinct alpha- and beta-tubulin isotypes are required for the positioning, differentiation and survival of neurons: new support for the 'multi-tubulin' hypothesis. Biosci Rep. 15;30(5):319-30.

84. Tortora G J, Nielsen M T. 2009. Principles of human anatomy. Hoboken, N.J., John Wiley. Ch22.

85. Wu H, Mahato RI. 2014. Mesenchymal stem cell-based therapy for type 1 diabetes. Discov Med. 17(93):139-43.

86. Yang C, Przyborski S, Cooke MJ, Zhang X, Stewart R, Anyfantis G, Atkinson SP, Saretzki G, Armstrong L, Lako M. 2008. A key role for telomerase reverse transcriptase unit in modulating human embryonic stem cell proliferation, cell cycle dynamics, and in vitro differentiation. Stem Cells 26(4): 850-63.

87. Young R W. 1967. The renewal of photoreceptor cell outer segments. J Cell Biol 33(1): 61-72.

88. Wawersik S, Maas R L. 2000. Vertebrate eye development as modelled in Drosophila. Hum Mol Genet 9(6): 917-25.

89. Zhao W, Ji X, Zhang F, Li, Ma L. 2012. Embryonic Stem Cell Markers. Molecules 17, 6196-6236.

90. Zuber ME, Gestri G, Viczian AS, Barsacchi G, Harris WA. 2003. Specification of the vertebrate eye by a network of eye field transcription factors. Development 130(21): 5155-67.